AN INVESTIGATION INTO SEASONAL TRENDS OF TERPENE EMISSIONS: A FOCUS ON MONOTERPENE AND SESQUITERPENE EMISSIONS OF NATIVE COLORADO TREE SPECIES

by

RYAN WOODFIN DALY

B.S./M.S. candidate, University of Colorado

A thesis submitted to the

Faculty of the Graduate School of the

University of Colorado in partial fulfillment

of the requirement for the degree of

Master of Science

Department of Mechanical Engineering

2010

This thesis entitled:
An Investigation into Seasonal Trends of Terpene Emissions
from Biogenic Sources: A Focus on Monoterpene and
Sesquiterpene Emissions of Native Colorado Tree Species
written by Ryan Woodfin Daly
has been approved for the Department of Mechanical Engineering

_____
Jana Milford, Committee Chair

_____
Detlev Helmig, Committee Member and Thesis Director

_____
Alex Guenther, Committee Member

Date: April 22, 2011

The final copy of this thesis has been examined by the signatories, and we
Find that both the content and the form meet acceptable presentation standards
Of scholarly work in the above mentioned discipline.

Abstract

Daly, Ryan Woodfin (M.S., Mechanical Engineering)

An Investigation into Seasonal Trends on Terpene Emissions from Biogenic Sources

Thesis directed by Associate Research Professor Detlev Helmig

Plants naturally emit a variety of highly reactive hydrocarbon compounds, classified as biogenic volatile organic compounds (BVOC), which are known to have large implications for atmospheric chemistry. Once released into the troposphere, BVOC participate in reactive nitrogen, hydroxyl and ozone chemistry as well as secondary organic aerosol formation. The resulting air quality impacts warrant a thorough understanding of BVOC emission behavior, critical for effective regional modeling and legislative decision-making. This work aims to improve the database and algorithms used in biogenic emission models by examining the seasonal trends of two classes of BVOC, monoterpene (MT) and sesquiterpene (SQT) hydrocarbons. A field site established at a local tree nursery provided an opportunity to easily monitor the emissions of naturally growing vegetation throughout a growing season. The emission rates of five tree species native to Colorado forests were measured monthly between February 2009 and February 2010. Biogenic emissions were found to exhibit seasonal variation with higher emission rates observed between spring and late summer, falling to a low through winter months. The seasonal behavior of BVOC emissions proves to be very complex. These findings are discussed and call into question the methods used for estimating annual emission rates.

Acknowledgements

I would like to thank Creekside Tree Nursery in Boulder, Colorado for generously providing this research with a field site and the vegetation used throughout this study. Additionally, I gratefully acknowledge Thomas Mefford of the Coorperative Institute for Research in Environmental Sciences (CIRES) and NOAA Earth System Research Laboratory for providing meteorological data used in the study. This research has been supported by a National Science Foundation grant.

I would like to give thanks to my research advisor Detlev Helmig for support and guidance throughout the project. Additional thanks are extended to Jana Milford for providing advice and assistance and to Alex Guenther for serving on my committee. I am grateful for the assistance of members of the Atmospheric Research Lab (a division of the Institute of Arctic and Alpine Research), particularly Jacques Hueber, David Tanner, Romain Baghi, Brooks Mason, Carly Baroch and Chris Borke without whose help this research would not have been possible.

Table of Contents

Table of Contents ……. v

List of Tables ……. vii

List of Figures ……. viii

Chapter 1 Introduction ……... 1

1.1 Problem Statement ……. 1

1.2 Background ……. 1

1.3 Research Motivation ……. 3

1.4 Thesis Organization ……. 4

Chapter 2 An Investigation Into Seasonal Trends of Terpene Emissions ……. 5

2.1 Abstract ……. 5

2.2 Introduction ……. 6

2.3 Methods ……. 8

2.3.1 Measurement Site and Sample Vegetation ……. 8

2.3.2 Experimental Methods ……. 9

2.3.3 Observed Emission Rate (ER) ……. 13

2.3.4 Basal Emission Rate (ε) ……. 14

2.3.5 Seasonal Correction Factor C_S ……. 15

2.4 Results and Discussion ……. 17

2.4.1 Emission Summary ……. 17

2.4.2 Short-Term Emissions ……. 27

2.4.3 Seasonal Speciation ……. 31

2.4.4 Seasonal Emission Magnitude ……. 33

2.4.5 Variation of Temperature Dependent β-factor ……..... 37

2.4.6 Seasonal Emission Rate Sensitivity Analysis …….....….... 40

2.4.7 SQT observations ……..... 43

2.5 Conclusions and Summary……..... 44

References ……..…….....…… 46

Appendix A – GC-FID/MS Analysis Parameters …….....…. 52

Appendix B – Bootstrap Statistics of the β-factor ……..…. 53

Appendix C – C5 - C15 Multi-Adsorbent Sampling Cartridge ……....… 67

Appendix D – SQT Recovery Rate Analysis: Loss to Experimental Materials …..…….... 79

Appendix E – Analyte Recovery from Branch Enclosure Studies .....……...… 84

Appendix F – Published Paper: PTR-MS for measuring SQT ...……...…….....…. 86

Appendix G – 2009 & 2010 CABINEX Field Campaign ……..….… 93

Appendix H – Contribution of flowering trees to urban atmospheric biogenic volatile organic compound emissions …….……. 101

List of Tables

Table 1: Summary of enclosure study data for each sample tree, listed by sample date.

Table 2: Seasonally averaged emission rates reported with respect to speciation (%) and basal emission rate (ε). Seasons are defined by month listed in brackets (ie. 'Summer [JJA]' represents averaged data between June, July and August).

Table 3: Seasonally compiled β-factor statistics. The mean, standard deviation about the mean, median, minimum and maximum β-factor statistics are shown with respect to categorized compounds for each tree studied. Total MT is the sum of all monoterpenes observed.

Table 4: The use of basal emission rates and β-factors used in case 1, 2, and 3 for analyzing their respective sensitivity to calculating non-normalized emission rates over an annual period.

List of Figures

Figure 1: Schematic of the experimental setup.

Figure 2: Estimated biomass dry-weight of Ponderosa Pine A over the study period.

Figure 3: Normalizing light and temperature correction factors $\exp^{\beta*T}$ (dark red, solid), C_T (light red, dashed) and C_L (blue) for calculating a basal emission rate, ε.

Figure 4: A modified seasonal correction factor $C_{S,mod}$ (open dots) used here is compared to the correction factor C_S (closed red dots) proposed by Staudt et al. (2000).

Figure 5: Four day time series of total MT emissions (black diamonds) for BS-b sampled in January, 2010. Enclosure temperature is shown in red, light radiation (PAR) is shown in blue.

Figure 6: Emission speciation of Ponderosa Pine A with respect to diurnal cycling illustrated with several enclosure experiments between spring-fall of 2009. Sample dates are listed at the top of each plot. Bars indicate a compounds percent contribution to total emission signal. White diamonds are overlaid upon speciation bars to indicate diurnal change in actual (non-normalized) emission rates.

Figure 7: Emission speciation of Ponderosa Pine B with respect to diurnal cycling illustrated with several enclosure experiments between spring-fall of 2009. Sample dates are listed at the top of each plot. Bars indicate a compounds percent contribution to total emission signal. White diamonds are overlaid upon speciation bars to indicate diurnal change in actual (non-normalized) emission rates.

Figure 8: Monthly averaged MT compound speciation. Percent contribution to the total MT basal emission rate is indicated by the vertical bars. The magnitude of the basal emission rate is shown as a white diamond overlaid upon the vertical bars.

Figure 9: Seasonally plotted basal emission rates per enclosure study. Error bars indicate one standard deviation. Please note differences in scale. Seasonally corrected basal emission rates generated using the methods presented by Staudt et al. (2000) are illustrated by the curve. Red dots indicate data in which enclosure temperature was not recorded. Instead, sample temperature was inferred from temperature data of a nearby weather station. Blue vertical bars indicate leaf/needle bud break and senescence. Parameters used in the seasonal correction term $C_{S,mod}$ (Equation 10) listed below along with regression statistics:

(a): Do=4, τ=12. r=0.68
(b): Do=3, τ =12. r=0.50
(c): D_O=8, τ =12. r=0.53
(d): D_O=6, τ=12. r=0.72
(e): D_O=7, τ=12. r=0.45
(f): D_O=9, τ=4. r=0.21

Figure 10: Temperature dependent β-factors with respect to sample date. BVOC compounds are shown slightly separated on the x-axis for clarity. Error bars indicate the 90% confidence interval. Symbols represent the following compounds: Total MT (solid white dot), α-pinene (blue cross), β-pinene (red triangle), 1,8-cineol (green square), 3-carene (green plus sign), camphene (orange dash), D-limonene (purple diamond), germacrene B (purple asterisk). Please note changes in scale.

Figure 11: Seasonal ER sensitivity analysis using measured data from the Bristlecone Pine. Ambient temperature measured from a nearby meteorological station in Boulder, CO is shown (top). Non-normalized emission rates were calculated using equation 4 for cases 1, 2, and 3 (middle). Emission rates were calculated for two weeks prior to and after each enclosure study. The difference (subtraction) between each case is shown (bottom).

Figure 12: Case 2 – Seasonal ER sensitivity analysis using constant β-factor reported for BP-b in combination with c) seasonal ε (shown in purple dots) or d) constant ε (shown in gold dots). Ambient air temperature is shown at the top. The difference of $ER_{\varepsilon,const}$ - $ER_{\varepsilon,seasonal}$ is shown at the bottom.

Figure 13: Aromatic recovery rate outlet::inlet for the five reference standard compounds. TIPB and NB are shown with basic curved lines to help illustrate the diurnal recovery rates. Ambient outdoor and enclosure temperatures are shown as solid lines.

Chapter 1 Introduction

1.1 Problem Statement

Biogenic volatile organic compounds (BVOC) are naturally emitted from most types of vegetation. Once released into the atmosphere, BVOC participate in reactive nitrogen, hydroxyl and ozone chemistry as well as secondary organic aerosol formation. Due to their reactive nature and resulting effects on atmospheric composition and air quality, a thorough understanding of BVOC emission behavior is critical for effective regional modeling and legislative decision-making. While BVOC emissions are generally reported in the literature as normalized basal emission rates based on short-term observations, several studies have called attention to the importance of accounting for seasonal emission variation. The focus of this thesis is an examination of the seasonal trends of BVOC emission rates. The emissions of several tree species native to Colorado forests were monitored over a 12-month period beginning February 2009 and ending February 2010. Emission rates of monoterpenes (MT) and sesquiterpenes (SQT) were quantified for over 1,300 enclosure samples providing a thorough examination into the seasonal behavior of BVOC.

1.2 Introduction

Vegetation naturally emit volatile organic compounds (VOC) into the atmosphere. These compounds, commonly referred to as biogenic volatile organic compounds (BVOC), include terpenoids such as isoprene, monoterpenes (MT) and sesquiterpenes (SQT), their oxygenated derivatives, as well as non-terpenoid compounds including methane, alkanes, alkenes, carbonyls, alcohols, esters, ethers and acids. Due to the high emission of terpenoids into the atmosphere and the importance of their reaction products within the lower troposphere, isoprene, MT and

SQT have attracted the attention of many atmospheric scientists. Once emitted, BVOC participate in reactive nitrogen and hydroxyl chemistry, alter ozone levels and play a key role in the formation and growth of secondary organic aerosols (SOA) (Chameides, et al., 1988, Fehsenfeld et al., 1992; Hoffmann et al., 1997). The capacity of BVOC to enhance O_3 and SOA are important not only to the composition of atmospheric trace gases and potential radiative forcing and climate change (Liao et al., 2007; Peñuelas and Staudt, 2009) but also to plant and human health (Rabl and Eyre, 1998; Dockery and Pope, 1994; Bell et al., 2004). Due to the highly reactive nature and resulting impacts on air quality, a thorough understanding of BVOC emission behavior is critical for effective regional modeling and legislative decision-making.

BVOC emission rates have been studied for well over two decades. Of the terpenoid compounds, isoprene is believed to be comparatively well understood (Arneth et al., 2008) while MT and SQT emissions have proven to be more difficult to characterize. Different species of vegetations have been shown to emit a varied array of MT and SQT compounds, each at a particular rate. Emission rates are known to vary with environmental conditions (temperature, light, relative humidity, soil type, etc.) (Tingey et al, 1980; Guenther et al., 1991; Staudt et al., 2000; Duhl et al., 2008; Rivoal et al., 2010), and can be altered by drought stress and herbivore infestation (Litvak and Monson, 1998; Grote et al., 2010; Joó et al., 2010). Accounting for each variable is complex and has proven difficult (Peñuelas and Llusiá, 2001; Grote and Niinemets, 2007; Arneth et al., 2008). While many recent studies have expressed the importance of considering an approach to estimating BVOC emissions based on vegetative enzymatic activity (Grote and Niinemets, 2007; Arneth et al., 2008; Grote et al., 2010), most emission rate data sets available to date report normalized basal emission rate calculated with respect to empirically observed light and temperature dependencies (described in section 2.3.4). Emission models such

as the Model of Emissions of Gases and Aerosols from Nature (MEGAN) use basal emission rate data for estimating regional and global terrestrial emissions (Guenther et al, 1993; Guenther et al,. 2006; Sakulyanontvittaya et al., 2008).

A growing number of studies have demonstrated that light and temperature normalized basal emission rates vary throughout a seasonal cycle (Llusia and Peñuelas, 2000; Staudt et al, 2000; Pio et al., 2005; Holzinger et al., 2006; Holzke el al., 2006; Hakola et al., 2009; Rivoal et al., 2010; Geron and Arnts, 2010). These findings have large implications with respect to both the magnitude as well as the timing of biogenic emissions. In an effort to improve biogenic emissions models such as MEGAN, seasonal emission characteristics of BVOC must be investigated.

1.3 Research Motivation

Seasonal variation in the emission of biogenic volatile organic compounds is poorly understood. Most BVOC emission rate data available to date report short-term studies of emissions with respect to light and temperature conditions. It is the goal of this study to bridge the gap between short-term emission data sets and long-term seasonal variation. This study investigates seasonal emission characteristics of monoterpene and sesquiterpene compounds with respect to light and temperature dependence over a one-year period. Findings will be suggested for use in biogenic emissions models such as MEGAN (Guenther et al., 2006) to account for seasonal emission variability unexplained by short-term emission rate data.

1.5 Thesis Organization

This thesis is divided into two chapters. Chapter 2 contains the contents of a research manuscript to be submitted to Chemosphere detailing the seasonal variation in BVOC emission. Submission to the publisher is to occur within four weeks of the due date to the University of Colorado. Related projects are included in the appendix with the goal of providing insight and lessons learned that may be useful for future biogenic emission projects.

Chapter 2

An Investigation into Seasonal Trends of Terpene Emissions

Ryan Woodfin Daly[1,2], Detlev Helmig[1,*], Alex Guenther[3], Jana Milford[2]

[1]Institute of Arctic and Alpine Research (INSTAAR), University of Colorado, Boulder CO 80309, USA
[2]Department of Mechanical Engineering, University of Colorado, Boulder CO 80309, USA
[3]National Center for Atmospheric Research (NCAR), Boulder CO 80307, USA

[*]Author to whom correspondence should be addressed:
Detlev.Helmig@colorado.EDU, phone: (303) 492-2509, fax: (303) 492-6388

Manuscript to be submitted to Chemosphere

2.1 Abstract

Biogenic volatile organic compound (BVOC) emissions were monitored from six tree species representative of Colorado forests for one complete seasonal cycle. The result is a comprehensive data set comprised of more than 1300 samples describing seasonal emissions with respect to observed light and temperature conditions. Studied vegetation include four coniferous tree species: *Pinus ponderosa*, *Picea pungens*, *Pseudotsuga menziesii* and *Pinus longaeva*, as well as two deciduous species: *Quercus gambelii* and *Betula occidentalis*. Monoterpene (MT) and sesquiterpene (SQT) emission rates were quantified using the branch enclosure method in combination with solid adsorbent cartridge sampling with subsequent analysis by thermal desorption, gas chromatography-mass spectrometry. MT dominated coniferous emissions, producing greater than 95% of the emission signal. MT demonstrated strong short-term correlation predominantly with temperature exposure. Basal emission rates were found to vary in magnitude of the studied period. Spring and summer emissions of the

coniferous species were found to be up to five times greater than in winter months, where total MT rates were found to be 1-3 $\mu g\ g^{-1}\ hr^{-1}$, falling to below 0.5 $\mu g\ g^{-1}\ hr^{-1}$in fall and winter. The percent contribution of a compound's emission signal to the total emission rate was also found to vary with season. The MT compounds 3-carene, 1,8-cineol and piperitone varied the greatest with respect to the total emission signal, between 0 – 60% in some cases. Very low levels of SQT were measured from the coniferous tree species. High rates of 0.8 $\mu g\ g^{-1}\ hr^{-1}$ of the SQT germacrene B were found emitted from *Q. gambelii*. Seasonal basal emission rate correction factors reported in the literature were applied to the measured data reported in this study. Predicted versus observed emission rates were found with mixed results. The β-factor used to describe temperature dependent emissions did not exhibit discernable trends over the studied period. The inherent seasonal variation in biogenic emissions cannot be well characterized solely by empirical light and temperature descriptors. Emission models based on basal emission rate data determined from short-term studies during summer seasons do not accurately account for the timing and magnitude of actual BVOC emissions across a season's period.

2.2 Introduction

Most types of vegetation emit an array of biogenic volatile organic compounds (BVOC) including isoprene, monoterpenes (MT), sesquiterpenes (SQT), their oxygenated derivatives as well as non-terpenoid compounds (Fuentes et al., 2000). BVOC have garnered the interest of the atmospheric chemistry community due to the importance of their reaction products within the lower troposphere. Once released into the atmosphere, BVOC participate in reactive nitrogen and hydroxyl chemistry, alter ozone levels and play a key role in the formation and growth of secondary organic aerosols (SOA) (Fehsenfeld et al., 1992; Hoffmann et al., 1997). The capacity of BVOC to enhance O_3 and SOA are important not only to atmospheric composition and

radiative forcing (Liao et al., 2007; Peñuelas and Staudt, 2009) but also to plant and human health (Rabl and Eyre, 1998; Dockery and Pope, 1994; Bell et al., 2004). Due to the highly reactive nature and resulting impacts on air quality, a thorough understanding of BVOC emission behavior is critical for effective regional modeling and legislative decision-making.

Recent studies have highlighted uncertainty in the ability to describe and model biogenic emission rates over a seasonal cycle. Emission rates are most commonly expressed using empirical light and temperature dependent algorithms. Once normalized to standard light and temperature conditions (1000 μmol m^{-2} s^{-1} and 30^{o}C, respectively), biogenic emissions and their reactant products are predicted using atmospheric emission models. Despite light and temperature normalization, BVOC emissions have been found to vary with growth season. Generally speaking emission rates have been found to be greatest between late spring and early fall. The relative ratio between normalized maximum and minimum normalized basal emission rates reported in the literature varies greatly from 0–10 (Kuhn et al., 2004; Hakola et al., 2006; Holzinger et al., 2006; Holzke et al., 2006; Lim et al., 2008; Keenan et al., 2009; Geron and Arnts, 2010) and 45-100+ (Staudt et al., 2000; Pio et al., 2005; Rivoal et al., 2010) for a given study. Several studies have also noted that individual BVOC compounds are emitted at different rates throughout the season with respect to other emissions from the same plant (Llusiá and Peñuelas, 2000; Hakola et al., 2001; Holke et al., 2006; Lim et al., 2008; Geron and Arnts, 2010; Rivoal et al., 2010).

This study further investigates BVOC emission patterns utilizing light and temperature based data sets, accounting for seasonal variation. MT and SQT emissions of four coniferous and two deciduous species native to Colorado forests were monitored monthly over the course of one year. Changes in basal emission rate magnitude, emission speciation by compound and the

empirical temperature dependent parameter β are investigated for seasonal variation. Additionally, the application of a seasonal emission correction factor proposed by Staudt et al. (2000) and Keenan et al. (2009) is investigated using the dataset gathered in this study.

2.3 Methods

This study was conducted over the course of one complete seasonal cycle between February 2009 and February 2010 at a field site located in Boulder, CO. BVOC emissions of four coniferous and two deciduous tree species native to Colorado forests were monitored using bag enclosure experiments with adsorbent cartridge sampling with subsequent analysis by gas chromatography and mass spectroscopy. Emissions rates were normalized to basal light and temperature parameters and a seasonal correction factor was calculated. These methods are described in the following sections.

2.3.1 Measurement site and sample vegetation

A field site was established at Creekside Tree Nursery located in Boulder, CO ($40^{o}2$'N. $105^{o}12$'W). An enclosed trailer housing all equipment was located within the nursery and surrounded by sample vegetation placed in a semi-circle pattern along the southern side of the trailer. All trees received full sun until mid afternoon, approximately 5:00 pm local time, during summer months due to a mature cottonwood that shaded the area in the afternoon. The six tree species were selected based on abundance in Colorado, their ability to grow at Boulder's altitude and weather conditions as well as ordering accessibility. All tree species were installed within their planting pots and packed with mulch. Each tree specimen was allowed one month to adjust to its surroundings before sampling commenced.

The following is a list of the studied tree species including the scientific name and common name used here in parentheses. Coniferous species include two *Pinus ponderosa* (Ponderosa Pine A & B), *Picea pungens* (Blue Spruce), *Pseudotsuga menziesii* (Rocky Mountain Douglas-fir) and *Pinus longaeva* (Bristlecone Pine). These tree specimens ranged from 4 to 6 years of age. Deciduous species were a 6-year-old *Quercus gambelii* (Gamble Oak) and a 7-year-old *Betula occidentalis* (Western River Birch).

2.3.2 Experimental Methods

Methods and equipment used for this study followed recommendations by Ortega and Helmig (2008) and will be described briefly here. Terpenoid emissions were monitored using the branch enclosure technique. Figure 1 shows the experimental setup in detail. Each tree specimen was sampled monthly. Enclosures were allowed 24 hours to equilibrate on the sample limb before sampling commenced. Using the methods described below, 10 to 20 samples were collected over a two to three day period before the enclosure was moved to the next tree specimen.

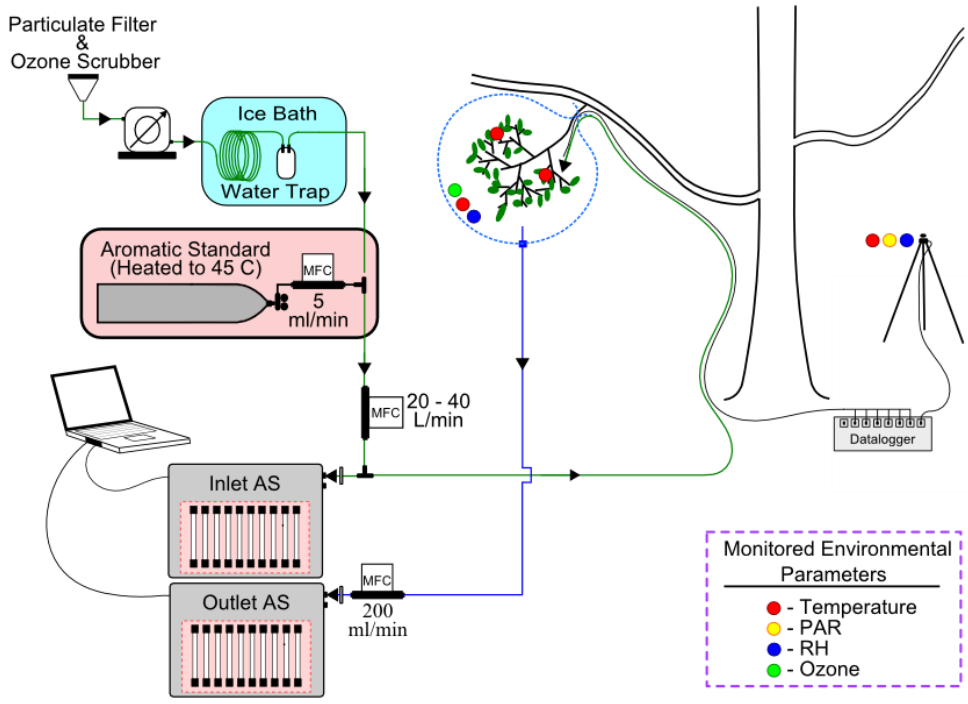

Figure 1: Schematic of the experimental setup.

For each tree, a limb was enclosed by a tedlar bag (Jensen Inert Products, Coral Springs, FL) that was cinched at the base of the limb by an exterior bungee cord, enclosing between 30L to 60L depending on size of the sample limb. Air leading to the enclosure, termed here as the enclosure purge air, was supplied by a high capacity (55 L min^{-1}) oil-free pump (Medo Corporation, Hanover Park, IL) and first scrubbed of VOC and particulates using a combination of an organic vapor and particulate respirator filter cartridge (Mersorb Part no. 463532; Mine Safety Appliances Company, Pittsburgh, PA) and charcoal scrubber (Fisher, 05-685A, 6-14 mesh). The purge air was then scrubbed free of ozone using a customized commercial scrubber composed of 40 MnO_2-coated copper screens (O.B.E. Corp. Fredericksburg, TX) and dried using a condensing water trap submerged in an ice bath (3/8" copper tubing, 1m length). Ozone was periodically monitored from the enclosure to ensure the purge air was free of any ozone (Monitor Labs 8810, Teledyne Technologies Inc., Englewood, CO). The purge air was delivered through

3/8" Teflon tubing at a mass flow controlled (MFC) flow rate varying between 20 L min^{-1} to 40 L min^{-1} dependent upon season. High purge rates of 35 L min^{-1} were used during the hotter summer season to reduce greenhouse heating within the enclosure while lower flow rates of 20 L min^{-1} were used during the winter season to maximize BVOC sensitivity. A reference gas standard composed of five aromatic compounds of similar volatility and molecular weight to MT and SQT was added to the purge flow at a rate of 5 ml min^{-1} for analyte recovery analysis and chromatography integration assistance. A 1/8" Teflon sample line extended from the branch enclosure to an automated adsorbent cartridge sampler (Helmig et al., 2004). A flow rate of 800 ml min^{-1} was pulled from the enclosure, of which 200 ml min^{-1} was directed to the sampler. Sample volumes varied between 12L and 24L dependent on season and time of day to produce a detectible signal.

To ensure consistency in emission sampling, one limb was selected per tree specimen for repeated monthly measurements throughout the study period. Monthly biomass dry weight measurements were taken to monitor the growth of each branch. Dry weight estimations were made by measuring the length of each branch per sample limb (to ¼" accuracy) noting the size and age of the leaf or needle (new growth, 1^{st} year, 2^{nd} year if applicable). Similarly sized leaves or needles were collected from nearby trees of the same species, which were dried (55 ^{o}C for 2 days) and weighed. Leaves and needles were not collected from the sample trees to reduce risk of shocking the plant, which might adversely affect emissions. Each sample limb was cut at the end of the sampling season for final dry-weight measurements. Using the monthly branch length and needle dry weight estimates described above, total dry-weight was estimated (Figure 2) throughout the study period and applied to the emission rate calculations described in section 2.3.3.

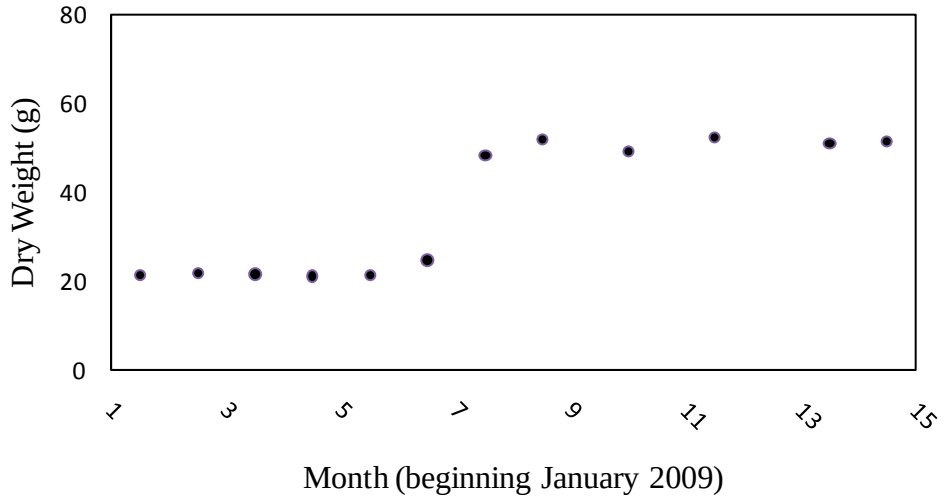

Figure 2: Estimated biomass dry-weight of Ponderosa Pine A over the study period.

Several environmental parameters were monitored during each sample period. Temperature was monitored both outdoor and within the enclosure using type K thermocouples (TC) (Omega Engineering). Within the enclosure, one TC measured the ambient temperature while two more were taped to a leaf or group of needles to monitor the vegetation temperature (usually slightly higher than ambient). Photosynthetically active radiation (PAR) was monitored at a central location with the surrounding vegetation. Relative humidity (Campbell Scientific) and ozone (Monitor Labs) were monitored outdoors and within the enclosure for quality control purposes. All data were logged onto a Campbell Scientific CX10 datalogger.

BVOC emissions were collected onto adsorbent cartridges made in house, discussed in detail in Appendix A. Briefly, ¼" glass tubes were packed with 0.126 g Tenax GR and 0.145 g Carboxen 1016 solid adsorbent (Sigma-Aldrich). Once collected, samples were stored in a freezer until analyzed by thermodesorption (Perkin-Elmer ATD400) and GC-FID/MS (Hewlet-Packard 5890/5970) using methods similar to those described by Helmig et al. (2004). Following GC-FID/MS analysis, each sample was manually integrated for MT, oxy-MT and

SQT. Compounds were identified using a combination of retention index (RI) and mass spectra comparison. RI were calculated for each compound with respect to the elution retention time of the GC and compared to the RI reported by Adams (1989). MS scans were compared to the National Institute of Standards and Technology (NIST) mass spectral database (NIST MS Search 2.0) if further identification assistance was needed.

2.3.3 Observed Emission Rate (ER) Calculation

Emission rates were determined in the following manner. BVOC mixing ratio (ppbV) were calculated according to equation 1.

$$MR_{[ppbV]} = \frac{A}{V \cdot ER} \cdot \frac{N}{ECN} \quad (1)$$

where PA is the integration peak area, V is the volume sampled, RF is the normalized per unit carbon calibrated GC-FID response factor, N is the number of carbons and ECN is the effective carbon number per compound. An emission rate in terms of μg ml^{-1} was then computed (equation 2) taking into consideration molecular weight (MW) of the compound and accounting for standard temperature and pressure of the sample volume.

$$ER_{[\mu g \cdot ml^{-1}]} = \frac{MR}{1 \cdot 10^{9}} \cdot \frac{P}{R \cdot T} \cdot MW \quad (2)$$

Finally, the observed emission rate (ER) in units of μg $g_{dry\ weight}^{-1}$ hr^{-1} is realized after taking into consideration the diluting purge flow rate (D) feeding the enclosure and dry weight (DW) of the enclosed biomass (equation 3).

$$ER_{[\mu g \cdot g^{-1} \cdot hr^{-1}]} = ER_{[\mu g \cdot ml^{-1}]} \cdot \frac{D}{DW} \quad (3)$$

2.3.4 Basal Emission Rate (ε)

BVOC emission rate data is most commonly reported in the literature as a normalized basal emission rate, denoted as ε henceforth. ε is the observed ER normalized to standard levels of temperature and light during the measurement period. ER that are observed to be dependent soley on temperature may be described by equation 4 (Tingey et al., 1980).

$$\varepsilon_{[T]} = \varepsilon \cdot e^{[\beta \cdot (T - T_S)]} \quad (4)$$

$\varepsilon_{[T]}$ is the observed ER at a given temperature and ε is the normalized emission rate at the basal temperature T_S (generally 30°C). β refers to the slope of the exponential regression of $\varepsilon_{[T]}$ and the sample temperature T. Compounds that demonstrated light and temperature dependant ER may be described by equations 5 - 7 (Guenther, 1997).

$$\varepsilon_{[L,T]} = \varepsilon \cdot C_L \cdot C_T \quad (5)$$

$$C_L = \frac{\alpha \cdot C_{L1} \cdot PAR}{\sqrt{1 + \alpha^2 \cdot PAR^2}} \quad (6)$$

$$C_T = \frac{e^{\frac{C_{T2}(T - T_S)}{R \cdot T_S \cdot T}}}{0.961 + e^{\frac{C_{T2}(T - T_M)}{R \cdot T_M \cdot T}}} \quad (7)$$

$\varepsilon_{[L,T]}$ is the observed ER at a given light and temperature condition, ε is the normalized basal emission (30°C and 1000 μmol s^{-1} m^{-2}). C_L and C_T are light and temperature correction factors, respectively. C_{L1} (1.066), C_{T1} (95000 J mol^{-1}), C_{T2} (230000 J mol^{-1}) and T_M (314 K or 41 °C), α (0.0027) are empirically defined parameters (Guenther et al., 1993). R (8.314 J K^{-1} mol^{-1}) is the ideal gas constant and T_S (303 K or 30 °C) is the standard basal temperature. T and PAR are the measured temperature and light for a given sample, respectively. Figure 3 displays the corrective

effect of normalizing a measured emission to a basal emission rate. Basal emission rates were calculated on a compound-by-compound basis utilizing equation 4 or 5 based on whether they displayed temperature-only or temperature-and-light dependent emissions, respectively.

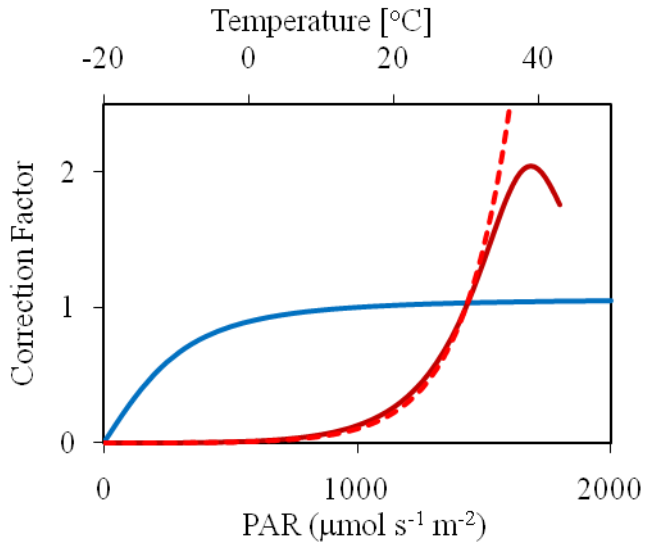

Figure 3: Normalizing light and temperature correction factors $exp^{\beta*T}$ (dark red, solid), C_T (light red, dashed) and C_L (blue) for calculating a basal emission rate, ε.

2.3.5 Seasonal Correction Factor C_S

Few studies to date have examined the application of an additional correction factor to compensate for seasonal emission changes. Staudt et al. (2000) proposed the addition of a seasonal correction factor, C_S, building on the standard basal emission rate equation described in section 2.3.3, described by equations 8 and 9.

$$\varepsilon_{[Season]} = \varepsilon \cdot C_L \cdot C_T \cdot C_S \quad (8)$$

$$C_S = 1 - \rho \cdot \left[1 - e^{\frac{(D-D_0)^2}{\tau}}\right] \quad (9)$$

ρ describes the emission amplitude (ε_{max} - ε_{min}) / ε_{max} over the growing season, D is the month of year, D_O is the month in which highest emissions are observed and τ is the length of the active-emitting season in months. Steinbrecher et al. (2009) used the correction factor C_S to model the annual variation of VOC emissions from vegetation across Europe. Keenan et al. (2009) applied an asymmetric exponential function similar to equation 9 to measure seasonal variation in basal emission rates. Other studies have developed study specific algorithms to describe seasonal variation (Pio et al., 2005; Holzinger et al., 2006).

In the present work, a simple modification $C_{S,mod}$ described by equation 10 is made to the originally published seasonal correction factor reported by Staudt et al. (2000) (equation 9).

$$C_{S,mod} = 1 - \rho \cdot \left[1 - e^{\frac{(\|\|D-D_O\|-6\|-6)^2}{\tau}}\right] \quad (10)$$

The original correction factor C_S works for cases in which the month with maximum emissions are during peak summer months, however fails to produce a seasonally repeating curve for a case where $D_O < 6$ or $D_O > 7$. Figure 4 depicts the difference between C_S used here and $C_{S,mod}$. As is evident, $C_{S,mod}$ produces a seasonally repeating curve regardless of the month of year defined with the maximum emission rate.

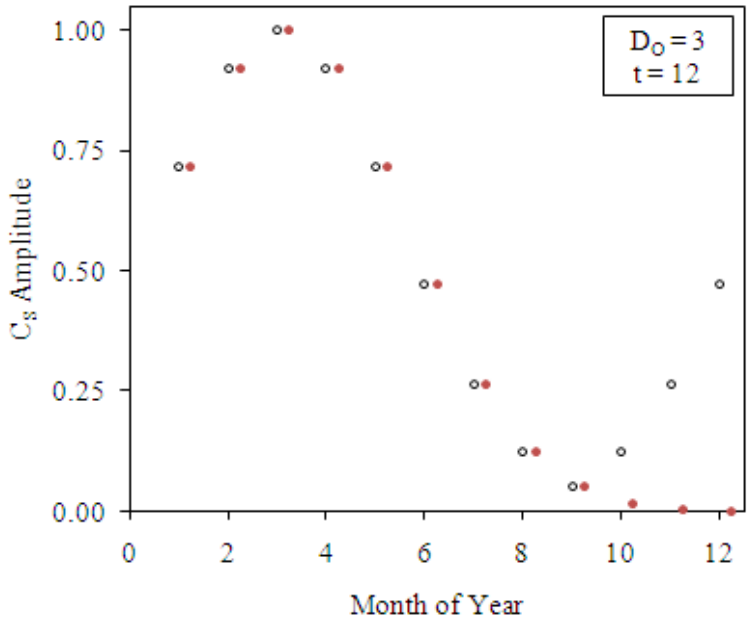

Figure 4. A modified seasonal correction factor $C_{S,mod}$ (open dots) used here is compared to the correction factor C_S (closed red dots) proposed by Staudt et al. (2000).

2.4 Results and Discussion

2.4.1 Emission Summary

Of more than 2000 cartridge samples that were collected during the twelve month study period, many of which were used for equipment calibration and testing, over 1300 were analyzed for BVOC and are reported here. Within this timeframe, emissions were monitored in a variety of weather conditions from winter temperature lows of -20°C to summer highs in excess of 35°C as well as full sun, rain, snow and high winds events. A summary of the collected data may be viewed in Tables 1 and 2.

Table 1 summarizes normalized basal emission rates ε for each enclosure experiment in order of date sampled. The table includes the number of cartridge samples contributing to the calculated ε, number of BVOC compounds observed, temperature range, temperature dependent β-factor and corresponding R^2 exponential regression statistic of MT and SQT emissions for

each plant. Total compound categories (total MT and SQT) refer to the sum of individual compound emissions. It should be noted that oxy-MT are included in total MT emissions reported henceforth. All coniferous species demonstrated strong MT emissions while SQT were found near or below the detection limit. As a result, SQT basal emission rates were often not calculated. Rather, the ratio of observed SQT to MT ER are listed along with the temperature and light radiation at which the emission occurred.

Emissions are further summarized in Table 2 with regard to seasonally averaged emissions and compound speciation. Basal emission rates were averaged quarterly over the study period to provide a seasonal snapshot. The sample period was divided into quarters defined as: Winter ’09 (February ’09), Spring ’09 (March, April and May ’09), Summer ’09, (June, July and August ’09), Fall ’09 (September, October and November ’09) and Winter ’10 (December ’09, January and February ’10). Table 2 reports the observed MT speciation and quarterly averaged basal emission rates ε.

Table 1: Summary of enclosure study data for each sample tree, listed by sample date.

Sample Dates	Total # of samples analyzed	Number of samples BVOC identified		Number of compounds per BVOC class		Temperature range		Total MT ε	Total MT β (MT)		Total SQT ε	Total SQT β (SQT)		Fraction of observed SQT :: MT at (temperature (°C) / PAR (μmol m^{-2} s^{-1}))	
		MT	SQT	MT	SQT	T_{min}	T_{max}	(μg g^{-1} hr^{-1})	(°C^{-1})	R^2	(μg g^{-1} hr^{-1})	(°C^{-1})	R^2		
Ponderosa Pine A															
Feb 27-28, '09	6	6	4	7	3	-8	19	3.15	0.10	0.83	-			0.04	(20 / 1000)
Mar 16-18, '09	12	12	2	7	6	5	32	3.41	0.11	0.91	-			0.04	(27 / 350)
Apr 6-8, '09	20	20	4	8	2	-1	30	6.03	0.11	0.10	0.07	0.03	0.13	0.01	(30 / 1600)
Apr 25-26, '09	10	10	-	7	-	8	11	2.58	0.11	0.19	-			-	
Jun 9-10, '09	10	10	3	7	1	9	27	3.11	0.10	0.94	-			0.01	(27 / 700)
Jun 20-21, '09	10	10	3	7	1	13	24	1.71	0.14	0.64	-			0.03	-
July 11-12, '09	10	10	4	7	3	18	36	1.14	0.10	0.62	-			0.02	-
Aug 8-9, '09	10	10	-	7	-	17	35	1.10	0.13	0.78	-			-	
Aug 19-21, '09	18	18	4	8	1	11	31	1.96	0.13	0.79	-			0.01	(31 / 1650)
Sept 16-17, '09	16	16	1	8	1	10	24	2.00	0.11	0.79	-			0.01	(24 / 350)
Oct 16-17, '09	8	8	3	8	2	0	32	1.19	0.08	0.84	-			0.02	(31 / 1050)
Oct 30-31, '09	9	9	4	8	1	-7	24	1.92	0.14	0.71	-			<.01	(20 / 1000)
Nov 6-10, '09	20	20	10	8	1	0	31	1.38	0.13	0.94	0.01	0.08	0.69	0.01	(31 / 1050)
Dec 21-24, '09	20	20	3	8	1	-4	21	0.70	0.10	0.71	-			0.01	(21 / 600)
Jan 11-13, '10	16	16	3	7	1	-6	27	2.01	0.13	0.92	-			0.01	(23 / 850)
Feb 6-10, '10	20	20	2	7	1	-13	12	1.96	0.12	0.95	-			0.01	(12 / 1150)
Ponderosa Pine B															
Feb 20-22, '09	19	19	4	7	1	-9	19	2.38	0.14	0.94	0.10	0.15	0.77	0.04	(19 / 900)
Mar 6-8, '09	9	9	-	7	-	2	15	4.59	0.18	0.93	-			-	
Apr 15-16, '09	5	5	1	7	1	6	26	2.32	0.15	0.94	-			0.02	(26 / 650)
May 27-28, '09	6	6	5	7	1	9	26	1.84	0.09	0.81	0.03	0.09	0.54	0.03	(25 / 1000)
Jun 29-30, '09	8	8	3	7	1	18	35	1.84	0.15	0.83	-			0.01	
Aug 21-24, '09	17	17	3	7	1	11	35	1.14	0.08	0.76	-			0.01	(35 / 1500)
Sept 15-17, '09	26	26	-	7	-	12	35	1.02	0.11	0.83	-			-	
Oct 16-20, '09	20	20	7	7	1	0	30	0.75	0.11	0.81	0.03	0.11	0.74	0.03	(29 / 1200)
Nov 12-14, '09	20	20	3	7	1	2	33	0.41	0.08	0.91	-			0.03	(33 / 1000)
Feb 6-10, '10	20	18	-	7	-	-13	12	0.28	0.11	0.68	-			-	

Table 1: Continued

Sample Dates	Total # of samples analyzed	Number of samples BVOC identified		Number of compounds per BVOC class		Temperature range		Total MT ε	β (MT)		Total SQT ε	β (SQT)		Fraction of observed SQT :: MT at (temperature (^{o}C) / PAR (μmol m^{-2} s^{-1}))	
		MT	SQT	MT	SQT	T_{min}	T_{max}	(μg g^{-1} hr^{-1})	(^{o}C^{-1})	R^2	(μg g^{-1} hr^{-1})	(^{o}C^{-1})	R^2		
Bristlecone Pine															
Feb 23-25, '09	17	17	3	12	1	2	31	7.41	0.23	0.88	-			< 0.01	(28 / 800)
Apr 22-24, '09	10	10	-	12	-	6	37	0.62	0.09	0.90	-			-	
May 9-10 , '09	10	10	-	12	-	11	26	0.34	0.09	0.78	-			-	
Jun 6-7, '09	10	10	-	12	-	10	26	0.74	0.12	0.53	-			-	
Jun 18-19, '09	10	10	-	12	-	10	26	0.59	0.13	0.89	-			-	
Jun 27-28, '09	10	10	-	12	-	15	36	0.16	0.07	0.54	-			-	
Jul 7-8, '09	6	6	5	13	1	14	28	1.51	0.13	0.83	0.01	0.07	0.61	0.01	(28 / 1450)
Jul 16-17, '09	10	10	2	13	1	20	39	0.77	0.11	0.71	-			< 0.01	(37 / -)
Aug 19-21, '09	17	17	-	10	-	11	31	1.15	0.08	0.56	-			-	
Aug 26-27, '09	11	11	5	13	1	11	40	1.46	0.07	0.72	0.07	0.10	0.81	< 0.01	(40 / 1600)
Sept 29-30, '09	10	10	2	13	1	10	39	0.84	0.15	0.98	-			< 0.01	(39 / 1200)
Oct 30-31, '09	10	10	-	12	-	-7	21	1.03	0.16	0.97	-			-	
Nov 6-10, '09	10	10	3	12	1	9	33	0.28	0.12	0.94	-			0.01	(32 / 1000)
Nov 17-19, '09	8	8	2	12	1	-1	24	0.11	0.06	0.35	-			0.02	(24 / 900)
Dec 15-15, '09	10	8	-	10	-	-5	17	0.25	0.10	0.88	-			-	
Jan 28-30, '10	20	16	-	11	-	-6	18	0.64	0.12	0.92	-			-	
Feb 2-4, '10	17	16	-	10	-	-5	21	0.42	0.12	0.93	-			-	
Feb 16-17, '10	10	10	-	9	-	-10	18	0.22	0.08	0.82	-			-	

Table 1: Continued

Sample Dates	Total # of samples analyzed	Number of samples BVOC identified		Number of compounds per BVOC class		Temperature range		Total MT ε	β (MT)		Total SQT ε	β (SQT)		Fraction of observed SQT :: MT at (temperature (°C) / PAR (μmol m^{-2} s^{-1}))	
		MT	SQT	MT	SQT	T_{min}	T_{max}	(μg g^{-1} hr^{-1})	($°C^{-1}$)	R^2	(μg g^{-1} hr^{-1})	($°C^{-1}$)	R^2		
Blue Spruce															
Feb 16-18, '09	20	18	-	7	-	0	29	0.76	0.15	0.77	-			-	
Feb 25-27, '09	19	17	-	7	-	-3	36	0.44	0.09	0.75	-			-	
Mar 4-6, '09	19	16	-	8	-	0	34	0.55	0.13	0.88	-			-	
Mar 25-26, '09	8	8	-	7	-	2	9	3.48	0.10	0.44	-			-	
Apr 17-19, '09	19	4	-	4	-	3	12	< 0.10	-		-			-	
May 7-8, '09	9	9	-	9	-	11	36	0.96	0.11	0.88	-			-	
May 29-30, '09	10	10	-	9	-	9	36	0.87	0.11	0.76	-			-	
Jul 2-3, '09	10	10	5	8	1	14	31	1.45	0.12	0.89	0.01	0.12	0.81	0.01	(31 / -)
Aug 11-12, '09	16	16	-	7	-	11	45	0.75	0.05	0.64	-			-	
Aug 21-24, '09	15	15	-	7	-	12	34	0.66	0.15	0.86	-			-	
Sept 12-13, '09	5	5	-	7	-	14	26	0.19	0.02	0.45	-			-	
Nov 11-14, '09	20	19	-	9	-	2	31	0.46	0.13	0.93	-			-	
Dec 3-5, '09	10	10	-	6	-	-17	7	0.16	0.06	0.83	-			-	
Jan 17-20, '10	17	17	-	8	-	-4	17	0.24	0.08	0.85	-			-	
Feb 11-13, '10	20	20	-	-	-	-8	25	0.38	0.07	0.64	-			-	
Douglas-fir															
Apr 20-22, '09	18	18	-	9	-	6	39	0.52	0.08	0.93	-			-	
May 12-13, '09	10	10	-	9	-	10	43	0.33	0.10	0.91	-			-	
May 19-20, '09	9	9	-	9	-	15	44	0.47	0.09	0.94	-			-	
Jun 13-14, '09	4	4	-	7	-	11	29	2.51	0.08	0.79	-			-	
Jun 25-26, '09	10	10	-	9	-	18	33	0.80	0.08	0.54	-			-	
Jul 8-9, '09	5	5	-	8	-	13	26	1.03	0.13	0.77	-			-	
Jul 14-15, '09	9	9	-	9	-	14	37	0.68	0.12	0.70	-			-	
Aug 11-14, '09	18	18	-	9	-	11	45	0.67	0.06	0.69	-			-	
Aug 24-25, '09	18	18	-	4	-	12	35	0.09	0.04	0.10	-			-	
Sept 15-18, '09	30	28	-	4	-	12	35	0.12	0.05	0.44	-			-	
Oct 22-24, '09	10	10	-	5	-	3	24	0.26	0.08	0.94	-			-	
Nov 17-20, '09	20	20	-	6	-	-3	28	0.18	0.06	0.85	-			-	
Dec 10-13, '09	20	11	-	6	-	-16	24	0.79	0.12	0.87	-			-	
Jan 22-26, '10	29	26	-	5	-	-7	30	0.16	0.07	0.60	-			-	
Feb 11-14, '10	19	19	-	6	-	-8	27	0.37	0.08	0.96	-			-	

Table 1: Continued

Sample Dates	Total # of samples analyzed	Number of samples BVOC identified		Number of compounds per BVOC class		Temperature range		Total MT			Total SQT			Fraction of observed SQT :: MT at (temperature (^{o}C) / PAR (μmol m^{-2} s^{-1}))
		MT	SQT	MT	SQT	T_{min}	T_{max}	ε (μg g^{-1} hr^{-1})	β (MT) (^{o}C^{-1})	R^2	ε (μg g^{-1} hr^{-1})	β (SQT) (^{o}C^{-1})	R^2	
Gamble Oak														
July 2-3, '09	10	-	5	-	1	14	28	-			0.35	0.19	0.81	-
Aug 15-16, '09	10	-	6	-	1	15	25	-			0.33	0.14	0.31	-
Aug 26-27, '09	14	-	9	-	1	11	37	-			0.45	0.14	0.69	-
Sept 23-24, '09	12	-	-	-	-	9	15	-			-			-
Sept 25-26, '09	10	-	3	-	1	7	25	-			1.17	0.26	1.00	-
Sept 27-29, '09	20	-	9	-	1	4	25	-			0.78	0.18	0.75	-
Oct 7-9, '09	17	-	9	-	1	4	31	-			0.07	0.09	0.84	-
Oct 13-16, '09	19	-	9	-	1	4	33	-			0.01	0.05	0.70	-
Western River Birch														
Aug 14 - Oct 15, '09	107	-	-	-	-			-			-			-

The Ponderosa Pines were observed to be the highest emitter with total MT ε upwards of 4 μg g^{-1} hr^{-1}. The emission was dominated by α and β-pinene. Combined, they contributed to 60-80% of the total emission. The oxygenated MT 1,8-cineol was the third most abundant emitted compound, found to make up 30% of the total MT emissions between late spring and summer periods. Both Ponderosa Pine A and B demonstrated similar emission patterns with highest basal emission rates found in the spring of 2009, which gradually tapered off throughout the remainder of the study period. Lowest basal emission rates were detected at levels below 0.50 μg g^{-1} hr^{-1} through the winter months. The Ponderosa pines were the only coniferous trees found to emit quantifiable levels of SQT. Six SQT were detected. Three SQT were indentified, including β-bourbonene, β-caryophyllene and γ-muurolene. β-caryophyllene accounted for 80% of the SQT emission. Similar to MT emissions, SQT demonstrate highest basal emission rates in the spring. Basal SQT emission rates were found to range between 0.01-0.10 μg g^{-1} hr^{-1}.

The Bristlecone Pine and Blue Spruce demonstrated highest normalized emission rates during the summer period. MT ε were found to exceed 1.5 μg g^{-1} hr^{-1}. Emissions were found at lower levels in both spring and fall, with normalized seasonal lows of less than 0.2 μg g^{-1} hr^{-1} in winter months. 3-carene was the most significant emission from the Bristlecone Pine, contributing to 40-60% of the total MT emission. α-pinene and D-limonene were observed to be the most significantly emitted compounds from Blue Spruce samples, however chemical speciation appears to become more dynamic through the summer months. Low levels of SQT were found in a limited number of enclosure experiments for both vegetation species. β-caryophyllene and the saturated SQT farnesane were observed from Blue Spruce samples while α-copaene was the only quantifiable SQT observed from the Bristlecone Pine. Basal

Table 2: Seasonally averaged emission rates reported with respect to speciation (%) and basal emission rate (ε). Seasons are defined by month listed in brackets (i.e. 'Summer [JJA]' represents averaged data between June, July and August).

	Winter '09 [F]		Spring '09 [MAM]		Summer '09 [JJA]		Fall '09 [SON]		Winter '10 [DJF]	
		ε		ε		ε		ε		ε
Compound Name	%	($\mu g\ g^{-1}\ hr^{-1}$)	%	($\mu g\ g^{-1}\ hr^{-1}$)	%	($\mu g\ g^{-1}\ hr^{-1}$)	%	($\mu g\ g^{-1}\ hr^{-1}$)	%	($\mu g\ g^{-1}\ hr^{-1}$)
Ponderosa Pine A										
α-pinene	56	1.60	49	2.05	46	0.96	42	0.48	63	1.01
camphene	4	0.10	5	0.10	3	0.05	4	0.04	4	0.03
β-pinene	23	0.54	26	0.99	20	0.33	18	0.26	20	0.36
mycrene	3	0.10	4	0.07	5	0.09	3	0.05	3	0.03
1,8-cineol	3	0.06	5	0.55	9	0.21	5	0.12	3	0.04
D-limonene	7	0.15	8	0.20	15	0.19	10	0.19	7	0.07
piperitone	2	< 0.01	1	0.51	1	0.37	17	0.68	-	-
Total MT		*3.15*		*4.01*		*1.82*		*1.62*		*1.56*
Ponderosa Pine B										
α-pinene	50	1.04	33	0.75	29	0.36	43	0.29	53	0.19
camphene	4	0.04	4	0.04	3	0.03	4	0.02	5	0.00
β-pinene	32	0.86	30	1.13	30	0.42	31	0.21	30	0.07
mycrene	3	0.03	8	0.19	10	0.13	5	0.04	2	0.01
1,8-cineol	3	0.04	15	0.27	21	0.33	10	0.09	1	0.00
D-limonene	6	0.05	8	0.06	5	0.08	6	0.04	7	0.01
piperitone	-	-	-	-	-	-	-	-	-	-
Total MT		*2.38*		*2.92*		*1.49*		*0.73*		*0.28*
Bristlecone Pine										
α-pinene	9	0.77	11	0.07	15	0.21	10	0.05	12	0.03
camphene	1	0.10	4	0.02	3	0.03	2	0.01	2	0.00
β-pinene	10	0.54	9	0.05	10	0.12	12	0.06	14	0.04
β-myrcene	3	0.21	5	0.03	7	0.07	3	0.01	3	0.01
3-carene	59	3.86	41	0.24	46	0.58	55	0.33	49	0.19
o-cymene	2	0.15	3	0.01	2	0.02	2	0.01	-	-
p-cymene	4	0.26	7	0.04	5	0.06	7	0.04	6	0.04
β-phellandrene	7	0.37	6	0.03	6	0.08	5	0.03	6	0.03
D-limonene	4	0.22	13	0.02	5	0.06	5	0.02	7	0.01
Total MT		*7.41*		*0.48*		*0.98*		*0.69*		*0.40*
Blue Spruce										
α-pinene	51	0.28	47	0.74	28	0.45	25	0.20	27	0.05
camphene	8	0.03	6	0.04	9	0.05	17	0.04	20	0.05
β-pinene	8	0.04	12	0.41	10	0.19	7	0.07	8	0.01
β-myrcene	-	-	4	0.06	6	0.07	5	0.04	5	0.03
3-carene	2	0.02	3	0.02	1	0.02	9	0.01	2	0.01
o-cymene	3	0.02	3	0.04	1	0.03	4	0.01	1	0.00
1,8-cineol	3	0.01	3	0.17	5	0.11	7	0.04	1	0.00
D-limonene	20	0.09	17	0.12	33	0.22	25	0.15	35	0.11
camphor	4	0.02	5	0.03	6	0.05	2	0.04	2	0.01
Total MT		*0.60*		*1.66*		*1.18*		*0.62*		*0.26*
Douglas-fir										
α-pinene			33	0.13	33	0.23	42	0.05	23	0.07
β-pinene			40	0.20	51	0.53	49	0.13	48	0.17
3-carene			12	0.06	6	0.10	2	< 0.01	18	0.06
o-cymene			3	0.14	2	0.02	3	< 0.01	4	0.01
α-phellandrene			4	0.03	2	0.02	-	-	1	0.01
D-limonene			7	0.04	6	0.06	4	0.01	6	0.01
Total MT				*0.44*		*0.96*		*0.18*		*0.44*

SQT emission rates calculated from a limited number of experiments ranged from 0.01-0.07 μg g^{-1} hr^{-1}.

It should be noted that Tables 1 and 2 report two extreme outliers for both the Bristlecone Pine and the Blue Spruce species. Samples collected from Bristlecone Pine between February 23-25, 2009 were found to exhibit very high normalized basal emissions in excess of 7 μg $g^{-1}hr^{-1}$. This emission rate is believed to be real and may be associated as a stress response as the result of considerable physical damage to the study plant in late January. Loreto and Sharkey (1993) noted that damage to one leaf of a plant caused the emissions of isoprene to increase from another, unharmed leaf. In this case, due to a power failure the enclosure purge pump ceased providing fresh air to the enclosure in late January of 2009. As a result of greenhouse heating, all needles turned brown and fell off the host limb within a week. A second branch was selected from the same tree for continued emission studies, reported here. By April the normalized emission rates appear to settle, falling in line with levels observed throughout the remainder of the season. In another instance, high basal emission rates were measured from the Blue Spruce in late March. The unusually high ε of 3.5 μg g^{-1} hr^{-1} may be attributed to the narrow enclosure temperature range (2^oC to 9^oC), resulting in poor temperature dependent ER correlation (R^2 = 0.44).

The Rocky Mountain Douglas-fir exhibited seasonal emission patterns similar to the Bristlecone Pine and Blue Spruce with maximum emission observed in early summer, falling to a minimum through winter months. Emissions were dominated by α and β-pinene, contributing 70-90% of the total MT emission. No SQT were observed. Two enclosure experiments were found with unusually high normalized basal emission rates. The first event occurred in mid June with reported ε of 2.5 μg g^{-1} hr^{-1}, more than double the next highest emission rate. Based on

sample calibration checks using the internal gas standard added to the purge flow rate, the normalized emission result appears to be correct. The second event occurred in December when the basal emission rate was found to be four times higher than rates observed in November 2009 and January 2010. The observed increase in MT emission might be attributable to a stress response to extreme cold temperatures of -16 ^{o}C followed by warming to 24^{o}C. During the warming period, enclosure temperatures were found to be in excess of 10^{o}C above the ambient air temperature.

The Gamble Oak was the only sample tree found to be the highest SQT emitter. The tree was acquired late into the growing season and already had fully developed foliage byt the time sampling commenced in July. Significant levels of germacrene B were detected with basal emission rates in excess of 0.30 $\mu g\ g^{-1}\ hr^{-1}$. The normalized emission signal was found to peak late into the growing season, near foliage senescence. Quickly thereafter, basal emission rates rapidly fell to zero. It should be noted that samples collected into October likely do not accurately account for actively emitting foliage. Biomass was measured by a number count of leaves intact with the branch, regardless of leaf activity. Therefore, the actual basal emission rates of samples taken into October are likely greater than reported here. Additionally, the high basal emission rate reported for samples collected between September 25-26, 2009 are based on only three measurements. Similar to the Gamble Oak, the Western River Birch was acquired late into the growing season. Samples were collected between mid August through October. No appreciable BVOC emissions were detected.

2.4.2. Short-Term Emissions

Each tree studied exhibited a pronounced response to short-term diurnal temperature and solar radiation cycling. Emissions increased with daylight and temperature, falling to a minimum over-night as shown in Figure 5. Most biogenic compounds observed in this study

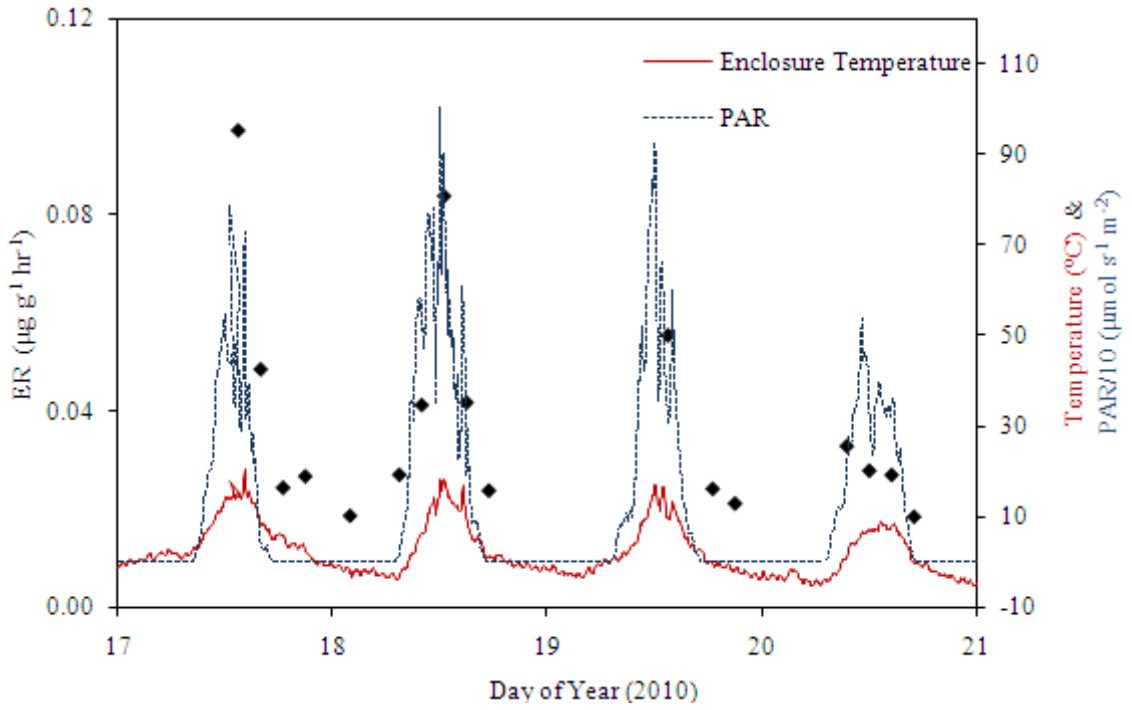

Figure 5: Four-day time series of total MT emission rates (black diamonds) measured from the Blue Spruce sampled in January, 2010. Enclosure temperature is shown in red, solar radiation (PAR) in blue. The emission rates shown are non-normalized.

were found to depend solely on temperature. These emission rates were normalized to basal emission rates following equation 4. However, a few MT were observed to exhibit light and temperature dependent emissions. Figures 6 and 7 demonstrate two compounds emitted from the two Ponderosa pine tree specimens that demonstrate light dependent emissions, 1,8-cineol and the oxygenated MT piperitone. Normalized basal emission rates for these light and temperature dependent compounds followed equations 5-7. In each plot, speciated MT compounds are

plotted along a diurnal timeframe for several enclosure experiments throughout the spring and summer seasons. Both 1,8-cineol and piperitone follow a light and temperature dependent emission pattern characterized by low to negligible emission rates by night, increasing through the day to a maximum during peak solar intensity and temperature. Actual total MT emission rates (non-normalized ER) are reported for each sample as a white diamond for the purpose of indicating diurnal change in emission magnitude. The magnitude of the total MT ER should not be used to infer change in emissions enclosure experiments.

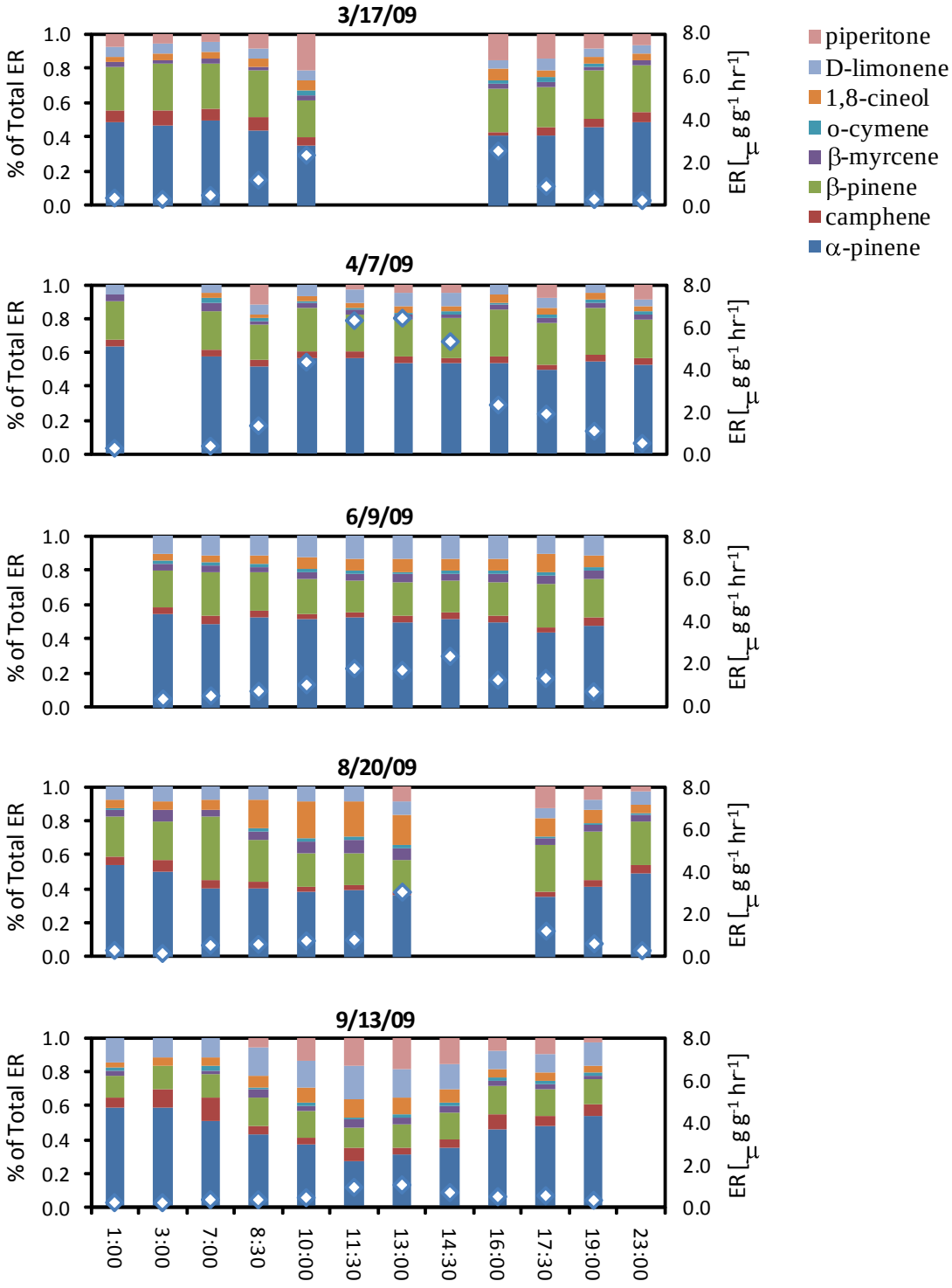

Figure 6: Emission speciation of Ponderosa Pine A with respect to diurnal cycling illustrated with several enclosure experiments between spring-fall of 2009. Sample dates are listed at the top of each plot. Bars indicate a compounds percent contribution to total emission signal. White diamonds are overlaid upon speciation bars to indicate diurnal change in actual (non-normalized) emission rates.

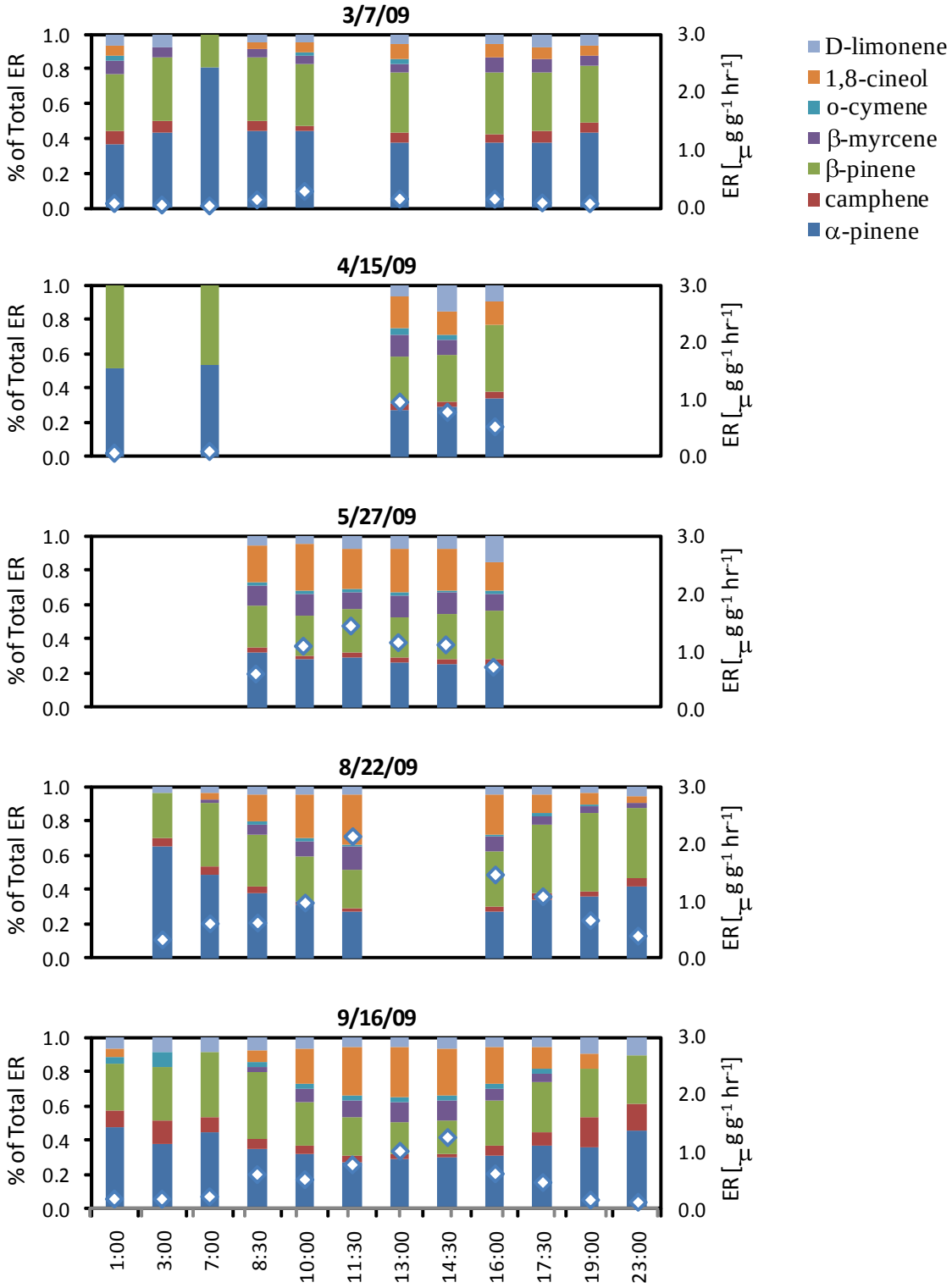

Figure 7: Emission speciation of Ponderosa Pine B with respect to diurnal cycling illustrated with several enclosure experiments between spring-fall of 2009. Sample dates are listed at the top of each plot. Bars indicate a compounds percent contribution to total emission signal. White diamonds are overlaid upon speciation bars to indicate diurnal change in actual (non-normalized) emission rates.

2.4.3. Seasonal Speciation

Compound speciation, or relative contribution to the total emission, varied throughout the sampling season. Figure 8 shows monthly averaged speciation for each coniferous tree sampled. The total MT basal emission rate is included, shown as white diamonds overlaying each reported month to help discern how changes in speciation affect the total emission. Ponderosa Pine A and B as well as the Bristlecone Pine demonstrated the most prominent seasonal variation. Among the compounds emitted by the Bristlecone Pine, 3-carene contributed upwards of 60% of the total emission, followed by α and β-pinene. Interestingly, the emission rate of 3-carene decreased between April and August. This decrease may explain the lowered total MT emission observed through the spring season. Throughout the remainder of the season, speciation between the MT compounds remained relatively constant.

The two Ponderosa Pine trees also exhibited interesting seasonal patterns with regard to speciation. First, the ratio of the speciated percent contribution to the total emission of the two most dominant compounds, α and β-pinene, remained nearly constant throughout the study period. In contrast, the speciated emission of 1,8-cineol and piperitone were found to vary dramatically over the sample season. These findings are illustrated in Figures 6 and 7, showing emission speciation with respect to a complete diurnal cycle for five measurement periods between March and September. Again, actual emission rates have been overlaid upon speciation data to provide a reference for gauging the diurnal variation in emission magnitude and should not be compared between enclosure experiments. In the case of 1,8-cineol, the percent contribution to the total MT emission was found to be less than 5% in March, however, increased to levels of 20 - 40% of the total MT signal through the summer months.

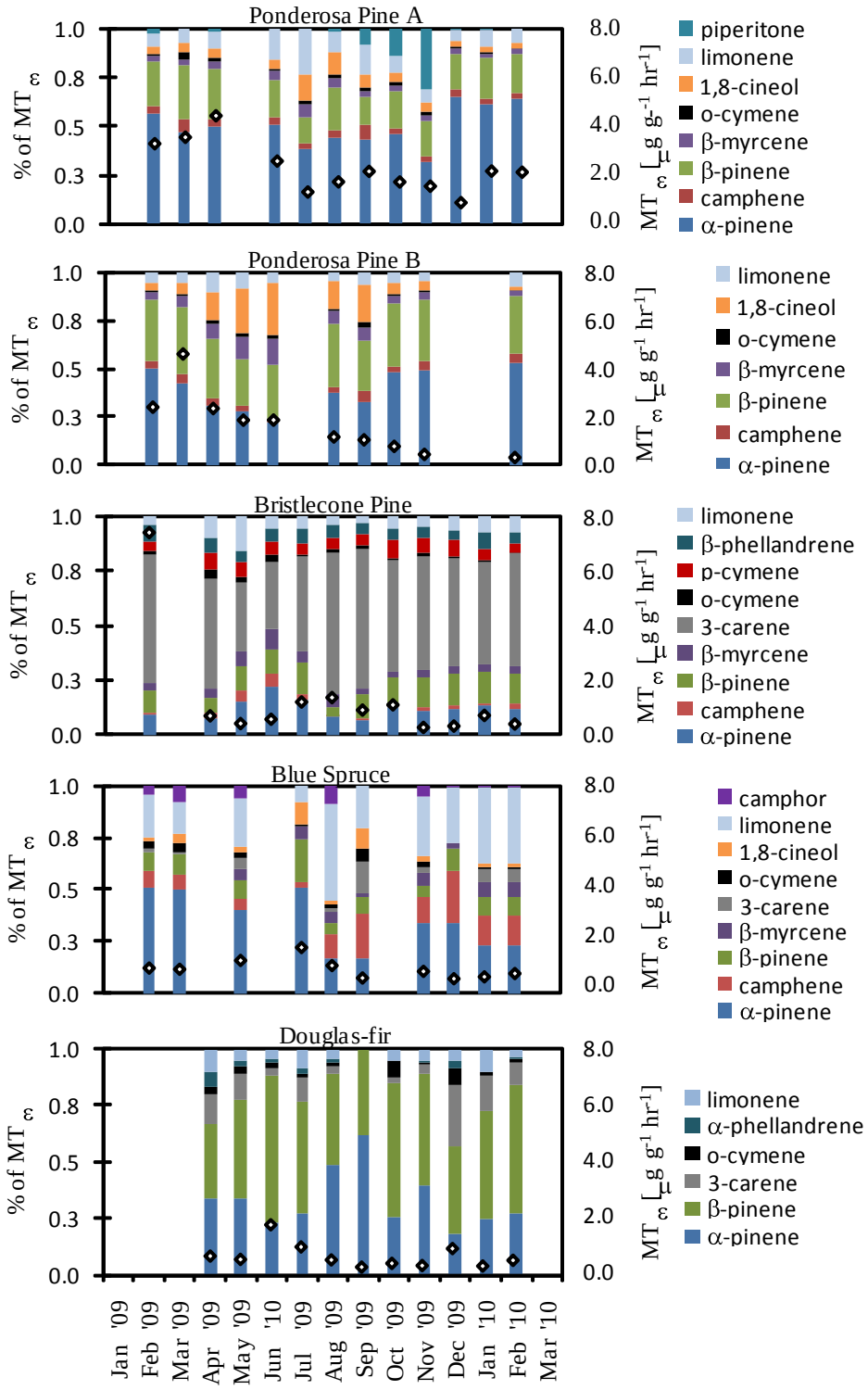

Figure 8: Monthly averaged MT compound speciation. Percent contribution to the total MT basal emission rate is indicated by the vertical bars. The magnitude of the basal emission rate is shown as a white diamond overlaid upon the vertical bars.

Likewise, the oxygenated MT piperitone demonstrated similar seasonal changes as shown in Figure 6. Piperitone was found in minimal quantities in early spring, and its emissions were not significant until fall when it quickly increased to 40% of the total emissions between September and November. Surprisingly, piperitone vanished from the emission spectrum through the remainder of the sampling season. This might have been a result of extreme cold temperatures observed in the later part of November. Furthermore, piperitone was found to be emitted solely from Ponderosa Pine A.

Biogenic volatiles serve as an interaction mechanism with insects, both as an attractant for pollination as well as a method of indirect defense against herbivore attack (Harborne, 1987; Knudsen and Tollsten, 1993; Paré and Tumlinson, 1997; Dicke, 1999; Gatehouse, 2000). It is possible Ponderosa Pine A emitted piperitone as a mechanism to interact with insects due to an unknown phonological response. Bruce and Cork (2001) investigated the response of the cotton bollworm, *Helicoverpa armigera* to volatile compounds emitted from African Marigold flowers. Piperitone was shown to evoke a positive reaction in demonstrating that the bollworm was attracted to the compound. In contrast, Bowers et al. (1993) found piperitone to be a strong insect repellant.

2.4.4 Seasonal Emission Magnitude

Accurately describing the timing and amplitude of BVOC emission rates over the course of a growing season is critical for accurate prediction of biogenic emissions. Staudt et al. (2000) proposed a method of estimating the seasonal basal emission based on length of the active emission season, emission amplitude, and timing of peak emissions as described in section 2.3.4. This method was applied to basal emission rate data compiled for Quercus ilex and Pinus pinea

by Keenan et al. (2009) who found good correlation between measured and predicted values of r = 0.83 and r = 0.86, respectively. Steinbrecher et al. (2009) used equation 10 to model seasonal BVOC emissions within Europe and neighboring countries. Here, the basal emission rates reported in Table 1 are plotted (Figure 9) with respect to sample date and overlaid with a curve projecting the seasonal basal emission following equation 9 and the methods described in section 2.3.4.

Unlike the reports of Keenan et al. (2009), mixed results were observed between basal emission rates and the predicted seasonal curve. The Bristlecone Pine and Blue Spruce displayed the best correlation with r = 0.53 and r = 0.72, respectively. Basal emission rates of the Douglas-fir demonstrated a similar profile to the predicted seasonal curve; however two outliers in late June and December result in poor correlation. The seasonally corrected emission rate curve clearly does not apply to the two Ponderosa pines of the Gamble Oak. Due to the late season emission peak of germacrene B observed from the Gamble Oak, the seasonally corrected emission curve would nearly double yearly emissions when compared to actual emission signal. Basal MT emission rates of Ponderosa Pine A and B reached a maximum in early spring, gradually tapering off through the remainder of the study season. As shown in Figure 9, normalized emission rates from both trees were not found to rise again in the spring as the seasonal correction curve predicts. Therefore, estimated annual emissions of the Ponderosa Pine would be overestimate if the seasonal correction factor was applied.

For all tree species studied, normalized emission rates were found to be far greater between spring and summer than fall and winter periods. Both Ponderosa Pine A and B demonstrated basal emission rate upwards of eight times higher between spring and winter measurements. The Bristlecone Pine, Blue Spruce and Douglas-fir displayed mid-summer

normalized emission rates five times higher than in winter. The Gamble Oak demonstrated a rapid increase in the measured basal emission rate in the fall, immediately preceding leaf senescence. Normalized emissions were found at levels in excess of two times higher than observed through the rest of the season.

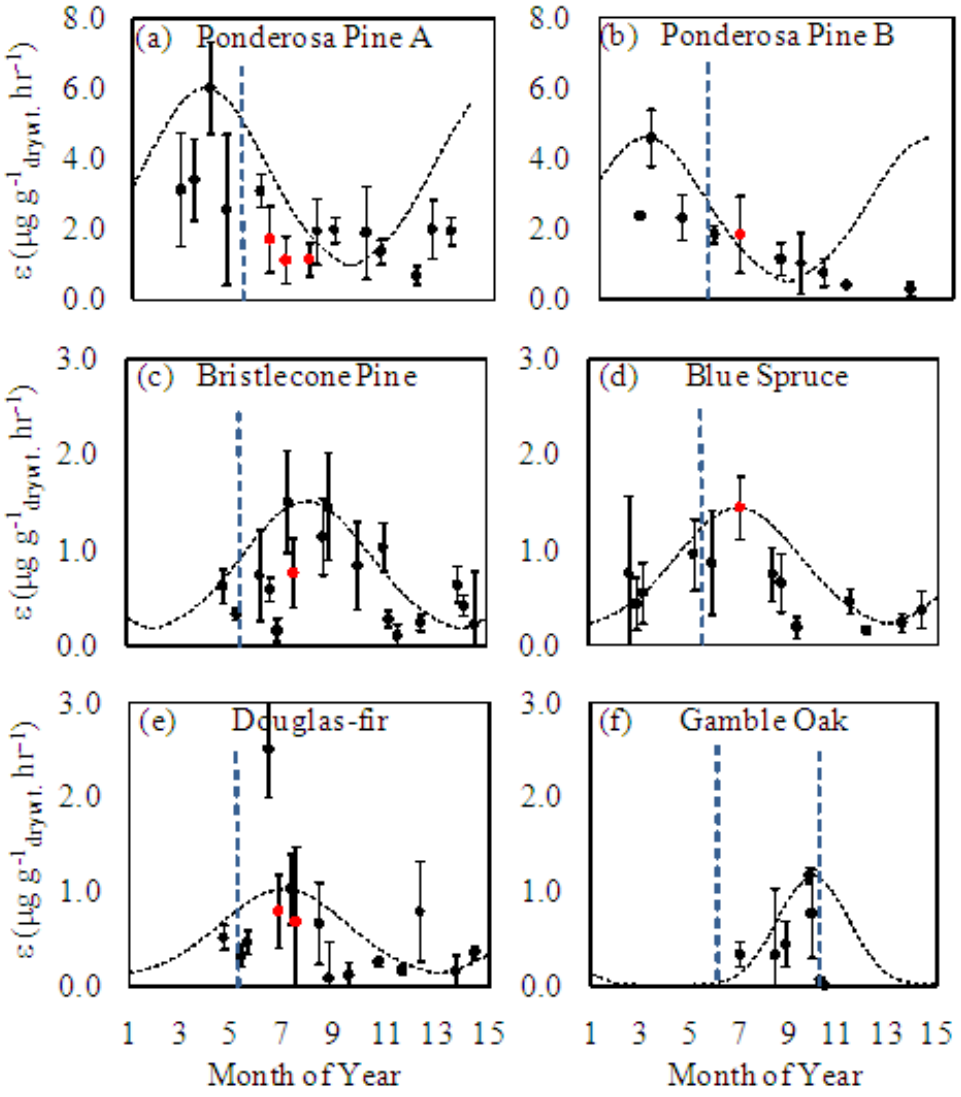

Figure 9: Seasonally plotted basal emission rates per enclosure study. Error bars indicate one standard deviation. Please note differences in scale. Seasonally corrected basal emission rates generated using the methods presented by Staudt et al. (2000) are illustrated by the curve. Red dots indicate data in which enclosure temperature was not recorded. Instead, sample temperature was inferred from temperature data of a nearby weather station. Blue vertical bars indicate leaf/needle bud break and senescence. Parameters used in the seasonal correction term $C_{S,mod}$ (Equation 10) listed below along with regression statistics:

(a): Do=4, τ=12. r=0.68
(b): Do=3, τ =12. r=0.50
(c): D_O=8, τ =12. r=0.53
(d): D_O=6, τ=12. r=0.72
(e): D_O=7, τ=12. r=0.45
(f): D_O=9, τ=4. r=0.21

2.4.5 Variation of Temperature Dependent β-factor

Most of the emitted compounds were observed to be temperature dependent. The β-factor, an empirical parameter that describes the slope of the exponential regression of observed ER to sample temperature, was further investigated for possible seasonal patterns. The β-factor of the three most prominently emitted compounds as well as the total MT emission are shown in Figure 10. Error bars indicate a 90% confidence interval generated using the bootstrapping technique; details are provided in Appendix B. Table 3 lists a summary of seasonally averaged β-factors for the three most dominantly emitted compounds as well as total MT for each tree studied. No discernable trends were identified in the β-factors over the study period. Rather, β-factors are scattered about a nominal value unique to the BVOC compound and vegetation specie ranging between 0.06 and 0.14 for MT. Accounting for all data collected in the study, a seasonally averaged MT β-factor of 0.11 $^{o}C^{-1}$ was calculated. This is slightly higher than the value of 0.09 $^{o}C^{-1}$ suggested by Guenther et al. (1993) for estimating temperature dependent MT emissions.

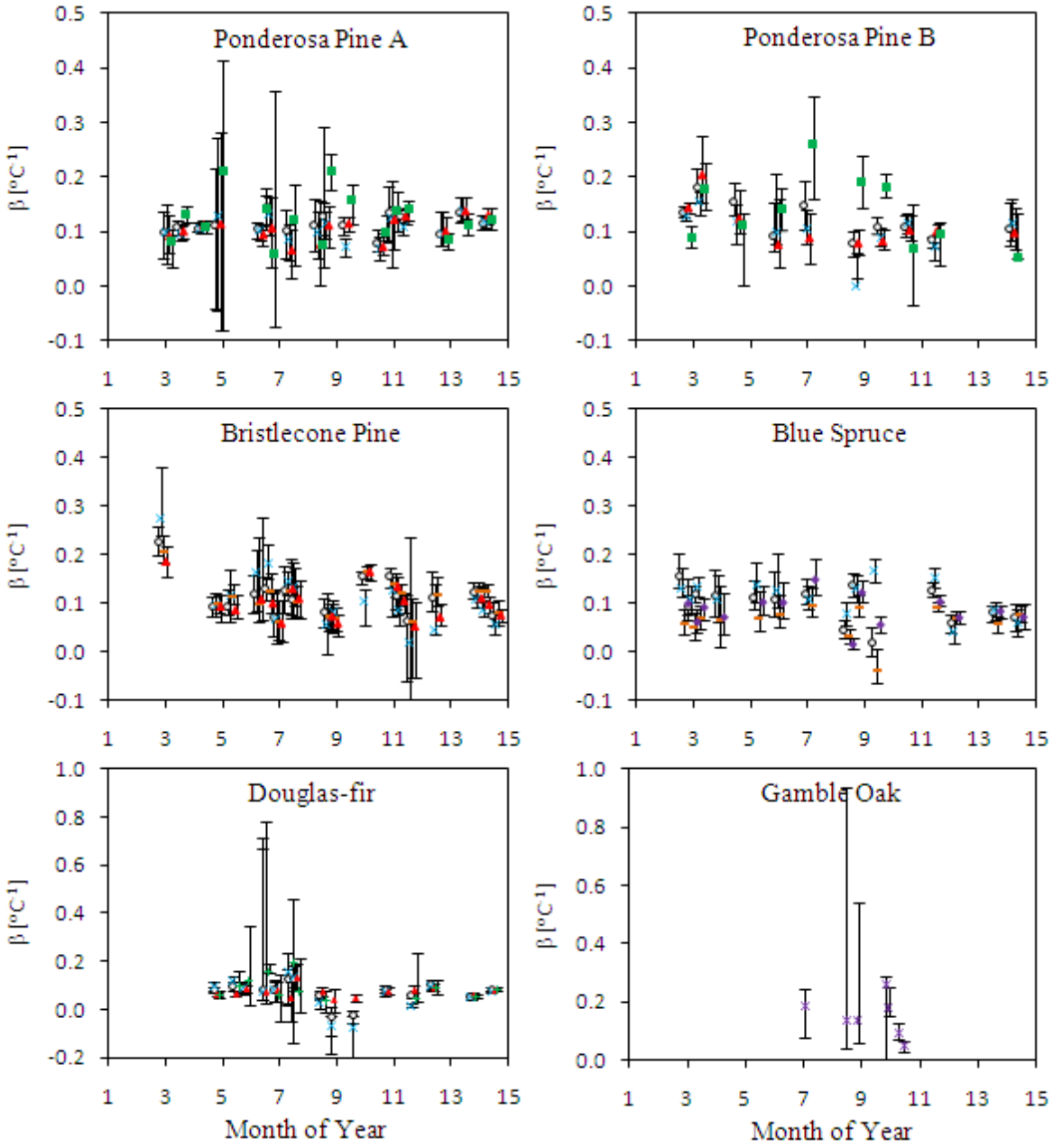

Figure 10: Temperature dependent β-factors with respect to sample date. BVOC compounds are shown slightly separated on the x-axis for clarity. Error bars indicate the 90% confidence interval. Symbols represent the following compounds: Total MT (solid white dot), α-pinene (blue cross), β-pinene (red triangle), 1,8-cineol (green square), 3-carene (green plus sign), camphene (orange dash), D-limonene (purple diamond), germacrene B (purple asterisk). Please note changes in scale.

Table 3: Seasonally compiled β-factor statistics. The mean, standard deviation about the mean, median, minimum and maximum β-factor statistics are shown with respect to categorized compounds for each tree studied. Total MT is the sum of all monoterpenes observed.

		Total MT	α-pinene	camphene	β-pinene	3-carene	1,8-cineol	limonene	germacrene B
Ponderosa Pine A	Mean	**0.11**	**0.10**		**0.10**		**0.12**		
	Std Dev	0.03	0.03		0.03		0.05		
	Median	0.11	0.10		0.11		0.12		
	min	*0.02*	*0.02*		*0.01*		*0.01*		
	max	*0.14*	*0.14*		*0.14*		*0.21*		
Ponderosa Pine B	Mean	**0.10**	**0.11**		**0.14**		**0.12**		
	Std Dev	0.03	0.04		0.07		0.03		
	Median	0.11	0.10		0.14		0.11		
	min	*0.04*	*0.08*		*0.05*		*0.08*		
	max	*0.16*	*0.20*		*0.26*		*0.18*		
Bristlecone Pine	Mean	**0.11**	**0.10**		**0.11**	**0.11**			
	Std Dev	0.06	0.04		0.04	0.04			
	Median	0.10	0.10		0.12	0.11			
	min	*0.02*	*0.05*		*0.01*	*0.06*			
	max	*0.28*	*0.19*		*0.21*	*0.23*			
Blue Spruce	Mean	**0.10**	**0.11**	**0.06**				**0.08**	
	Std Dev	0.04	0.04	0.03				0.03	
	Median	0.10	0.12	0.07				0.09	
	min	*0.02*	*0.04*	*0.03*				*0.02*	
	max	*0.15*	*0.17*	*0.09*				*0.15*	
Douglas-fir	Mean	**0.08**	**0.08**	**0.08**		**0.09**			
	Std Dev	0.03	0.04	0.02		0.05			
	Median	0.08	0.08	0.08		0.08			
	min	*0.04*	*0.01*	*0.04*		*0.03*			
	max	*0.13*	*0.16*	*0.13*		*0.19*			
Gamble Oak	Mean								**0.13**
	Std Dev								0.08
	Median								0.14
	min								*0.05*
	max								*0.26*

2.4.6 Seasonal Emission Rate Sensitivity Analysis:

BVOC emission rate data is most commonly reported based on short-term studies and mid-growth season. A sensitivity analysis was performed to demonstrate how application of the basal seasonal emission rates observed in this study compare to rates based on short-term measurements when extrapolated over an annual time frame. Non-normalized MT emission rates were calculated based on the temperature dependent emission rate equation described earlier (equation 4). Ambient air temperature reported from a nearby weather station was used to calculate the non-normalized emission rates. Three cases were investigated for the Bristlecone Pine tree, each case is outlined in Table 4 for clarity. Case 1 computes non-normalized emission

Table 4: The use of basal emission rates, ε, and β-factors used in cases 1, 2, and 3 for analyzing their respective sensitivity in calculating non-normalized emission rates over an annual time period.

	Case 1	Case 2	Case 3
ε	Seasonally Changing	Seasonally Changing	Constant ($0.94\ \mu g\ g^{-1}\ hr^{-1}$)
β	Seasonally Changing	Constant ($0.09\ ^oC^{-1}$)	Constant ($0.09\ ^oC^{-1}$)

rates utilizing the seasonally changing basal emission rate and β-factor measured in this study. Case 2 limits the β-factor to a constant value of $0.09\ ^oC^{-1}$, the value most commonly used in the literature for estimating basal MT emission rates (Guenther et al., 1993, Ortega et al, 2008b). Case 3 constrains both the basal emission rate and β-factor, representing a scenario in which short-term mid-growing season data are used to estimate annual emission rates. A constant basal emission rate of $0.94\ \mu g\ g^{-1}\ hr^{-1}$ was used, derived from the average of the summer season observations gathered in this study. Following equation 4, hourly non-normalized emission rates

were equated for two weeks before and after each enclosure study. The seasonally changing basal emission rates and β-factors used in case 1 and case 2 are listed in Table 1.

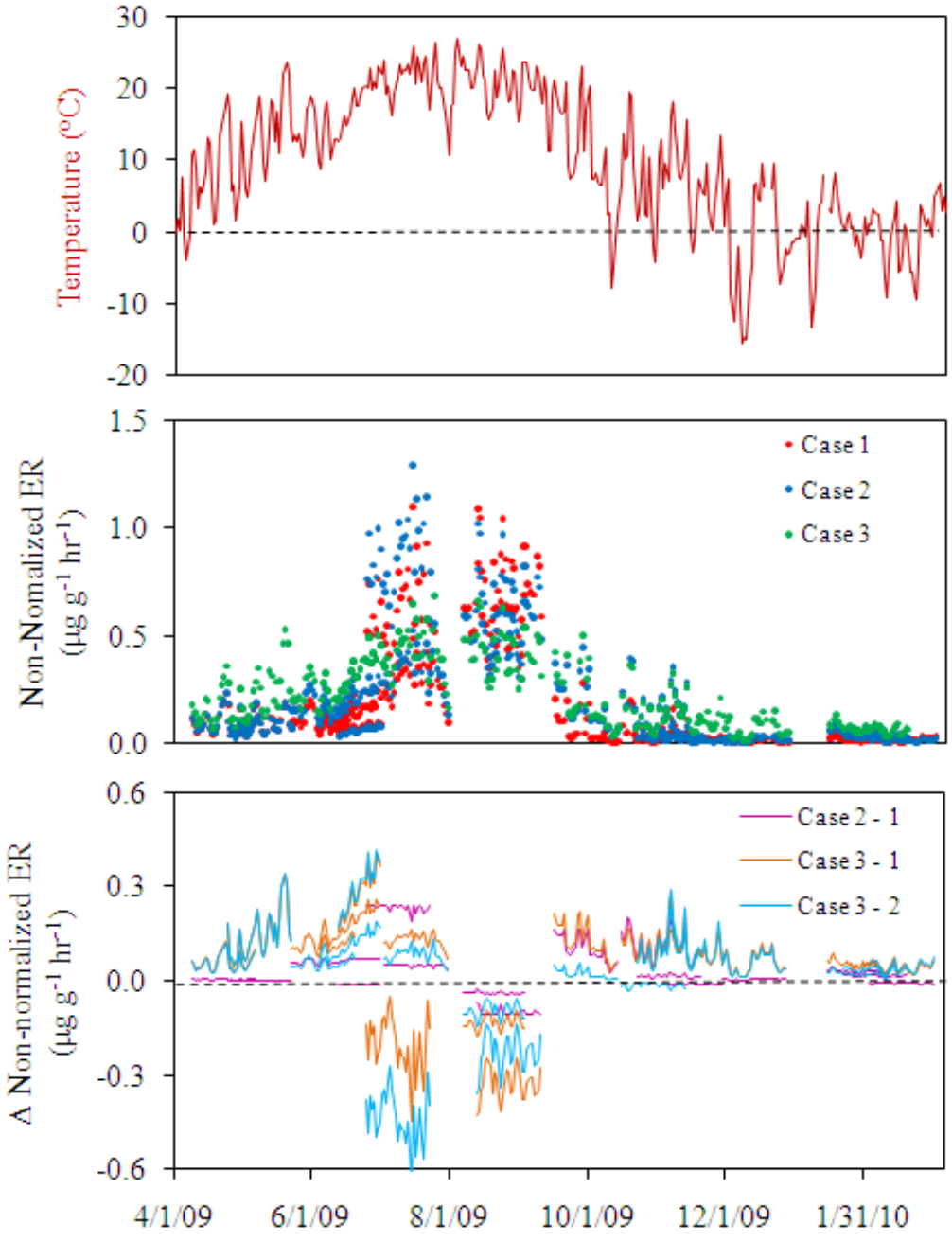

Figure 11: Seasonal ER sensitivity analysis using measured data from the Bristlecone Pine. Ambient temperature measured from a nearby meteorological station in Boulder, CO is shown (top). Non-normalized emission rates were calculated using equation 4 for cases 1, 2, and 3 (middle). Emission rates were calculated for two weeks prior to and after each enclosure study. The difference (subtraction) between each case is shown (bottom).

The calculated non-normalized emission rates detailed in case 1, 2, and 3 are shown in Figure 11 along with the respective difference (subtraction) between each case. The difference in non-normalized emission rates with respect to the incorporation of seasonally changing β-factor verse a constant β-factor may be seen in the bottom plot of Figure 11, 'Case 2 – 1'. The subtracted difference between case 2 and case 1 was found to be less than 0.3 $\mu g\ g^{-1}\ hr^{-1}$ across the studied period, with very little day-to-day variation. The delta in emission rates between case 2 and case 1 is smallest during winter periods as a consequence of low emission rates associated with cold temperatures. Greater deltas, as large as 0.6 $\mu g\ g^{-1}\ hr^{-1}$, were found between case 2 and case 3 where seasonally changing basal emission rates and a constant basal emission rate were input to calculate the non-normalized emission rates, respectively. Additionally, higher summer and lower winter season emission rates were observed between case 2 and case 3. It should also be noted that day-to-day summer season fluctuation are greater in case 2 than in case 3 while the reverse is true through the winter period. Thus, case 3 which calculates non-normalized emission rates with respect to a fixed β-factor and 'short-term' fixed basal emission rates may underestimate actual BVOC emissions during summer months and overestimate emission rates in the winter.

These findings illustrate the importance of incorporating accurate seasonally varying basal emission rate data for reliable modeling of annual BVOC emissions. The annually integrated non-normalized MT emission from the Bristlecone Pine were found to be approximately equal between all cases, however, the timing and magnitude varied dramatically between each case. The application of seasonally changing versus constant β-factors did not result in a clear benefit to seasonal emission modeling. This is likely due to the fact that seasonal patterns were not observed in the β-factor, as discussed in section 2.4.5.

2.4.7 SQT observations

Sesquiterpene emissions were found at rates lower than expected. Helmig et al. (2007) studied SQT emissions from several pine trees finding on average the total SQT basal emission rate at 30^{o}C to be 16% of the total MT emission signal. Some pines such as the Loblolly pine and the Ponderosa pine have been measured to emit SQT at levels equal to or greater than MT (Helmig et al., 2006; Bouvier-Brown et al., 2009). In this study SQT were scarcely observed from all four pine species, contributing up to a maximum of 4% of the total MT basal emission rate. Due to the limited SQT data gathered in this study, no inferences may be made about seasonal behavior. Instrument detection limit for measuring SQT were 50 pptV.

Total SQT basal emission rates of the Ponderosa pines trees studied here ranged between <0.01 – 0.07 $\mu g\ g^{-1}\ hr^{-1}$, up to 4% of the total MT emission. Six SQT were observed, three of which were positively identified as β-caryophyllene, γ-muurolene and β-bourbonene. Helmig et al. (2007) reported basal SQT emission rates in the same range as this study, however, the total SQT emission was 14% of the total MT emission. Baker and Sinnott (2009) and Bouvier-Brown et al. (2009) studied Ponderosa pines of the Sierra Nevada Mountains, CA, finding high SQT basal emission rates of up to 0.21 $\mu g\ g^{-1}\ hr^{-1}$, 20 – 200% of the total MT signal. Additionally, they reported a different set of dominant SQT compounds, comprised of α and β-farnesene and α-bergamotene. Kim et al. (2010) found lower SQT basal emission rates between 0.006-0.034 $\mu g\ g^{-1}\ hr^{-1}$, 1% of the total MT signal, using a PTR-MS at a Ponderosa stand in southern Colorado. It should be noted that lower ratios of SQT to MT have been reported from Colorado studies than California.

β-caryophyllene was the only SQT identified from Blue Spruce emissions. Basal emission rates varied between <0.01 – 0.15 $\mu g\ g^{-1}\ hr^{-1}$, 1% of the measured total MT emission

signal. Ortega et al. (2008) found maximum SQT basal emission rates of 0.04 $\mu g\ g^{-1}\ hr^{-1}$, a value lower than reported here, however, more significant in comparison to the MT emission signal at a fraction of 20% of the measured total MT emission rate. The SQT α-copaene was the only identified SQT emitted from the Bristlecone pine, with peak basal emission rates of 0.07 $\mu g\ g^{-1}\ hr^{-1}$, 2% of the total MT emission. No SQT were found emitted from the Douglas-fir. The Gamble Oak was the largest SQT emitter, where basal emission rates of Germacrene B were found to vary between 0.35 – 0.98 $\mu g\ g^{-1}\ hr^{-1}$.

The apparent variability in SQT emissions reported from various studies warrants further research. The low ratio of SQT to MT basal emission rates found in this study may be attributed to differences in geographical climate between studies. Physiological conditions may play a role including factors such as the tree nursery setting used in this study opposed to natural forest stands research be others. Additionally, genealogical differences within tree species may result in variation in the emission pattern.

2.5 Conclusions and Summary

MT dominated the observed BVOC emission from coniferous tree species. The SQT germacrene B was found to be the dominant emission from Gamble Oak. Normalized basal emission rates were found to vary throughout the season. Generally speaking, basal emission rates were greatest in spring and summer months, measured at a level of two to eight times greater than minimal emission levels observed in the fall or winter seasons. The percentile contribution of individual BVOC compounds to the total emission varied between compounds. α and β-pinene were found to be emitted at a near constant ratio whereas 1,8-cineol, 3-careen and piperitone varied dramatically across the studied period, with maximum contribution to the total emission rate in mid to late summer. The application of a seasonal correction factor applied

to normalized basal emission rates demonstrated mixed results. It is recommended that such a correction factor be applied only to well-characterized data sets with well defined growth season and maxima emission rates.

β-factor's used for defining temperature dependent basal emission rates did not demonstrate any discernable seasonal trends. Rather, the variation in measured β-factors seem to be scattered about a nominal value specific to the type of emitted compound and type of vegetation. The averaged MT β-factor measured in this study was found to be 0.11 $^{o}C^{-1}$. A simple modeling exercise examined three cases in which MT emissions were estimated over a growing season with respect to seasonally fixed or variable basal emission rates and β-factors. Findings illustrate the importance of incorporating accurate seasonally varying basal emission rate data to better account for the timing and magnitude of actual BVOC emissions across a season's period.

Total SQT emission rates observed from the coniferous species were found to be 1 – 4% of the total MT signal. These findings fall in contrast to several previous studies that report SQT to be emitted at higher ratios with respect to MT. Factors such as geographical setting, physiological condition and differences in genealogy may be root causes for these discrepancies. Further research is warranted to more fully understand the emission behavior of SQT.

References

Adams, R., P., 1989. Identification of essential oils by ion trap mass spectrometry. Academic Press, San Diego.

Arneth, A., Monson, R. K., Schurgers, G., Niinemtes, Ü., Palmer, P. I., 2008. Why are estimates of global terrestrial isoprene emissions so similar (and why is this not so for monoterpenes)? Atmospheric Chemistry and Physics, 8, 4605-4620.

Baker B. and Sinnott, M., 2009. Analysis of sesquiterpene emissions by plants using solid phase microextraction. Journal of Chromatography A, 1216, 8442-8451.

Bao, H., Shrestha, K. L., Kondo, A., Kaga A., Inoue, Y., 2010. Modeling in the influence of biogenic volatile organic compound emissions on ozone concentration during summer season in the Kinki region of Japan. Atmospheric Environment, 44, 421-431.

Bell, M.L., McDermett, A., Zeger, S.L., Samet, J.M., Dominici, F., 2004. Ozone and short-term morality in 95 US communities, 1987-2000. JAMA 292, No. 19, 2372-2378.

Bertin, N., Staudt, M., Hansen, U., Seufert, G., Ciccioli, P., Foster, P., Fugit, J.L., Torres, L., 1997. Diurnal and seasonal course of monoterpene emissions from Quercus ilex L. under natural conditions: application of the light and temperature algorithms. Atmospheric Environment, 31, 135–144.

Bouvier-Brown, N.C., Holzinger, R., Palitzsch, K., Goldstein, A.H., 2007. Quantifying sesquiterpene and oxygenated terpene emissions from live vegetation using solid-phase microextraction fibers. Journal of Chromatography, 1161, 113–120.

Bouvier-Brown, N.C., Holzinger, R., Palitzsch, K., Goldstein, A.H., 2009. Large emissions of sesquiterpenes and methyl chavicol quantified from branch enclosure measurements. Atmospheric Environment, 43, 389-401.

Bowers, W.S., Ortego, F., You X.Q., Evans, P.H., 1993. Insect repellants from the Chinese Prickly Ash Zanthoxylum-Bungeanum. Journal of Natural Products, 56, 935-938.

Bruce, T. J., Cork, A., 2001. Electrophysical and behavioral responses of female Helicoverpa ameriga to compounds identified in flowers of African Marigold, Tagetes erecta. Journal of Chemical Ecology, 27, 1119-1131.

Chameides, W.L., Lindsay, R.W., Richardson, J., Kaing, C.S., 1988. The role of biogenic hydrocarbons in urban photochemical smog: Atlanta as a case study. Science, 241, 1473-1475.

Dettmer, K., Engewald, W., 2002. Adsorbent materials commonly used in air analysis for adsorptive enrichment and thermal desorption of volatile organic compounds. Analytical and Bioanalytical Chemistry, 373, 490–500.

Dicke, M., 1999. Evolution of induced indirect defense of plants. IN: Harwell CD, Trollian R (eds) The ecology and evolution of inducible defenses. Princeton University Press, Princeton NJ, 62-88.

Dockery, D.W., Pope, C.A., 1994. Acute respiratory effects of particulate air pollution. Annual Review of Public Health, 15, 107-132.

Duhl, T., Helmig, D., Guenther, A., 2008. Sesquiterpene emissions from vegetation: a review. Biogeosciences, 5, 761-777.

Fehsenfeld, F., Calvert, J., Fall, R., Goldan, P., Guenther, A.B., Hewitt, C.N., Lamb, B., Liu, S., Trainer, M., Westberg, H., Zimmermann, P., 1992. Emissions of volatile organic compounds from vegetation and the implications for atmospheric chemistry. Global Biogeochemical Cycles, 6 (4), 389-430.

Fuentes J. D., Lerdau, M., Atkinson, R., Baldocchi, D., Bottenheim, J.,W., Ciccioli, P, Lamb., E., Geron, C., Gu, L., Guenther, A., Sharkey, T. D., Stockwell, W., 2000. Biogenic hydrocarbons in the atmospheric boundary layer: A review. Bulletin of the American Meteorological Society, 81, 1537-1575.

Gatehouse, J., 2002. Plant resistance towards insect herbivores: A dynamic interaction. New Phytologist, 156, 145-169.

Geron, C., Guenther, A., Pierce, T., 1994. An improved model for estimating emissions of volatile organic compounds from forests in the eastern United States. Journal of Geophysical Research, 99, 12773-12792.

Grote, R., Niinemets, Ü., 2007. Modeling volatile isoprenoid emissions – a story with split ends. Plant Biology, 10, 8-28.

Grote, R., Keenan, T., Lavoir, A.-V., Staudt, M., 2010. Process-based simulation of seasonality and drought stress in monoterpenes emission models. Biogeosciences, 7, 257-274.

Guenther, A.B., Zimmerman, P.R., Harley, P.C., Monson, R.K., Fall, R., 1993. Isoprene and monoterpene emission rate variability: model evaluations and sensitivity analyses. Journal of Geophysical Research, 98, 12609-12617.

Guenther, A., Hewitt, C.N., Erickson, D., Fall, R., Geron, Ch., Graedel, T., Harley, P., Klinger, L., Lerdau, M., McKay, W.A., Pierce, T., Scholes, B., Steinbrecher, R., Tallamraju, R., Taylor, J., Zimmerman, P., 1995. A global-model of natural volatile organic compound emissions. Journal of Geophysical Research, 100, 8873-8892.

Guenther, A.B., 1997. Seasonal and spatial variations in natural volatile organic compound emissions. Ecological Applications, 7, 34-45.

Hakola, H., Tarvainen, V., Back, J., Ranta, H., Bonn, B., Rinne, J., Kulmala, M., 2005. Seasonal variation of mono- and sesquiterpene emission rates of Scots Pine. Biogeosciences, 3, 93-101.

Hansen, U., Seufert, G., 2003. Temperature and light dependence of b-caryophyllene emission rates. Journal of Geophysical Research, 108. doi:10.1029/2003JD003853.

Harborne, J.B., 1987. Chemical signals in the ecosystem. Annals of Botany, 60, 39-57.

Harper, M., 2000. Sorbent trapping of volatile organic compounds from air. Journal of Chromatography, 885, 129–151.

Helmig, D., Vierling, L., 1995. Water adsorption capacity of the solid adsorbents Tenax TA, Tenax GR, Carbotrap, Carbotrap C, Carbos-ieve SIII, and Carboxen 569 and Water management techniques for the atmospheric sampling of volatile organic trace gases. Analytical Chemistry, 67, 4380–4386.

Helmig, D, Revermann, T., Pollmann, J., Kaltschmidt, O., Jimenez-Hernandez, A., Bocquet, F., David, D., 2003. Calibration system and analytical considerations for quantitative sesquiterpene measurements in air. Journal of Chromatography A, 1002, 193-211.

Helmig, D., Bocquet, F., Pollmann, J., Revermann, T., 2004. Analytical techniques for Sesquiterpene emission rate studies in vegetation enclosure experiments. Atmospheric Environment, 38, 557-572.

Helmig, D., Ortega, J., Guenther, A., Herrick, J.D., Geron, C., 2006. Sesquiterpene emissions from loblolly pine and their potential contribution to biogenic aerosol formation in the Southeastern U.S. Atmospheric Environment, 40, 4150-4157.

Hoffmann, T., Odum, J.R., Bowman, F., Collins, D., Klockow, D., Flagan, R.C., Seinfeld, J.H., 1997. Formation of organic aerosols from the oxidation of biogenic hydrocarbons. Journal of Atmospheric Chemistry, 26, 189-222.

Holzke, C., Hoffmann, T., Jaeger, L., Koppmann, R., Zimmer, W., 2006. Diurnal and seasonal variation of monoterpene and sesquiterpene emissions from Scots Pine (*Pinus silvestris L.*). Atmospheric Environment, 40, 3174-3185.

Joó, E., Langenhove, H. V., Šimpraga, M., Steppe, K., Amelynck, C., Schoon, N., Müller, J.-F., Dewulf, J., 2010. Atmospheric Environment, 44, 227-234.

Kempf, K., Allwine, E., Westberg, H., Claiborn, C., Lamb, B., 1996. Hydrocarbon emissions from spruce species using environmental chamber and branch enclosure methods. Atmospheric Environment, 30, 1381–1389.

Keenan, T., Niinemets, Ü., Sabate, S., Gracia, C., Peñuelas, J., 2009. Seasonality of monoterpenes emission potentials in Quercus ilex and Pinus pinea: Implications for regional VOC emissions modeling. Journal of Geophysical Research, 114, D22202.

Kim, S., Karl, T., Guenther, G., Tyndall, G., Orlando, J., Harley, P., Rasmussen, R., Apel, E., 2010. Emissions and ambient distributions of biogenic volatile organic compound (BVOC) in a ponderosa pine ecosystem: interpretation of PTR-MS mass spectra. Atmospheric Chemistry and Physics, 10, 17-59-1771.

Komenda, M., Parusel, E., Wedel, A., Koppmann, R., 2001. Measurements of biogenic VOC emissions: sampling, analysis and calibration. Atmospheric Environment, 35, 2069–2080.

Knudson, J.T., Tollsten, L., 1993. Trends in floral scent chemistry in pollination syndromes – floral scent composition in moth-pollinated taxa. Botanical Journal of the Linnean Society, 113, 263-284.

Laothawornkitkul, J., Taylor, J. E., Paul, N. D., Hewitt, C. N., 2009. Biogenic volatile organic compounds in the Earth system. New Phytologist, 183, 27-51.

Litvak, M.E., Monson, R.K., 1998. Patterns of induced and constitutive monoterpene production in conifer needles in relation to insect herbivory. Oecologia, 114, 531-540.

Liao, J., Henze, D., Seinfeld, J. H., Wu, S., Mickley, L. J., 2007. Biogenic secondary organic aerosol over the United States: Comparison of climatological simulations with observations. Journal of Geophysical Research, 112, D06201.

Loreto, F., Sharkey, T.D., 1993. Isoprene emission by plants is affected by transmissible wound signals. Plant, Cell & Environment, 16, 563-570.

Niinemets, Ü., Tenhuenen, J.D., Harley, P.C., Steinbrecher, R., 1999. A model of isoprene emission based on energetic requirements for isoprene synthesis and leaf photosynthetic properties for *Liquidambar* and *Quercus*. Plant Cell Environment, 22, 1319-1335.

Niinemets, Ü, Seufert, G., Steinbrecher, R., Tenhunen, J.D., 2002. A model coupling foliar monoterpene emissions to leaf photosynthetic characteristics in Mediterranean evergreen *Quercus* species. New Phytologist, 153, 257-273.

Ortega J., Helmig, D., 2008. Approaches for quantifying reactive and low-volatility biogenic organic compound emissions by vegetation enclosure techniques – Part A. Chemosphere, 72, 343-364.

Ortega, J., Helmig, D., Daly, R.W., Tanner, D.M., Guenther, A.B., Herrick, J.D., 2008. Approaches for quantifying reactive and low-volatility biogenic organic compound emissions by vegetation enclosure techniques – Part B: Applications. Chemosphere, 72, 365-380.

Paré, P.W., Tumlinson, J.H., 1997. Induced synthesis of plant volatiles. Nature, 835, 30-31.

Peñuelas, J., Llusiá, J., 2001. The complexity of factors driving volatile organic compound emissions by plants. Biologia Plantarum, 44, 481-487.

Peñuelas, J., Staudt, M., 2009. BVOCs and global change. Trends in Plants Science, 15, 133-144.

Pio, C. A., Silva., P. A., Cerqueira, M. A., Nunes, T. V., 2005. Diurnal and seasonal emissions of volatile organic compounds from cork oak (Quercus suber) trees. Atmospheric Environment, 39, 1817-1827.

Pollmann, J., Ortega, J., Helmig, D., 2005. Sampling of atmospheric sesquiterpenes: sampling losses and mitigation of ozone interference. Environmental Science Technology, 39, 9620.

Pressley, S., Lamb, B., Westberg, H., Guenther, A., Chen, J., Allwine, E., 2004. Monoterpene emissions from a Pacific Northwest old-growth forest and impact on regional biogenic VOC emission estimates. Atmospheric Environment, 38, 3089–3098.

Rabl, A. and Eyre, N., 1998. An estimate of regional and global O3 damage from precursor NOx and VOC emissions. Environment International, 24, 835-850.

Rapparini, F., Baraldi R., Facini, O., 2001. Seasonal variation of monoterpene emission from *Malus domestica* and *Prunus avium*, Phytochemistry, 57, 681–687.

Rivoal, A., Fernandez, C., Lavoir, A. V., Olivier, R., Lecareux C., Greff, S., Roche, P., Vila, B., 2010. Environmental control of terpene emissions from Cistus monspeliensis L. in natural Mediterranean shrublands. Chemosphere, 78, 942-949.

Schnee, C., Kollner, T.G., Gershenzon, J., Dengenhardt, J., 2002. The maize gene terpene synthase 1 encodes a sesquiterpene synthase catalyzing the formation of (E)-b-farnesene, (E)-nerolidol, and (E,E)-farnesol after herbivore damage. Plant Physiology, 130, 2049-2060.

Schnitzer, J.P., Bauknecht, N., Bruggemann, N., Einig, W., Forkel, R., Hampp, R., Heiden, A.C., Heizmann, U., Hoffmann, T., Holzke, C., Jaeger, L., Klauer, M., Komenda, M., Koppmann, C., Kreuzwieser, J., Mayer, H., Rennenberg, H., Smiatek, G., Steibrecher, R., Wildt, J., Zimmer, W., 2002. Emission of Biogenic Volatile Organic Compounds: An Overview of Field, Laboratory and Modeling Studies Performed during the 'Tropospheric Research Program' (TFS) 1997–2000. Journal of Atmospheric Chemistry, 42, 159-177.

Shao, M., Czapiewski, K.V., Heiden, A.C., Kobel, K., Komenda, M., Koppman, R., Wildt, J., 2001. Volatile organic compound emissions from Scots pine: mechanisms and description by algorithms. Journal of Geophysical Research, 1006, 20483-20491.

Staudt, M., Bertin, N., Hansen, U., Seufert, G., Ciccioli, P, Foster, P., Frenzel, B., Fugit, J.L., 1997. Seasonal and diurnal patterns of monoterpene emissions from *Pinus pinea (L.)* under field conditions. Atmospheric Environment, 31, 145-156.

Staudt, M., Bertin, N., Frenzel, B., Seufert, G., 2000. Seasonal Variation in amount and composition of monoterpenes emitted by young Pinus pinea trees – Implications for emission modeling. Journal of Atmospheric Chemistry, 35, 77-99.

Steeghs, M., Bais, H.P., de Gouw, J., Goldan, P., Kuster, W., Northway, M., Fall, R., Vivanco, J.M., 2004. Proton-transfer-reaction mass spectrometry as a new tool for real time analysis of root-secreted volatile organic compounds in Arabidopsis. Plant Physiology, 135, 47–58.

Steinbrecher, R., Smiatek, G., Köble, R., Seufert, G., Theloke, J., Hauff, K., Ciccioli, P., Vautard, R., Curci, G., 2009. Intra- and inter-annual variability of VOC emissions from natural and semi-natural vegetation in Europe and neighboring countries. Atmospheric Environment, 43, 1380-1391.

Tingey, D T., Manning, M., Grothaus, L. C., Burns, W., F,. 1980. Influence of light and temperature on monoterpene emission rates from slash pine (Pinus elliotti). Plant Physiology, 65, 797-801.

Tholl, D., Boland, W., Hansel, A., Loreto, F., Rose, U.S.R., Schnitzler, J.P., 2006. Practical approaches to plant volatile analysis. Plant Journal, 45, 540–560.

Wang, Q., Han , Z., Wang., T., Zhang., R., 2008. Impacts of biogenic emissions of VOC and NOx on tropospheric ozone during summertime in eastern China. Science of Total Environment ,395, 41-49.

Yassaa, N., Williams, J., 2007. Enantiomeric monoterpene emissions from natural and damaged Scots pine in a boreal coniferous forest measured using solid-phase microextraction and gas chromatography/mass spectrometry. Journal of Chromatography, 1141, 138–144.

Appendix A: GC-FID/MS Analysis Parameters

Adsorbent cartridges were analyzed by thermodesorbtion GC/MS with FID detection. Instrument parameters are described below.

Thermodesorbtion was performed by a Perkin-Elmer ATD-400 automated cartridge desorber set to the following parameters:
Hydrogen purge flow rate: 50 ml min^{-1}
Outlet-split flow rate: 10.2 ml min^{-1}
GC x-fer flow rate (Column flow rate): 2.1 ml min^{-1}

Desorption temperature: 300 ^{o}C
Desorption time: 30 min
Micro cold-trap sample temperature: -20 ^{o}C
Micro cold-trap desorption temperature: 325 ^{o}C
GC x-fer temperature: 275 ^{o}C

GC/MS flow rates:
Carrier gas: Hydrogen
Column flow rate: 2.1 ml min^{-1}
MS split flow rate: 0.4 ml min^{-1}
FID split flow rate: 1.7 ml min^{-1}
FID supplemental hydrogen flow rate: 21.6 ml min^{-1}
FID air flow rate: 245 ml min^{-1}

GC oven Program:
Hold 40 ^{o}C 5 minutes
Ramp 6 ^{o}C min to 200 ^{o}C
Hold 200 ^{o}C 5 minutes

GC Column specs:
Manufacturer: J. & W. Scientific
Column type: DB-1
Length: 30m
Inner diameter: 0.320mm
Film thickness: 0.025mm

Appendix B – Bootstrap statistics of the β-factor

A detailed analysis of the statistical 'bootstrap' method used in Chapter 2 to analyze any seasonal patterns in the measured β-factor.

1 - Introduction

1.1 - Overview

The bootstrap method used in Chapter 2 is described in detail here. The bootstrap is a methodology of measuring the accuracy of an estimator. Using the technique of resampling, it allows for the estimation of a sample distribution by assembling a number of randomly generated resamples from the original sample distribution, thereby creating a larger sample population. The bootstrap was used in Chapter 2 to estimate confidence intervals about the β-factor statistics of seasonal BVOC emission data.

1.2 The Bootstrap Method

The bootstrap method may be applied to an independent and identically distributed population. The method may be implemented by the computer-based generation of a number of resamples of the original sample distribution. Resamples are constructed from random sampling of the original dataset with replacement to create a new sample set of equal size of the original. A number of resamples are performed to build a larger sample population representative of the original dataset from which measures of statistical accuracy may be performed. The number of suggested resamples varies, however 1,000 to 10,000 is suggested for measuring a confidence interval (Efron and Tibshirani, 1986).

1.3 – Application: β-factor

The bootstrap method was used in this study to estimate confidence intervals about the β-factor statistic measured in Chapter 2. The β-factor is used for describing the temperature dependant emission rates of biogenic volatile organic compounds (BVOC) measured from branch enclosure studies. β is calculated as the slope of the exponential regression of a temperature dependant emission rate with respect to sample temperature. See Figure B1 for an example of exponentially fit emission data.

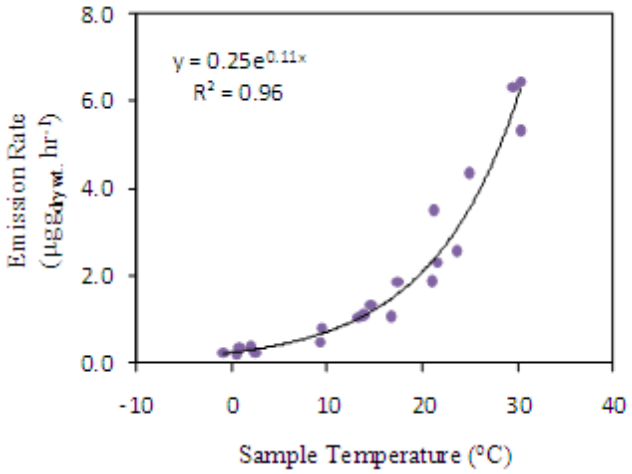

Figure B1: Temperature dependence MT emissions from Ponderosa Pine A sampled April 6-8, 2009.

Mathematically, the β-factor may be represented by equation 1 where ER is the measured emission rate (μg $g_{dry\ wt.}$ hr^{-1}), a and β are empirically defined parameters from the best fit exponential regression and T is the sample temperature.

$$ER = a \cdot e^{\beta(T)} \quad (1)$$

The emphasis of Chapter 2 was to analyze properties of the methods used to model and estimate BVOC emission rates for seasonal patterns and trends. The β-factor is used by emission models to calculate emission rates and was therefore important to analyze with respect to seasonal variation. The bootstrap method was used develop a confidence interval (CI) about each branch enclosure experiment for the entire study.

CI were generated for the emission rates of the three most dominant monoterpene (MT) compounds as well as for total MT for each vegetation species studied. These species include the Ponderosa Pine, Blue Spruce, Bristlecone Pine and Douglas-fir. The sesquiterpene compound germacrene B was also analyzed from the specie Gamble Oak. Five thousand resamples were computed for all MT datasets and ten thousand for total MT and germacrene B datasets. Figures B2 and B3 demonstrate reduction in standard error with increasing number of resamples.

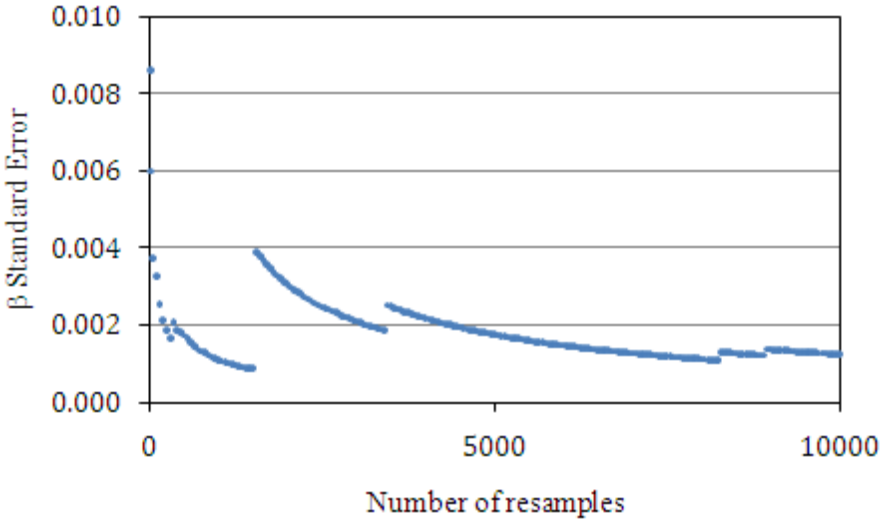

Figure B2: Plot of the bootstrapped standard error of β with respect to the number of resamples performed. Data was chosen from a Ponderosa Pine sampled June 27-28, 2009. The measured β was 0.07 with a R^2 statistic of 0.54. This example represents a case of poor exponential regression between emission rate and sample temperature. By resampling 10,000 times, the bootstrap method smoothes out potential oddities even in dataset with small number of data points or in this case poor regression.

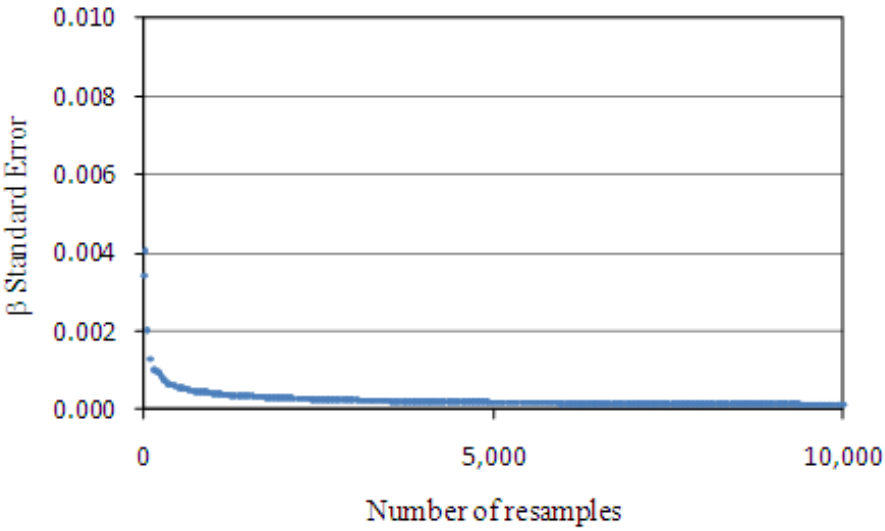

Figure 3: Plot of the bootstrapped standard error of β with respect to the number of resamples performed. Data was chosen from a Ponderosa Pine sampled April 23-24, 2009. The measured β was 0.09 with a R^2 statistic of 0.90. This example represents a case of excellent exponential regression between emission rate and sample temperature.

A 90% confidence interval $\alpha = 0.05$ was chosen to investigate the change in the β-factor over the measurement period. Graphical data is shown in two manners below in section 2. First, β-factors are shown in the form of a scatter plot. Measured β is laid across the x-axis with respect to season and error bars indicating the outer range of the 90% CI. The second manner, shown for only a few vegetation species, illustrates the seasonal variation in β using a histogram to demonstrate the probability distribution of the β-factor for each enclosure study of the course of the season. This data is discussed in chapter 2 and may be seen in more detail below.

2 – Data

Table B1 provides a list of seasonally averaged β-factors for the most dominant MT compounds, total MT as well as the sesquiterpene germacrene B. Data is described in tables and plots in the following sections, listed by vegetation species. β-factors of individual compounds per tree enclosure experiment are detailed in section 2 below. Additionally, visual representations of the 90% confidence intervals are plotted for each enclosure per study tree, again shown below in section 2.

Table B1: Seasonally averaged β-factor statistics listed by vegetation specie and emitted compound.

		Total MT	α-pinene	camphene	β-pinene	3-carene	1,8-cineol	limonene	germacrene B
Ponderosa Pine A	n	16	16		16		16		
	Mean	0.11	0.10		0.10		0.12		
	Std Dev	0.03	0.03		0.03		0.05		
	Median	0.11	0.10		0.11		0.12		
	min	*0.02*	*0.02*		*0.01*		*0.01*		
	max	*0.14*	*0.14*		*0.14*		*0.21*		
Ponderosa Pine B	n	10	10		9		10		
	Mean	0.10	0.11		0.14		0.12		
	Std Dev	0.03	0.04		0.07		0.03		
	Median	0.11	0.10		0.14		0.11		
	min	*0.04*	*0.08*		*0.05*		*0.08*		
	max	*0.16*	*0.20*		*0.26*		*0.18*		
Bristlecone Pine	n	18	18		18	18			
	Mean	0.11	0.10		0.11	0.11			
	Std Dev	0.06	0.04		0.04	0.04			
	Median	0.10	0.10		0.12	0.11			
	min	*0.02*	*0.05*		*0.01*	*0.06*			
	max	*0.28*	*0.19*		*0.21*	*0.23*			
Blue Spruce	n	14	14	14				14	
	Mean	0.10	0.11	0.06				0.08	
	Std Dev	0.04	0.04	0.03				0.03	
	Median	0.10	0.12	0.07				0.09	
	min	*0.02*	*0.04*	*0.03*				*0.02*	
	max	*0.15*	*0.17*	*0.09*				*0.15*	
Douglas-fir	n	15	15	15		15			
	Mean	0.08	0.08	0.08		0.09			
	Std Dev	0.03	0.04	0.02		0.05			
	Median	0.08	0.08	0.08		0.08			
	min	*0.04*	*0.01*	*0.04*		*0.03*			
	max	*0.13*	*0.16*	*0.13*		*0.19*			
Gamble Oak	n								8
	Mean								0.13
	Std Dev								0.08
	Median								0.14
	min								*0.05*
	max								*0.26*

2.1 – Ponderosa Pine

Table B2.1.1: Ponderosa Pine A. β-factor and exponential regression statistic summarized by branch enclosure experiment and emitted compound(s).

	ε MT		α-pinene		β-pinene		1,8-cineol	
Sample Date	β	R^2	β	R^2	β	R^2	β	R^2
Feb 27-28, '09	0.10	0.83	0.09	0.80	0.09	0.77	0.08	0.74
Mar 16-18, '09	0.11	0.91	0.10	0.88	0.10	0.88	0.13	0.92
Apr 6-8, '09	0.11	0.10	0.11	0.96	0.11	0.97	0.11	0.95
Apr 25-26, '09	0.11	0.19	0.13	0.23	0.11	0.13	0.21	0.19
Jun 9-10, '09	0.10	0.94	0.10	0.92	0.09	0.91	0.14	0.94
Jun 20-21, '09	0.02	0.15	0.02	0.16	0.01	0.11	0.01	0.06
July 11-12, '09	0.10	0.62	0.08	0.65	0.08	0.48	0.12	0.54
Aug 8-9, '09	0.12	0.64	0.10	0.69	0.08	0.26	0.07	0.33
Aug 19-21, '09	0.13	0.79	0.12	0.83	0.11	0.60	0.21	0.82
Sept 16-17, '09	0.11	0.79	0.07	0.75	0.11	0.91	0.16	0.73
Oct 16-17, '09	0.08	0.84	0.07	0.82	0.07	0.78	0.10	0.87
Oct 30-31, '09	0.14	0.71	0.12	0.49	0.12	0.92	0.14	0.85
Nov 6-10, '09	0.13	0.94	0.11	0.91	0.13	0.91	0.14	0.88
Dec 21-24, '09	0.10	0.71	0.09	0.66	0.10	0.75	0.09	0.90
Jan 11-13, '10	0.13	0.92	0.14	0.91	0.14	0.92	0.11	0.88
Feb 6-10, '10	0.12	0.95	0.12	0.96	0.13	0.93	0.12	0.80
Median	0.11		0.10		0.11		0.12	
Mean	0.11		0.10		0.10		0.12	
Std Dev	0.03		0.03		0.03		0.05	

Table B2.1.2: Ponderosa Pine B. β-factor and exponential regression statistic summarized by branch enclosure experiment and emitted compound(s).

	ε MT		α-pinene		β-pinene		1,8-cineol	
Sample Date	β	R^2	β	R^2	β	R^2	β	R^2
Feb 20-22, '09	0.13	0.92	0.14	0.96	0.09	0.90	0.14	0.94
Mar 6-8, '09	0.16	0.96	0.20	0.83	0.18	0.86	0.18	0.93
Apr 15-16, '09	0.12	0.92	0.12	0.93	-		0.15	0.94
May 27-28, '09	0.10	0.90	0.08	0.60	0.14	0.96	0.09	0.81
Jun 29-30, '09	0.11	0.87	0.09	0.72	0.26	0.75	0.15	0.83
Aug 21-24, '09	0.04	0.51	0.08	0.76	0.19	0.74	0.08	0.76
Sept 15-17, '09	0.09	0.77	0.08	0.62	0.18	0.91	0.11	0.83
Oct 16-20, '09	0.11	0.84	0.10	0.79	0.07	0.25	0.11	0.81
Nov 12-14, '09	0.07	0.80	0.10	0.96	0.10	0.82	0.08	0.91
Feb 6-10, '10	0.11	0.78	0.10	0.70	0.05	0.99	0.11	0.68
Median	0.11		0.10		0.14		0.11	
Mean	0.10		0.11		0.14		0.12	
Std Dev	0.03		0.04		0.07		0.03	

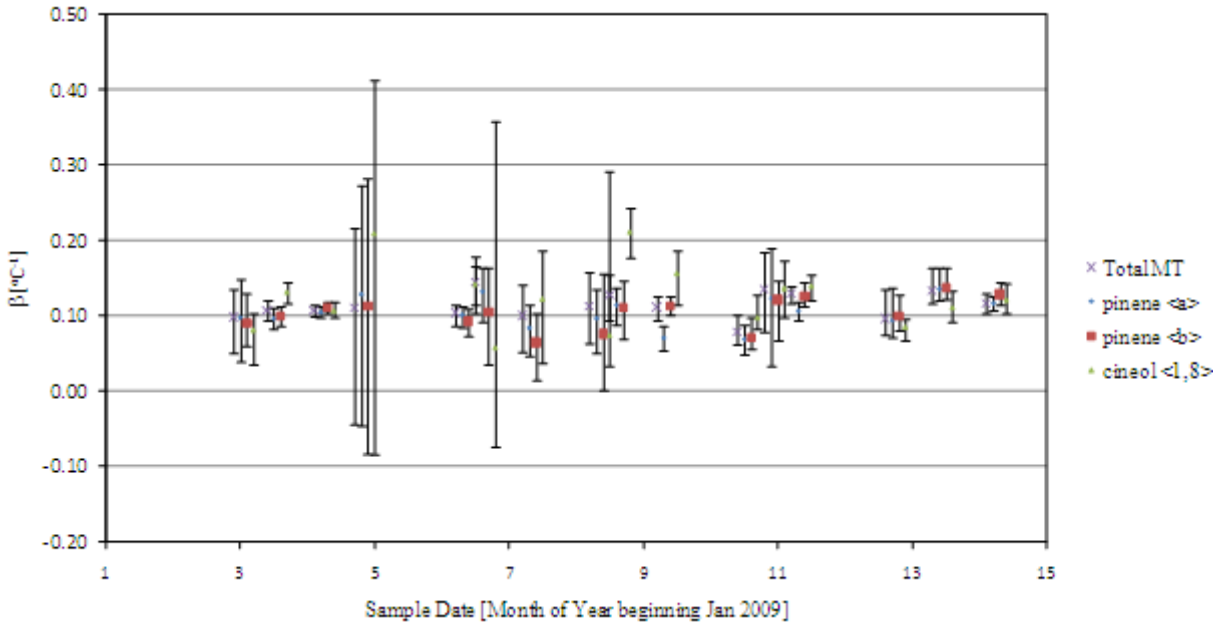

Figure B2.1.1: Ponderosa Pine A. Measured β-factor plotted with 90% CI shown by error bars. Total MT and the three most dominant MT emitters are shown by enclosure experiment with dates slightly offset for clarity.

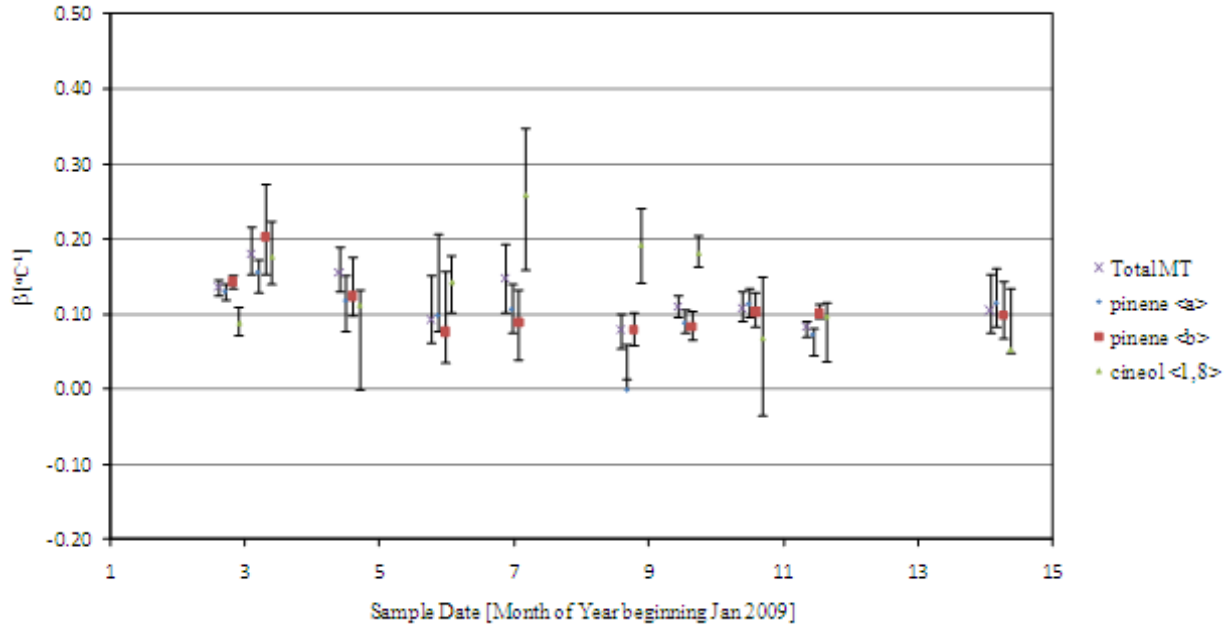

Figure B2.1.2: Ponderosa Pine B. Measured β-factor plotted with 90% CI shown by error bars. Total MT and the three most dominant MT emitters are shown by enclosure experiment with dates slightly offset for clarity.

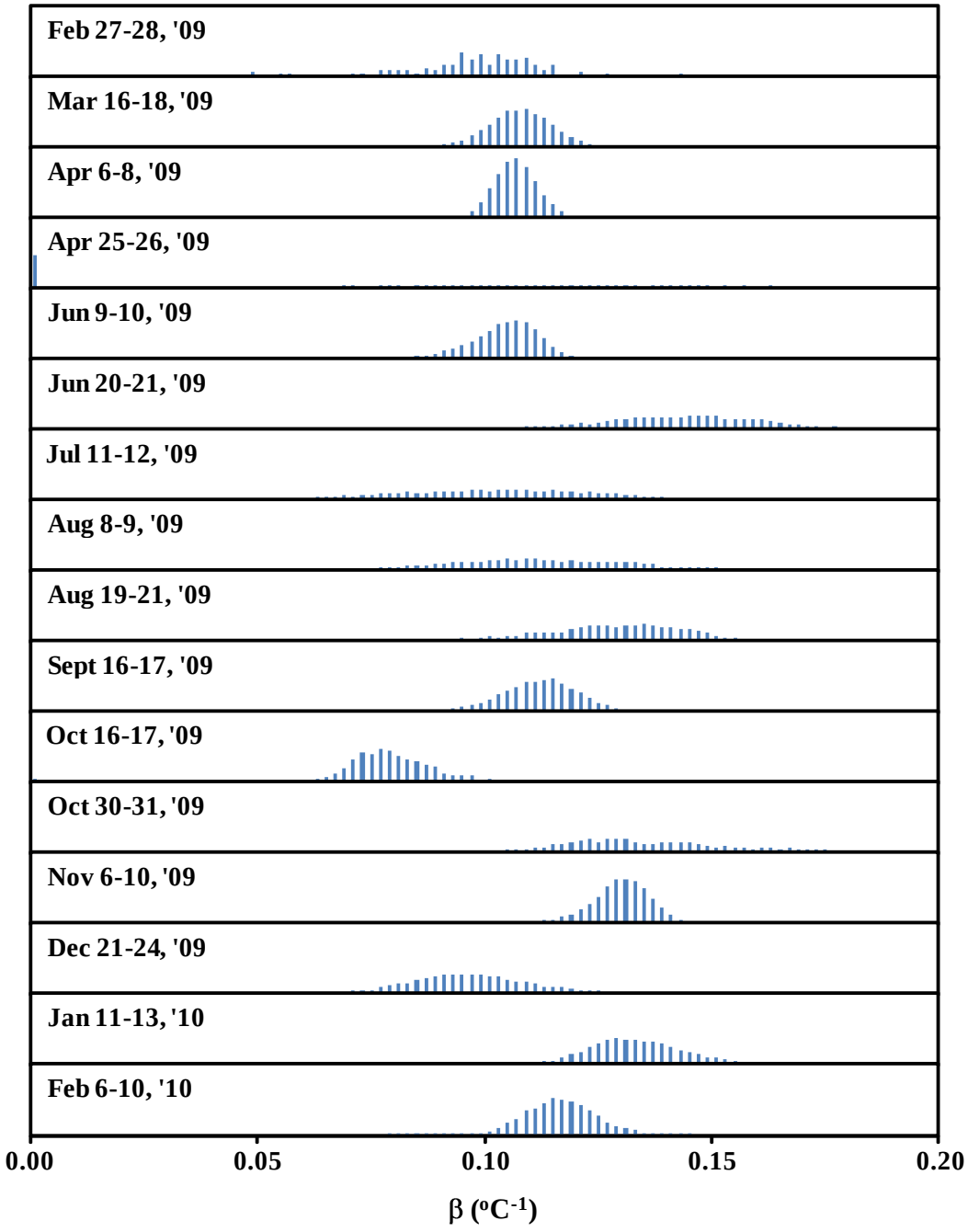

Figure B2.1.3: Ponderosa Pine A. Total MT β-factor plotted as a histogram. The probability distribution of the β-factor is shown along the y-axis where the min and max probability values are 0.0 and 0.2, respectively. β-factor values are listed on the x-axis. Each plotted box is one enclosure dataset listed in order of date sampled from top to bottom.

2.2 – Blue Spruce

Table B2.2.1: Blue Spruce. β-factor and exponential regression statistic summarized by branch enclosure experiment and emitted compound(s).

	ε MT		α-pinene		camphene		limonene	
Sample Date	β	R^2	β	R^2	β	R^2	β	R^2
Feb 16-18, '09	0.15	0.77	0.13	0.81	0.06	0.64	0.10	0.63
Feb 25-27, '09	0.09	0.75	0.11	0.79	0.05	0.49	0.06	0.60
Mar 4-6, '09	0.13	0.88	0.13	0.88	0.07	0.81	0.09	0.81
Mar 25-26, '09	0.10	0.44	0.09	0.44	0.05	0.13	0.06	0.22
May 7-8, '09	0.11	0.88	0.14	0.87	0.07	0.71	0.10	0.80
May 29-30, '09	0.11	0.76	0.13	0.81	0.08	0.77	0.10	0.83
Jul 2-3, '09	0.12	0.89	0.11	0.84	0.09	0.83	0.15	0.88
Aug 11-12, '09	0.05	0.64	0.08	0.73	0.03	0.58	0.02	0.27
Aug 21-24, '09	0.15	0.86	0.13	0.77	0.09	0.66	0.11	0.83
Sept 12-13, '09	0.02	0.45	0.17	0.99	0.00	0.00	0.04	0.93
Nov 11-14, '09	0.13	0.93	0.15	0.94	0.09	0.94	0.11	0.95
Dec 3-5, '09	0.06	0.83	0.04	0.64	0.07	0.87	0.07	0.95
Jan 17-20, '10	0.08	0.85	0.09	0.84	0.06	0.71	0.08	0.86
Feb 11-13, '10	0.07	0.64	0.06	0.54	0.08	0.81	0.07	0.63
Median	0.10		0.12		0.07		0.09	
Mean	0.10		0.11		0.06		0.08	
Std Dev	0.04		0.04		0.03		0.03	

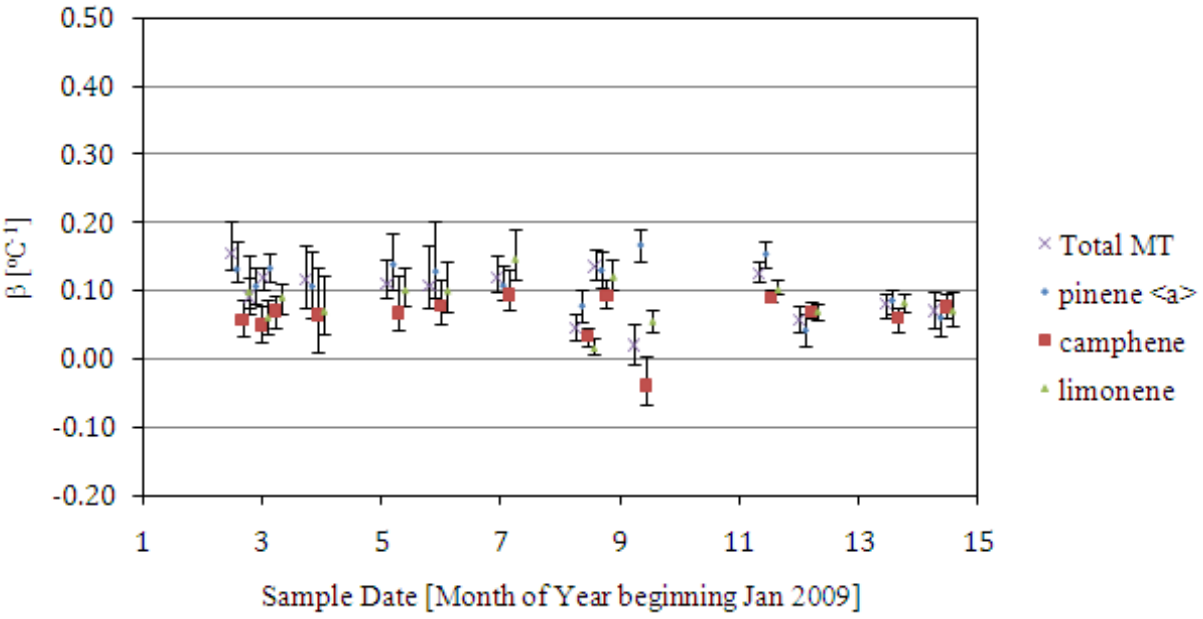

Figure B2.2.1: Blue Spruce. Measured β-factor plotted with 90% CI shown by error bars. Total MT and the three most dominant MT emitters are shown by enclosure experiment with dates slightly offset for clarity.

2.3 – Bristlecone Pine

Table B2.3.1: Bristlecone Pine. β-factor and exponential regression statistic summarized by branch enclosure experiment and emitted compound(s).

	ε MT		α-pinene		β-pinene		3-carene	
Sample Date	β	R^2	β	R^2	β	R^2	β	R^2
Feb 23-25, '09	0.28	0.94	0.19	0.89	0.21	0.88	0.23	0.88
Apr 22-24, '09	0.10	0.91	0.09	0.93	0.10	0.89	0.09	0.90
May 9-10 , '09	0.12	0.73	0.10	0.47	0.00	0.00	0.09	0.78
Jun 6-7, '09	0.16	0.50	0.11	0.61	0.10	0.60	0.12	0.53
Jun 18-19, '09	0.18	0.94	0.10	0.89	0.12	0.80	0.13	0.89
Jun 27-28, '09	0.07	0.38	0.06	0.49	0.06	0.53	0.07	0.54
Jul 7-8, '09	0.14	0.96	0.13	0.78	0.13	0.75	0.13	0.83
Jul 16-17, '09	0.14	0.74	0.11	0.73	0.10	0.71	0.11	0.71
Aug 19-21, '09	0.06	0.22	0.07	0.55	0.07	0.55	0.08	0.56
Aug 26-27, '09	0.08	0.79	0.06	0.67	0.07	0.68	0.07	0.72
Sept 29-30, '09	0.10	0.85	0.17	0.98	0.16	1.00	0.15	0.98
Oct 30-31, '09	0.13	0.94	0.14	0.96	0.14	1.00	0.16	0.97
Nov 6-10, '09	0.09	0.84	0.11	0.93	0.12	0.94	0.12	0.94
Nov 17-19, '09	0.02	0.60	0.05	0.35	0.01	0.34	0.06	0.35
Dec 15-15, '09	0.05	0.77	0.07	0.88	0.12	0.91	0.10	0.88
Jan 28-30, '10	0.11	0.91	0.11	0.90	0.13	0.95	0.12	0.92
Feb 2-4, '10	0.09	0.88	0.10	0.92	0.13	0.96	0.12	0.93
Feb 16-17, '10	0.06	0.75	0.08	0.91	0.08	0.74	0.08	0.82
Median	0.10		0.10		0.11		0.11	
Mean	0.11		0.10		0.10		0.11	
Std Dev	0.06		0.04		0.05		0.04	

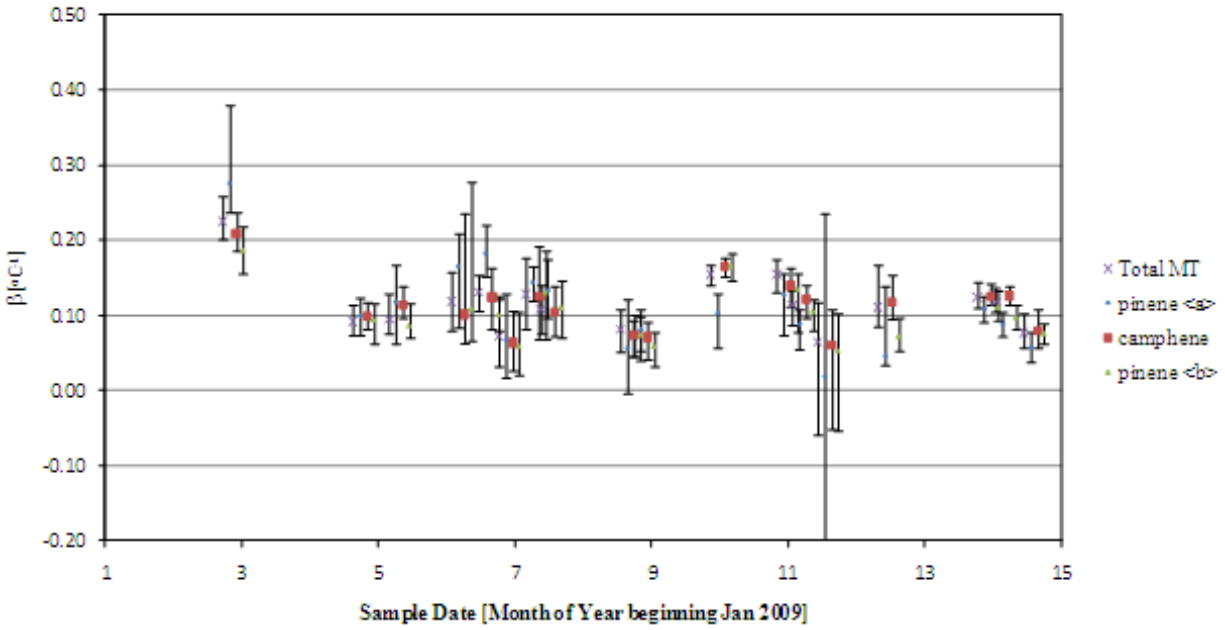

Figure B2.3.1: Bristlecone Pine. Measured β-factor plotted with 90% CI shown by error bars. Total MT and the three most dominant MT emitters are shown by enclosure experiment with dates slightly offset for clarity.

2.4 – Douglas-fir

Table B2.4.1: Douglas-fir. β-factor and exponential regression statistic summarized by branch enclosure experiment and emitted compound(s).

	ε MT		α-pinene		β-pinene		3-carene	
Sample Date	β	R^2	β	R^2	β	R^2	β	R^2
Apr 20-22, '09	0.08	0.93	0.09	0.91	0.06	0.93	0.06	0.89
May 12-13, '09	0.10	0.91	0.12	0.92	0.07	0.91	0.09	0.76
May 19-20, '09	0.09	0.94	0.09	0.90	0.09	0.93	0.12	0.97
Jun 13-14, '09	0.08	0.79	0.07	0.78	0.08	0.73	0.15	1.00
Jun 25-26, '09	0.13	0.77	0.16	0.71	0.05	0.29	0.19	0.78
Jul 8-9, '09	0.06	0.69	0.03	0.21	0.08	0.78	0.03	0.19
Jul 14-15, '09	0.04	0.10	0.00	0.00	0.04	0.10	0.00	0.00
Aug 11-14, '09	0.05	0.44	0.00	0.00	0.05	0.44	0.00	0.00
Aug 24-25, '09	0.08	0.94	0.08	0.88	0.08	0.87	0.00	0.00
Sept 15-18, '09	0.06	0.85	0.02	0.25	0.08	0.83	0.05	0.64
Oct 22-24, '09	0.12	0.87	0.10	0.90	0.10	0.93	0.09	0.60
Nov 17-20, '09	0.07	0.60	0.05	0.89	0.07	0.83	0.05	0.87
Dec 10-13, '09	0.08	0.96	0.07	0.95	0.08	0.98	0.08	0.97
Jan 22-26, '10	0.08	0.54	0.01	0.58	0.08	0.61	0.06	0.24
Feb 11-14, '10	0.12	0.70	0.14	0.78	0.13	0.71	0.08	0.33
Median	0.08		0.07		0.08		0.06	
Mean	0.08		0.07		0.08		0.07	
Std Dev	0.02		0.05		0.02		0.06	

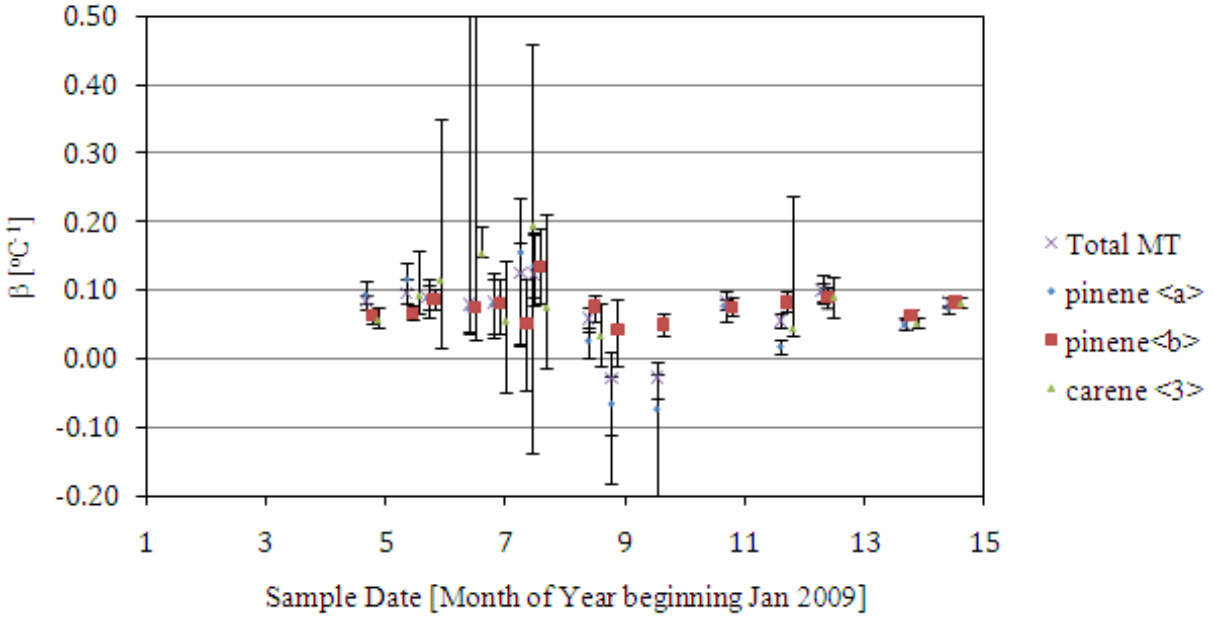

Figure B2.4.1: Douglas-fir. Measured β-factor plotted with 90% CI shown by error bars. Total MT and the three most dominant MT emitters are shown by enclosure experiment with dates slightly offset for clarity.

2.5 – Gamble Oak

Table B2.5.1: Gamble Oak. β-factor and exponential regression statistic summarized by branch enclosure experiment and emitted compound, the sesquiterpene germacrene B.

	ε SQT	
Sample Date	β	R^2
Aug 2-3, '09	0.19	0.81
Aug 15-16, '09	0.14	0.31
Aug 26-27, '09	0.14	0.69
Sept 23-24, '09	0.00	0.00
Sept 25-26, '09	0.26	1.00
Sept 27-29, '09	0.18	0.75
Oct 7-9, '09	0.09	0.84
Oct 13-16, '09	0.05	0.70
Median	0.14	
Mean	0.13	
Std Dev	0.08	

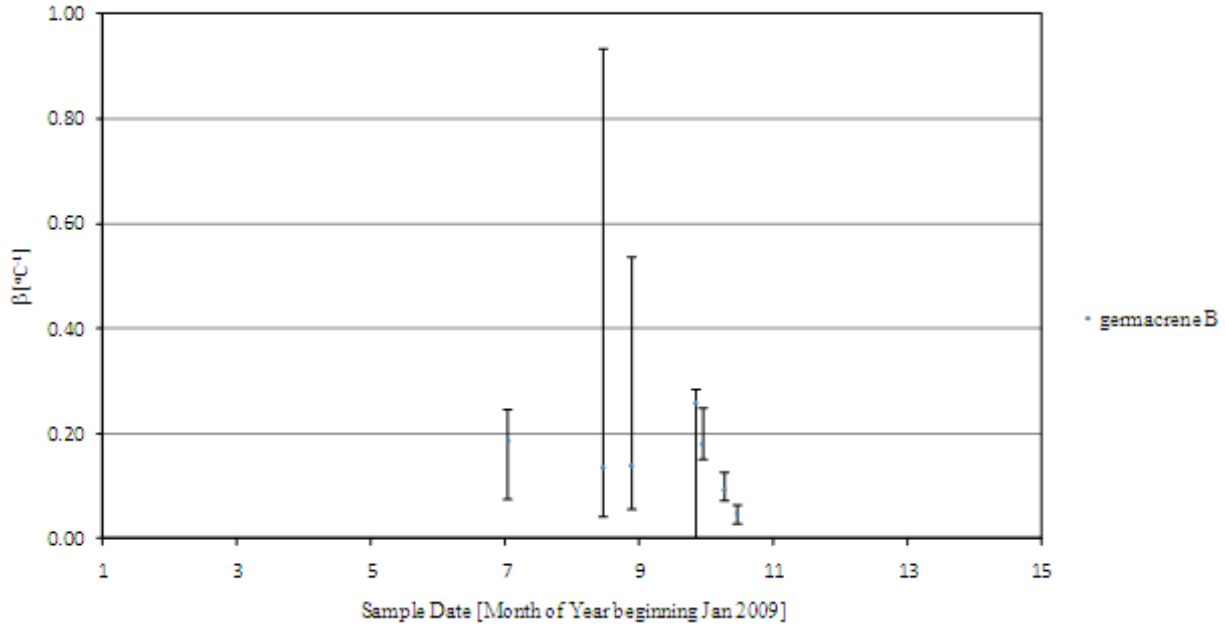

Figure B2.5.1: Gamble Oak. Measured β-factor plotted with 90% CI shown by error bars. β-factors are shown by enclosure experiment date.

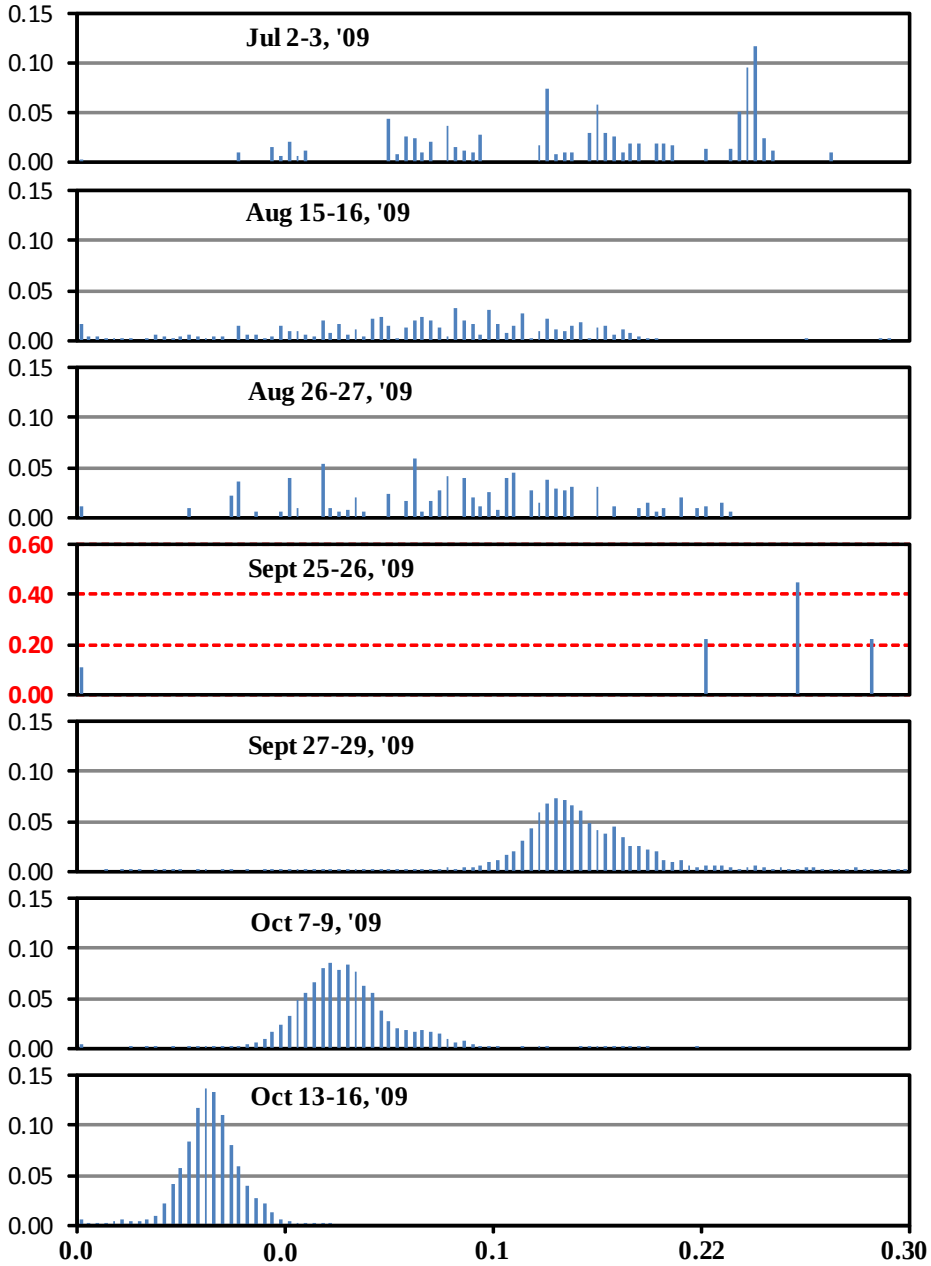

Figure B2.5.2: Gamble Oak. Germacrene B β-factors plotted in the format of a histogram. The probability distribution of the β-factor is shown along the y-axis where the min and max probability values are 0.00 and 0.15, respectively, unless otherwise stated. β-factor values are listed on the x-axis. Each plotted box is one enclosure dataset listed in order of date sampled from top to bottom.

3 – Conclusions

As discussed in Chapter 2, there are no discernable patterns in the seasonal variation of measured short term β-factors of temperature dependent BVOC emissions. Rather, the measured β-factors seem to vary around a nominal value. A generalized β-factor of 0.09 is recommended in the literature for modeling MT emission rates (Guenther et al., 1993). Several more recent studies have found larger β-factors for MT especially SQT. Ortega et al. (2008) found MT β–factors in the range of 0.12 – 0.17 $^{o}C^{-1}$ and 0.15 – 0.21 $^{o}C^{-1}$ for SQT. Seasonally averaged total MT values found in this study were between 0.10 and 0.11 for all studied vegetation other than the Douglas-fir, with a value of 0.08. While β-factors likely vary between vegetation species and type of BVOC compound, the recent findings of higher β -factors should be taken into consideration. Based on these results, the use of a β-factor of 0.09 may result in the under prediction of MT emission rates.

References:

Efron B. and Tibshirani R., 1986. Bootstrap methods for standard errors, confidence intervals, and other measures of statistical accuracy. Statistical Science, 1, 54-77.

Guenther, A.B., Zimmerman, P.R., Harley, P.C., Monson, R.K., Fall, R., 1993. Isoprene and monoterpene emission rate variability: model evaluations and sensitivity analyses. Journal of Geophysical Research, 98, 12609-12617.

Ortega, J., Helmig, D., Daly, R.W., Tanner, D.M., Guenther, A.B., Herrick, J.D., 2008. Approaches for quantifying reactive and low-volatility biogenic organic compound emissions by vegetation enclosure techniques – Part B: Applications. Chemosphere 72, 365-380.

Appendix C – C_5 to C_{15} Multi-Sorbent Sampling Cartridge

Project Duration: May – August, 2008
Conducted by Andrea Wilken, a student intern, with the guidance and assistance of Ryan Daly

Goal: A lab and field study to develop a multi-sorbent sampling cartridge for the simultaneous collection of C_5 – C15 BVOC

This report is broken into the following sections:

1.1 – Introduction
1.2 – Adsorbent Cartridge Construction Guide
1.3 – Experimental Methods
1.4 – Results/Discussion
1.5 – Comment / suggestions for improvement

1.1 - Introduction

Sorbent-based sampling techniques have widely been used for the collecting of Biogenic Volatile Organic Compounds (BVOC). Due to the broad volatility range between BVOC compounds such as isoprene (C_5H_8) and sesquiterpenes (SQT) ($C_{15}H_{24}$), sampling to date has been limited to partial collection of the total BVOC class at one time. That is, sorbent sampling of BVOC has been forced to focus on a limited portion of the total BVOC molecular weight spectrum (ie. isoprene, monoterpenes, sesquiterpenes, or a combination of two of these) at one time to avoid analyte breakthrough and/or low detection limits. In this study, combinations of sorbent materials were examined in an effort to develop a multi-sorbent based sample cartridge capable of retaining isoprene, monoterpenes and sesquiterpenes in one sample.

There are many sorbent materials available today for the sampling of BVOC. The challenges inherent in this study were in the selection of a 'strong' and 'weak' sorbent for the collection of the isoprene, most volatile, and SQT, least volatile, respectively. Helmig et al. (2004) and Pollmann et al. (2006) provided general guidelines for material selection. Helmig et al. (2004) surveyed several sorbent materials for collecting SQT samples including Tenax TA, Tenax GR, Carbotrap, Carbotrap C, Unibeads and glass beads. Likewise, Pollmann et al. (2006) described several solid-adsorbent materials for the collection of C_2-C_6 non-methane hydrocarbons including Carboxen 1000, Carbosieve S III, molecular sieve 5A, molecular sieve 4A, silica gel, Carboxen 563, activated alumina, Carbotrap and Carboxen 1016. A brief summary of their findings are described in Table C1.

Table C1: Summary of adsorbent materials for sampling of non-methane hydrocarbons.

Adsorbent study for retention of $C_2 – C_6$ NMHC'. Pollmann et al. (2006)		
Adsorbent material	**Strength**	**Comments**
Carboxen 1000	Very Strong	Versatile adsorbent for $C_2 – C_6$
Carbosieve S III	Very Strong	Poor desorption of $C_4 – C_6$. Too strong for isoprene studies
Molecular sieve 5A	Strong	Found to alter the composition of compounds. High level of contamination
Molecular sieve 4A	Medium	Best suited for compound heavier than hexane
Silica gel	Medium	Best for C_5 and larger. Difficult to handle
Carboxen 563	Strong	Versatile adsorption/desorption range applicable to $C_3 – C_6$.
Activated alumina	Medium	70-90% recovery of $C_4 – C_6$ compounds
Carbotrap	Medium	Performed best for compound C_5 and heavier. Material found to disintegrate while handling and repeated heating cycles, causing an increase head pressure through the tube.
Carboxen 1016	Strong	Good retention of near 100% for compounds C_4 and greater.

Adsorbent study for retention of SQT. Helmig et al. (2004)		
Adsorbent material	**Strength**	**Comments**
Tenax GR	Weak	SQT recovery of 90% or better. Lower recovery for oxy-SQT.
Tenax TA	Weak	SQT recovery of 90% or better. Lower recovery for oxy-SQT. Material volume loss (shrinking) was observed from repeated desorption cycles.
Carbotrap	Weak	SQT recovery of 90% or better. Lower recovery for oxy-SQT.
Carbotrap C	Weak	SQT recovery of 90% or better. Lower recovery for oxy-SQT.
Unibeads	Very weak	Poor SQT recovery with increasing relative humidity.
Glass Beads	Very weak	Poor SQT recovery with increasing relative humidity.

Based on the review listed above, Carboxen 563 and 1016 were chosen to capture high volatility BVOC as both materials exhibited complete recovery of $C_4 – C_6$ NMHC (encompassing isoprene). Carboxen 1000 was also considered, however it is believed to be too strong of an adsorbent and might not fully desorb heavier BVOC. For sampling lower volatility BVOC such as MT and SQT, Tenax GR was chosen. While Tenax TA is used in many other studies, Pollman et al. (2006) found the material to 'shrink' after repeated thermal cycles causing tunneling through the adsorbent bed. Therefore only Tenax GR was considered. Three combinations of adsorbent materials were constructed for comparison: Tenax GR only, Tenax GR & Carboxen 563, and Tenax GR & Carboxen 1016. The following sections describe

methods for making the adsorbent cartridges used here as well as an analysis of the recovery rate potential for each type of cartridge.

1.2 Adsorbent Cartridge Construction Guide

Sample adsorbent cartridges were made in house by Andrea Wilken and Ryan Daly. Glass cartridges were manufactured from borosilicate glass tubing made to the specifications shown in Figure C1 (Allen Scientific Glass Inc., Boulder, CO).

Adsorbent Cartridges were made using the following procedure:

Materials

- Borosilicate glass tube (Allen Scientific Glass Inc., Boulder, CO)
- Carboxen 563 20/45 mesh size (Supelco, Bellefonte, PA)
- Carboxen 1016 60/80 mesh size (Supelco, Bellefonte, PA)
- Tenax GR 20/35 mesh size (Supelco, Bellefonte, PA)
- Silane treated glass wool (Supelco, Bellefonte, PA)
- Stainless steel wire (Malin Co. Brook Park, OH)

- Funnel (brass Swagelok fitting with ¼" teflon ferrule)
- Long rod for packing tubes (small allen wrench or screwdriver)
- Glass wool remover (dentist tool / tweezers)
- Razor blade
- Analytical gloves

Material Preparation

All materials used for making the adsorbent cartridges must be cleaned with solvent and baked to 300^{o}C before use. Soaking the materials in methanol within a sonic bath for 20 minutes followed by a 300^{o}C bakeout is sufficient for sterilization.

Glass tubes should undergo a leak test using the Perkin Elmer ATD-400 thermal desorber prior to the addition of adsorbent. From experience, several tubes have been found to have cracked or warped ends due to manufacturing defects. A simple one minute desorbtion test using the ATD-400 can determine whether the cartridge is suitable for use.

Retention springs can be from stainless steel wire. Using a vise, secure a skinny tool (small allen wrench, screw driver, etc.) oriented vertically such that the stainless steel wire may be wrapped around it. The goal is to create a small torsion spring by wrapping the wire around the tool and cutting the ends. Holding the wire with two hands, wrap the wire around the tool 2 times (720^{o}). Upon releasing your grip, the wire should relax, forming a 90-120^{o} angle between the two sides. Using wire snips, cut the each end of the wire ¼ cm from the center circle. For efficiency, many springs can be made along the same strand of wire and cut later. All retention springs must be cleaned using the method described above.

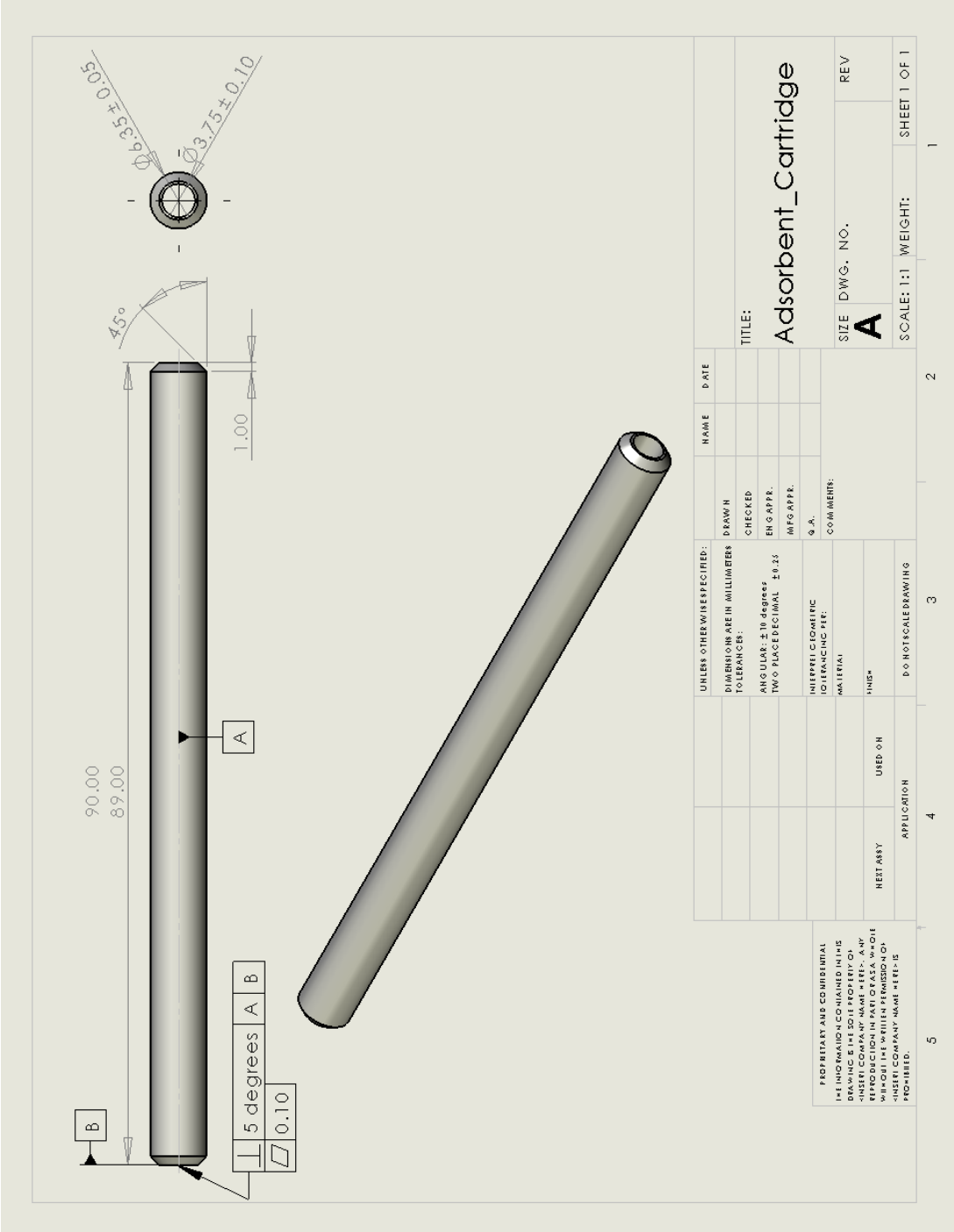

Figure C1: Manufacturing drawing for glass tubing.

Analytical Concerns

The adsorbent bed must be arranged so that the sampled compounds are absorbed first by the weaker substrate, followed by the stronger adsorbent. This is to prevent heavier compounds from becoming retained on the stronger adsorbent from which they will never thermally desorb. During practice, this means that the flow path must enter the side with the weak substrate during sampling, and reversed during desorption. Since many adsorbents look alike, it is important to take note of the three digit ID number printed on each tube. Tubes without numbers or with numbers which can be read in either direction such as 999 (666) or 606 (909) should not be used. The weakest adsorbent should always be packed on the left side of the tube when reading the number upright. (See below)

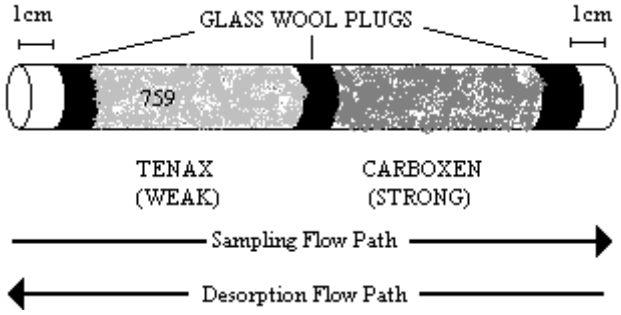

Furthermore, it is important to leave a 1cm margin on both ends of the desorption tube. This ensures that the entire substrate is heated evenly during desorption and that the entire analytical mass is thereby removed from the cartridge.

Method

1. Analytical gloves should be worn at all times to prevent contamination. Hand oils or other contaminants can easily be transferred to analytical materials through touch, posing concerns for the recovery of heavy BVOC such as SQT.
2. Extract a long strand of glass wool (a pinch, 2 in. long) from the container and bend it over itself a few times so that it forms round tip on one end. Twist the strand of glass wool into the right end of the tube (when reading the tube label left to right) 7-8mm from the end. Using a razor blade, cut the excess glass wool flush at the end of the tube. This may take a couple of tries to get a clean surface and care should be taken not to damage the glass tube end with the blade. (See below)

3. Use a clean (see above) allen wrench or some other long skinny tool to push the plug to the other end of the tube leaving a 1 cm margin from the end of the tube.
4. Add a retention spring to the end of the tube to prevent the glass wool plug from moving. The spring can protrude into the 1 cm margin if necessary. (see below)

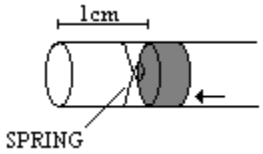

5. Adsorbent materials were added to cartridges in amounts determined by weight. The following weights were used per cartridge type:

Material	**Weight (g)**
Tenax GR only	0.24
Tenax GR / Carboxen 563	0.10 / 0.11
Tenax GR / Carboxen 1016	0.10 / 0.31

6. Using the funnel, slowly pour the weakest adsorbent in to the glass tube. Gently shake or tap the cartridge to settle the adsorbent material to the bottom. Take care not to pack or compress the material, which may lead to an increased head pressure through the tube during sampling.
7. If making a multi-adsorbent package, repeat step 2, adding a glass wool plug to the middle of the tube. This will isolate the first adsorbent from the second adsorbent. Add just enough pressure to conglomerate any loose adsorbent, but no more! Tubes that are packed too tightly will present problems during sampling by resisting airflow.
8. Repeat steps 3-6 for the second, stronger adsorbent.
9. Repeat step 2, creating a final glass wool plug to cap the stronger adsorbent material. Press a retention spring into the end of the tube, securing the right end of the adsorbent package.
10. The finished adsorbent cartridge should have approximately 1 cm between the end of the tube and the glass wool plug on both sides. You may need to increase or decrease the amount of glass wool used for plugs. (The importance is consistency)
11. Once packed with adsorbent, cartridges should undergo a pressure test. Place a vacuum pump and MFC in line with a vacuum gauge. Regulate the air flow to 500 ml min^{-1}. Place an adsorbent cartridge with the strong adsorbent side (right side when reading the cartridge left to right) towards the vacuum gauge. The observed pressure drop should not exceed 0.8”Hg. Refer to Figure below.

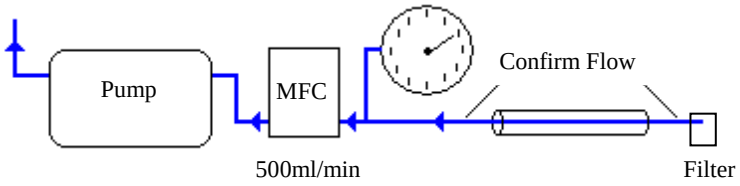

12. Condition finished cartridges for 2 hours at 325°C and 50 ml min^{-1} flow of nitrogen using one of the following methods:
    GC oven with manifold- Attach glass tubes to manifold using ¼” Vespel ferrules, orienting each tube so that the direction of flow from passed from strongest to weakest adsorbent. Control the nitrogen flow rate to ensure 50-100 ml min^{-1} pass through each tube. Ramp the GC temperature at a rate of 10°C min^{-1}.
    Perkin Elmer ATD-400- The ATD 400 should be programmed to a 60 minute desorption at 325°C for each tube. After the cycle, turn the tubes 180 degrees, and run again.

13. Update the Adsorbent Cartridge Log describing the newly constructed cartridge. Record the cartridge ID, adsorbents used and vacuum test pressure observed.

Finished cartridges are shown in Figure C2.

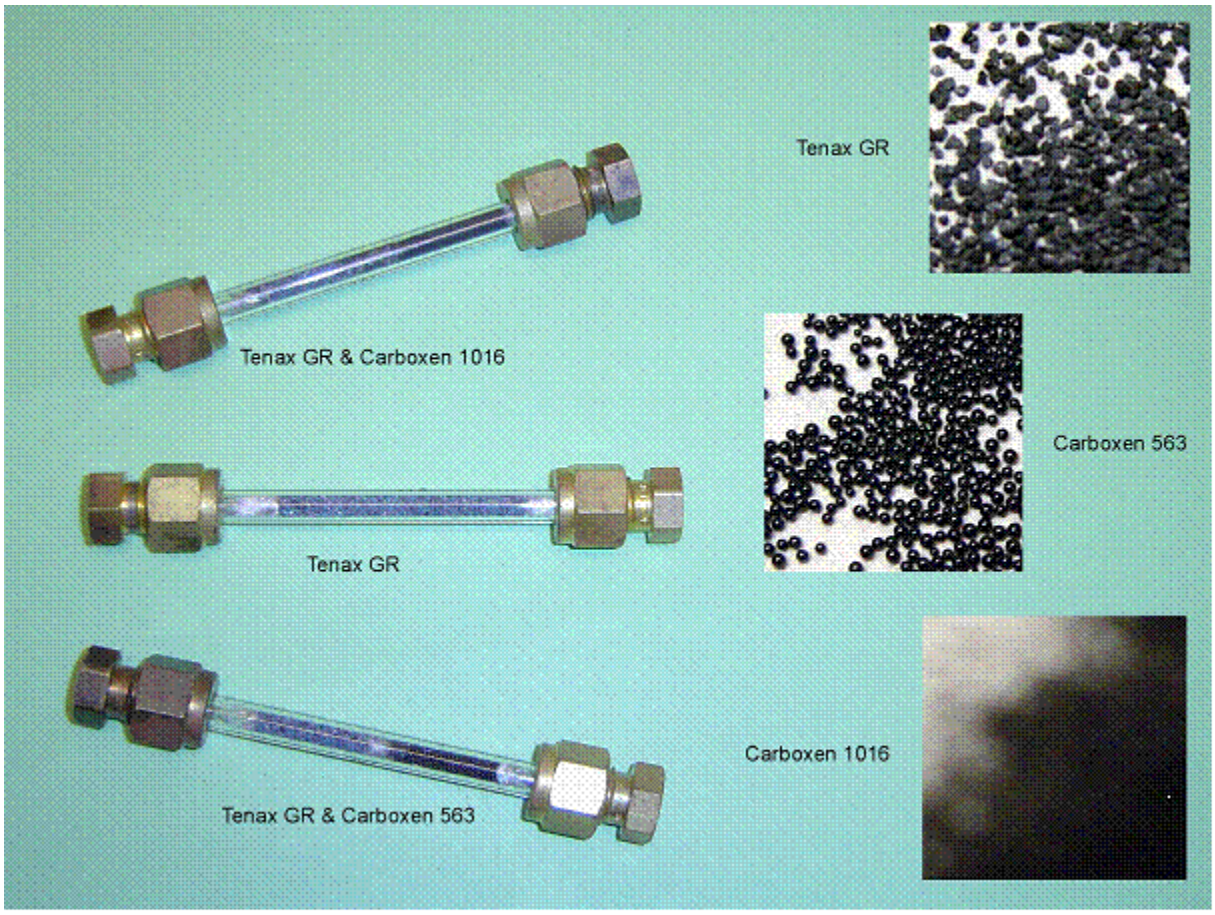

Figure C2: Finished Adsorbent cartridges.

1.3 - Experimental Methods

A capillary diffusion system (CDS) described in detail by Helmig et al. (2003) was used to generate mixing ratios between 1.0-0.1 ppmV of gas phase BVOC which were further diluted for sampling. The CDS generated a steady output of three MT (α-pinene, β-pinene and D-limonene) and a mixture of compounds from a compressed gas standard (isoprene, isooctane, n-dodecane, n-tridecane, n-tetradecane, n-pentadecane and n-hexadecane). While no sesquiterpenes were analyzed in this study, n-tetradecane and n-hexadecane span the volatility range of most SQT providing confidence that SQT were represented. The gas mixture was diluted to low ppbV levels using charcoal scrubbed air. The sampled mixing ratio per compound was 7 ppb isoprene, 10 ppb isooctane, 24 ppb α-pinene, 25 ppb β-pinene, 24 ppb D-limonene, 19 ppb n12, 20 ppb n13, 12 ppb n14, 13 ppb n15 and 11 ppb n16.

Cartridge samples were collected using the same methods used in field observations. Using an automated cartridge sampler (described in detail by Helmig et al. (2004)), samples were collected for one hour at a flow rate of 200ml min^{-1}, capturing a total volume of 12L. Sampled cartridges were then analyzed by thermal desorption GC/MS (Perkin Elmer ATD-400, Hewlett-Packard 5980/5970). Cartridges were thermally desorbed for 30 minutes at a temperature of 270^{o}C and desorption flow of hydrogen at 50ml min^{-1}. GC parameters were the following: H_2 carrier gas flow 4.8ml min^{-1}, FID H_2 46ml min^{-1}, FID air 374ml min^{-1}; GC oven program: -20^{o}C for 5 min, ramp 6^{o}C min^{-1} to 200^{o}C, hold 5 min. A cryogenic oven program starting at -20^{o}C was found to be most effective for separation of isoprene.

The gas mixture generated by the CDS was simultaneously directed to an Online-GC system through a heated injection loop. Due to the simplicity of this system, minimal losses are expected therefore providing a reference to measure recovery rates of compounds sampled onto the cartridges. The same cryogenic oven program was used for this system.

The recovery of the sampled compounds was measured as the ratio of the peak area (PA) integrated from both analytical systems. That is, recovery (R) is defined as:

$$R = \frac{PA_{GC/MS}}{PA_{Online-GC}}$$

where a higher R indicates greater recovery. This method was used due to sampling error in the experiments. The true sample flow rate used during cartridge collection is unknown due to user error, a problem that was not discovered until the last weeks of the experiment. A more valid method for analyzing recovery would be to calculate the mixing ratio of each compound from both cartridge and Online-GC sample. Evaluating the ratio of mixing ratios would provide far greater insight than the comparison of peak area.

1.4 – Results/Discussion

Recovery rate analysis was broken into two parts: MT compounds and compressed gas compounds (isoprene, isooctane, n12-n16). It was discovered that sampling all compounds simultaneously was not desirable due to drastic differences in concentration (ppb for MT and ppm for compress gas compounds). Ten cartridges of each type of adsorbent package were sampled simultaneously with injection to the Online-GC. Each cartridge was then run on the GC/MS. Peak areas were integrated and compared, shown in Figures C3 and C4. Figure C3 shows general agreement between all three cartridge types for the heavier n12-n16 compounds. The single adsorbent Tenax GR cartridges displayed zero recovery of isoprene and isooctane, a

finding that was expected. The cartridges with Carboxen 1016 showed slightly greater recovery of isoprene than the cartridges with Carboxen 563. All three cartridge types exhibited good recovery of MT, however the cartridges filled with Carboxen 563 were heavily contaminated making integration very difficult for some compounds such as β-pinene which co-eluded with a contaminant.

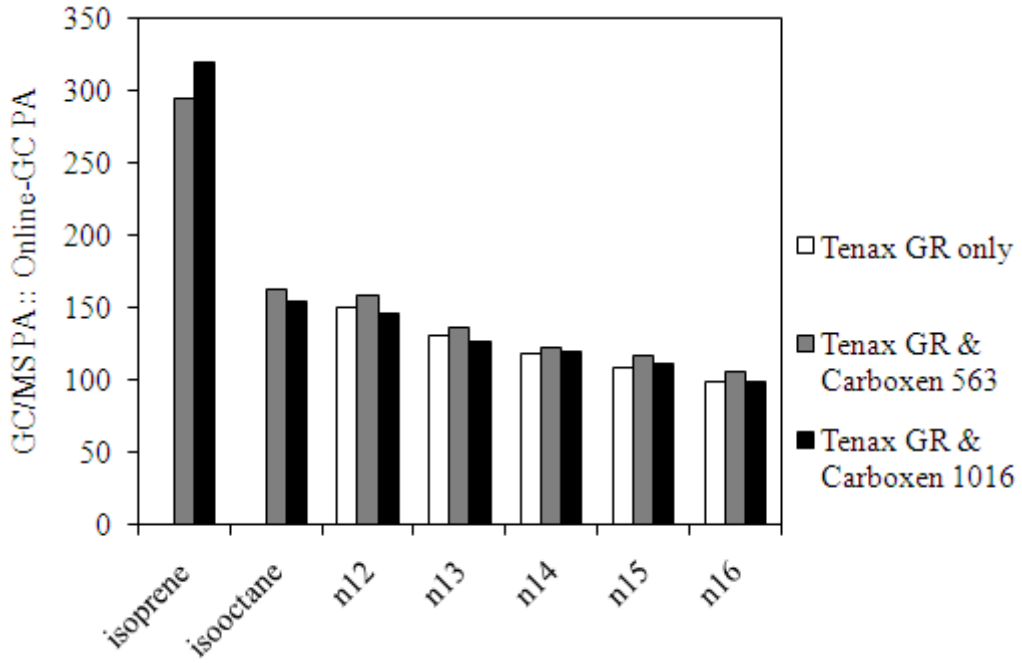

Figure C3: Recovery of C_5-C_{16} for each type of adsorbent package, shown as the ratio of the peak areas (PA) of the analytical cartridge desorber GC/MS system 'GC/MS' and the online GC coupled to the capillary diffusion system 'Online-GC'.

The contamination of all the Carboxen 563 filled tubes was thoroughly investigated and found to be attributed to the Carboxen 563 adsorbent material itself. This was determined by constructing two new multi-adsorbent cartridges (Tenax GR and Carboxen 563), running them on the GC/MS system at each step of the production process. Starting with clean, empty glass tubes the chromatograms were extremely clean. After adding Tenax GR and glass wool plugs, few contaminant peaks were observed. After adding the Carboxen 563, many more contaminant peaks were observed, most of which eluted where MT were expected. The distributor of the Carboxen 563 was notified of the apparent contamination. However, they were unwilling to replace the material. The differences between the Carboxen 1016 and 563 adsorbent packages may be seen in Figure C5.

Both multi-adsorbent cartridges exhibited good recovery of all compounds between C_5 and C_{16}, proving that they are both capable of measuring the full spectrum of BVOC simultaneously. However, due to the contamination level of the Carboxen 563, its use in the production of multi-adsorbent packages is not recommended. Therefore, the multi-adsorbent cartridge composed of Tenax GR and Carboxen 1016 is favored for the simultaneous measuring of gas phase BVOC ranging from isoprene to sesquiterpenes.

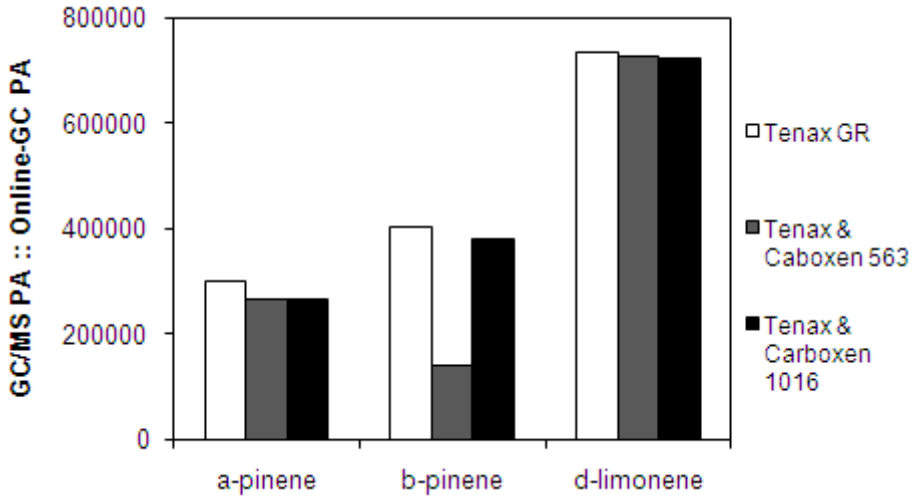

Figure C3: Recovery of C_5-C_{16} for each type of adsorbent package, shown as the ratio of the peak areas (PA) of two analytical instruments.

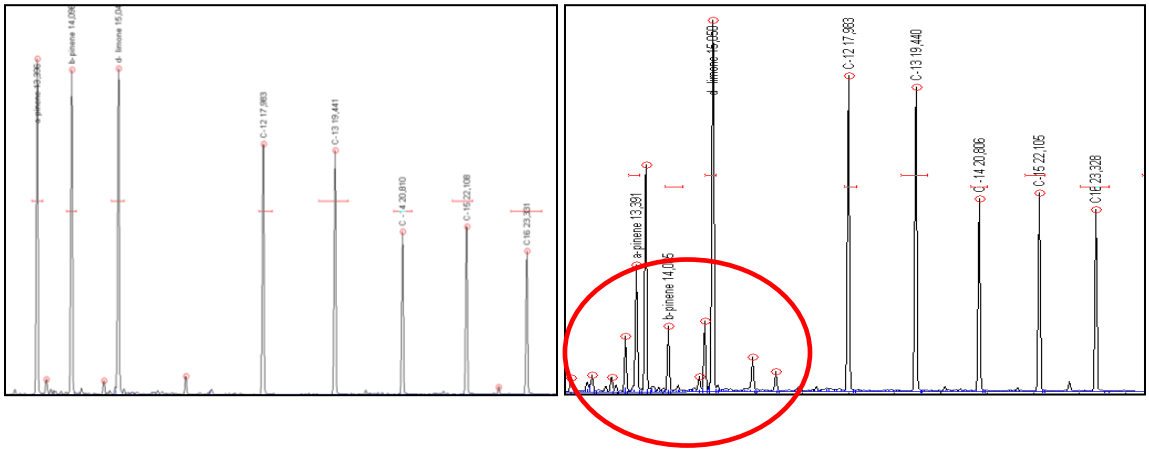

Figure 5: Difference between contamination levels of Carboxen 1016 (left) and Carboxen 563 (right).

1.5 Comments / Suggestions for Improvement

This was a study conducted by a visiting undergraduate student with a background in analytical chemistry. Due to an unfortunate bicycle crash in her second week, Andrea was incapable of using both of her arms for an entire month. This limitation severely impacted the productivity of the study, limiting the amount of data collected to very few samples. Although the results seem fairly conclusive that a multi-adsorbent cartridge composed of Tenax GR and Carboxen 1016 are suitable to the measurement of isoprene through SQT, more data could show more conclusive evidence by proving the observed mixing ratios of cartridge and Online-GC compared well. Additionally, an investigation into breakthrough volumes would provide more information on the limits of these cartridges for field studies. Finally, a study on the time period these cartridges are capable of retaining the higher volatility compounds once sampled would

provide useful insight into the amount of time sample cartridges may be stored before run by GC/MS.

A further investigation into the capability of the multi-adsorbent cartridge for monitoring high-volatility NMHC has been conducted by Ryan Daly using a compressed gas standard containing low molecular weight compounds ranging from ethane to octane. Using the known mixing ratio of each compound, a recovery analysis was investigated and briefly summarized here. Mixing ratios of the compounds ranged from high pptV levels to 10 ppbV. Using similar sampling methods used in field studies, cartridges composed of the Tenax GR & Carboxen 1016 adsorbent package combination were used to sample the gas. A needle valve controlled the flow rate to 250ml min^{-1}. Cartridges were sampled for increments of 30 to 75 minutes collecting a total volume of 8 to 20 liters. The recovery rates for 16 integrated peaks, representing 17 compounds, are shown in Figure C6. Recovery rates reported here are the ratio of the observed mixing ratio to the known theoretical mixing ratio for each compound. That is:

$$R = \frac{MR_{observed}}{MR_{theoreticd}}$$

Clearly, the Tenax GC & Carboxen 1016 multi-adsorbent cartridges demonstrate excellent recovery of compounds between C_5 isopentane and higher. Unfortunately, this example exhibited a co-ellusion of pentane and isoprene (using a GC oven program ranging between 40°C to 200°C). However, by integrating and entire peak and accounting to the mixing ratios of both compounds, recovery of ±10% was observed. Furthermore, a second desorption analysis for each sample cartridge confirmed complete desorption of all compounds from the adsorbent package, Figure C7.

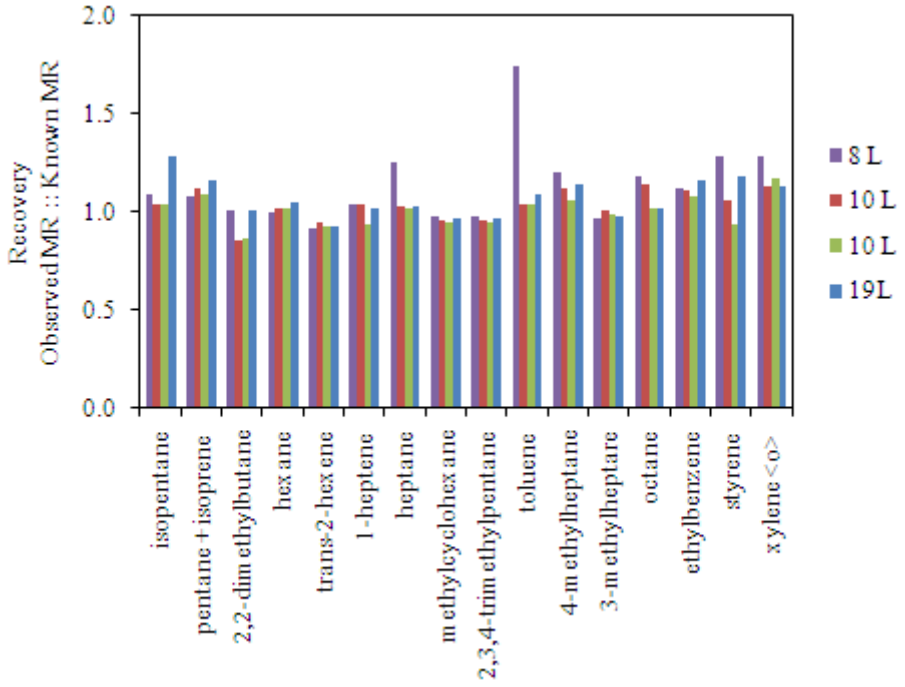

Figure C6: Recovery of C_5 – C_8 for ranging in volume from 8-19 liters.

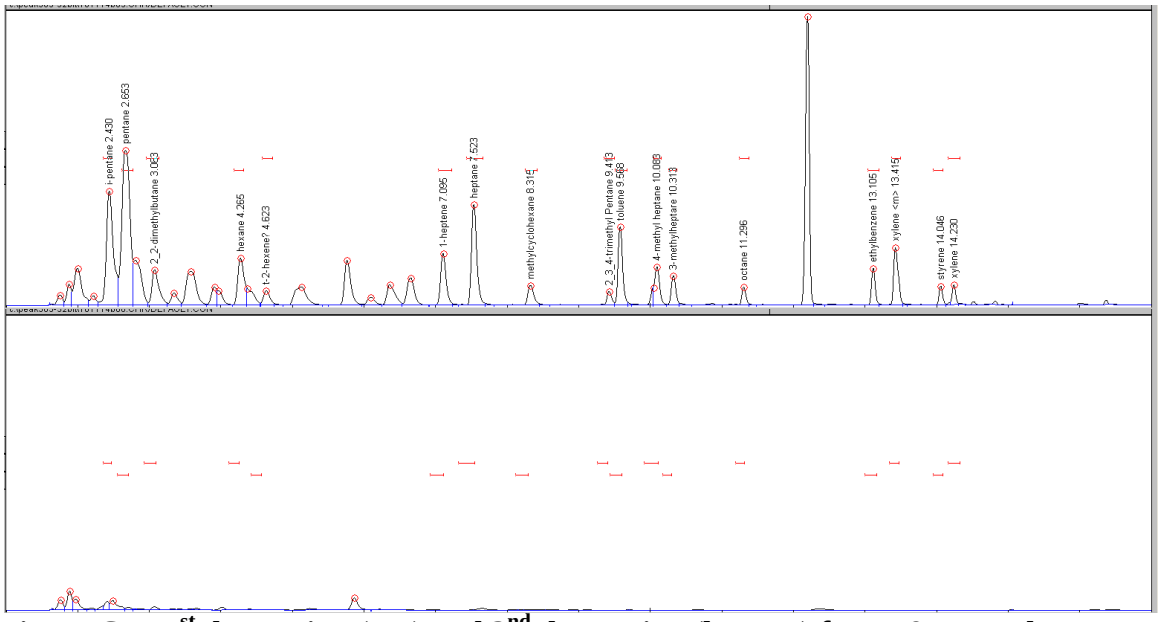

Figure C7: 1st desorption (top) and 2nd desorption (bottom) for a 19L sample.

References

Helmig, D., Revermann, T., Pollmann, J., Kaltschmidt, O., Hernández, A.J., Bocquet, F., David, D., 2003. Calibration system and analytical considerations for quantitative sesquiterpenes measurements in air. Journal of Chromatography A, 1002, 193-211.

Helmig, D., Bocquet, F., Pollmann, J., Revermann, T., 2003. Analytical techniques for sesquiterpenes emission rate studies in vegetation enclosure experiments. Atmospheric Environment, 38, 557-572.

Pollmann, J., Helmig, D., Hueber, J., Tanner D., Tans, P., 2006. Evaluation of solid adsorbent materials for cryogen-free trapping-gas chromatographic analysis of atmospheric C2-C6 non-methane hydrocarbons. Journal of Chromatography A, 1134, 1-15.

Appendix D – SQT Recovery Rate Analysis: Loss to Experimental Materials

Project Duration: September – October, 2009
Conducted by Éva Joó with the guidance and assistance of Ryan Daly. Éva was a visiting graduate student from Gent University, Belgium.

Goal: A laboratory study to examine potential loss of SQT to adhesion to enclosure material over hot/cold diurnal cycling.

Introduction

Previous studies have shown heavy, low volatility compounds such as nonylbenzene (NB) exhibit diurnal variation (higher mixing ratios observed during warm day time than cold night periods) (Ortega et al., 2008). These findings pose great analytical challenges for accurately measuring sesquiterpenes (SQT) emission rates from vegetation using the branch enclosure method. In this study, diurnal recovery rate losses forced by diurnal cycling were investigated in a controlled laboratory setting. A capillary diffusion system was used to generate low level mixing ratios of nine hydrocarbon compounds of varying volatility that were flown into an empty bag enclosure. Mixing ratios were monitored at the inlet and outlet of the enclosure by adsorbent cartridge sampling with subsequent GC/MS analysis. The enclosure was placed outside of an office window exposed to direct sunlight and outdoor temperatures ranging from 0^{o}C to 40^{o}C.

Experimental Methods

Capillary Diffusion System (CDS)

A CDS described by Helmig et al. (2003) was used to generate ppbV levels of low volatility SQT and aromatic compounds. Briefly, the CDS was setup with nine channels, each used to generate one of the following compounds: 1,3,5-triisopropylbenzene (tIPB); nonylbezene (NB); aromadendrene (ARO); β-caryophyllene (CAR); α-humulene (HUM); caryophyllene-oxide (CAROX); neoclovene (NEO); isolongifolene-9-one (ILO); δ-cadinene (CAD). Any number of the nine compounds could be selected for sampling at one time.

Experimental Setup

A purge flow rate of 12 L min^{-1} served to dilute and carry the gas mixture generated by the CDS to the empty bag enclosure. The purge flow was drawn from ambient outdoor air and purified using a combination of a particulate filter, MnO2 ozone scrubber and activated Carbon scrubber before mixing with the CDS. The purge flow rate was controlled using a rotometer. Once mixed with the CDS, a 50m line of 3/8" teflon tubing carried the gas mixture to the empty bag enclosure installed outside of an office window. Three automated adsorbent cartridge samplers were used for monitoring analyte mixing ratios. The first was located immediately after the purge air mixed with the output of the CDS to measure 'maximum' concentrations of the compounds of interest. Two more cartridge samplers were placed at the inlet and outlet of the bag enclosure. A datalogger recorded ambient temperature and light readings and well as temperature and relative humidity within the enclosure. Figure D1 shows the experimental setup in more detail. Figure D2 shows the enclosure assembly on the south facing side of the building.

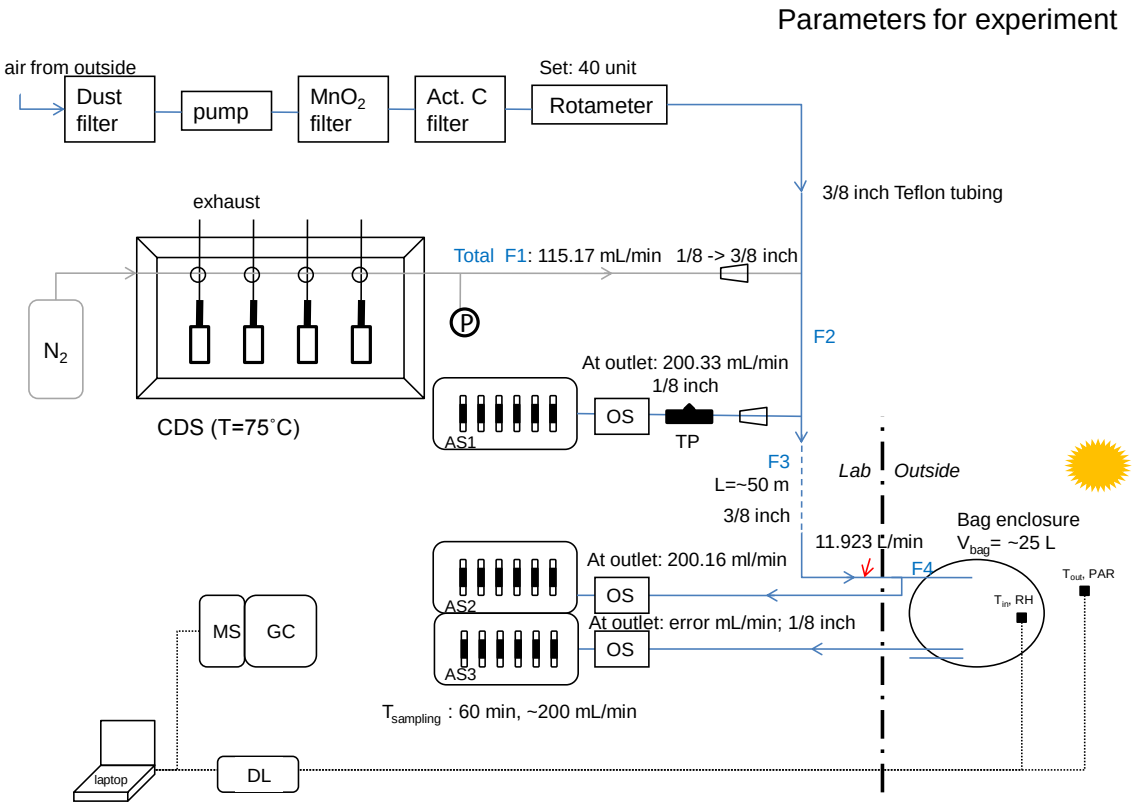

Figure D1: Experimental Setup. OS – ozone scrubber, DL – datalogger, TP – optional T connection with septa, AS – autosampler.

Figure D2: Empty bag enclosure assembled on the outside of the building.

GC/MS-FID analysis

Samples were collected onto multi-adsorbent cartridges composed of Tenax GR & Carboxen 1016. Once collected, sample cartridges were analyzed by thermal desorption GC/MS with FID detection (Perkin Elmer ATD-400, Hewlett-Packard 5980/5970). Cartridges were desorbed under 50 ml min^{-1} H2 for 30min at 300^{o}C. Following secondary focusing, a H2 carrier gas transferred the sample to the GC. The following GC parameters were used: H_2 carrier gas flow 4.8ml min^{-1}, FID H_2 46ml min^{-1}, FID air 374ml min^{-1}; GC oven program: 40^{o}C for 5 min, ramp 6^{o}C min^{-1} to 200^{o}C, hold 5 min. FID detection was used for quantitative analysis while the MS was used for identification of peaks.

Results

Following GC/MS analysis, compounds were analyzed for recovery by comparison of the observed mixing ratios measured at the inlet and outlet of the enclosure. Striking discoveries were made with regard to the diurnal behavior of many of the compounds. Previous studies have indicated that heavier, lower volatility compounds exhibit low recovery at night while a surplus is observed during the warmer day period. These observations are believed to be caused by compound settling to material surfaces during cold nighttime periods. Therefore, lower than expected abundances are observed. With daytime warming, the excess abundance from nighttime accumulation led to greater than expected missing ratios. Results from this study do not support these findings. Rather, the recovery rates of some of the heavier compounds such as humulene (HUM) and δ-cadinene (CAD) demonstrated opposite trends with lower recovery during peak daylight and high temperatures.

Recovery rates for each compound may be seen in Figure D3. It should be noted that many of the SQT studied do not exhibit any diurnal cycling trends. TIPB, NEO, CAR, AROM demonstrated excellent recovery accurate to within 5% regardless of enclosure temperatures and time of day. However, as noted earlier, interesting recovery rates were observed for HUM and CAD. Both compounds show good recovery accurate to within 10% during nighttime periods. However, with daylight the recovery rates drop to as low as 50%. These observations may be explained by increased photolysis during day periods. Increased levels of ozone within the enclosure may account for the degradation on these compounds. However, ozone reaction rate constants do not directly explain the loss (see Pollmann et al., 2005). Additionally, care was taken to ensure removal of ozone from the enclosure purge flow through the use of a MnO_2 ozone scrubber as well as activated carbon scrubber. Ozone levels were not measured from the enclosure.

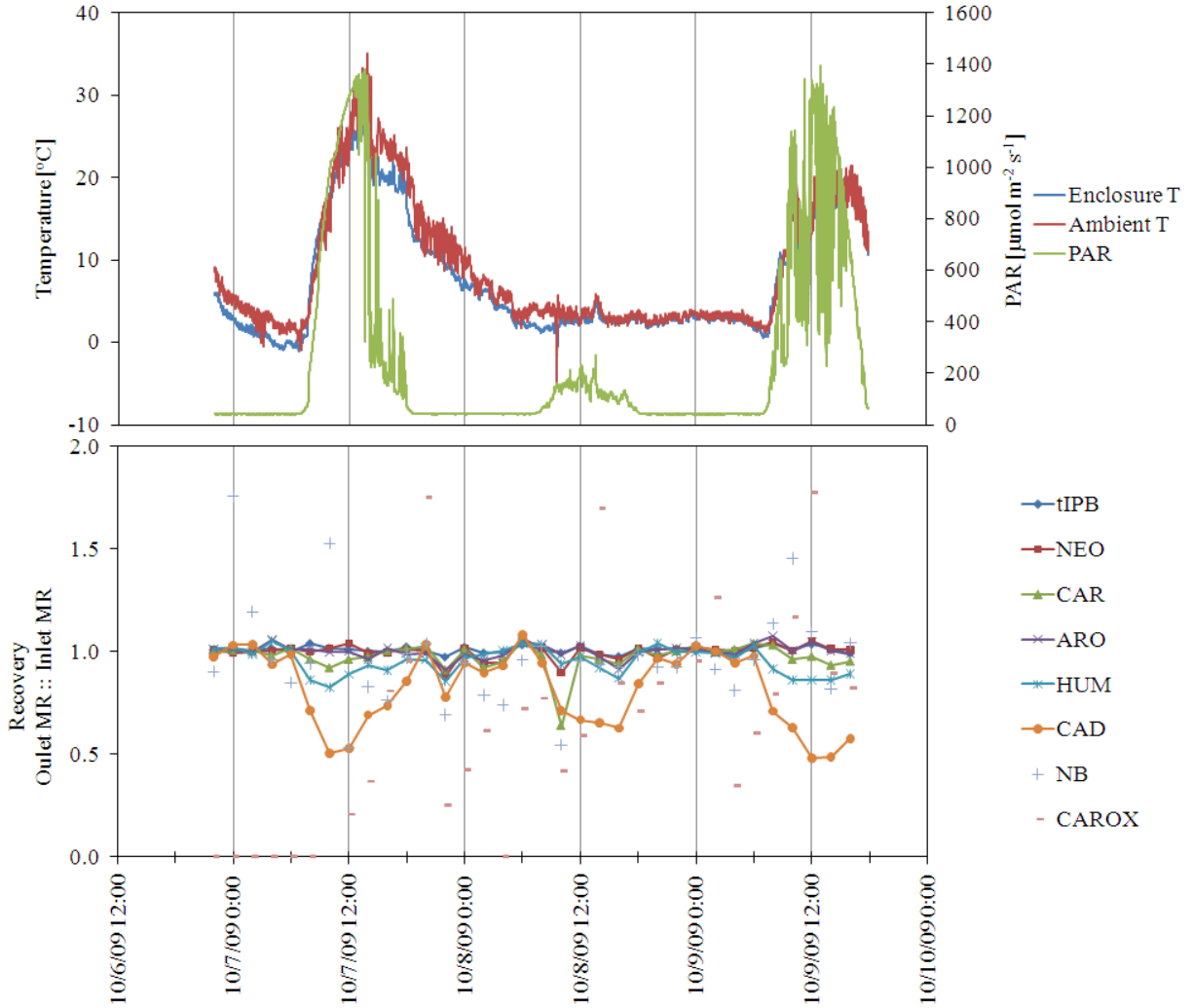

Figure D3: Temperature and light levels are shown in comparison with the recovery rates observed for each of the SQT compounds over a three day period.

Unfortunately, peak integration of NB and CAROX proved difficult due to co-elusion of the two compounds and incomplete desorption. Quantification of these compounds were attempted, however, the resulting mixing ratio estimations varied widely as shown in Figure D3. A second desorption analysis found NB was not fully recovered. Desorption time and temperature were adjusted from 20min to 30min and 275 to 300 ^{o}C to ensure complete removal of NB for future studies.

Discussion

Recovery rates of SQT compounds were analyzed for potential loss to bag enclosure material surfaces over diurnal temperature cycling. Expected diurnal recovery trends reported in other studies were not observed. Most SQT compounds displayed excellent recovery between enclosure outlet and inlet samples regardless of the period of day and temperature exposure. These findings provide confidence that measurements of at least low to mid-range volatility SQT from enclosure studies are representative of true levels. Surprisingly, δ-cadinene and caryophyllene-oxide exhibited significant recovery loss during peak daylight and temperature.

Losses are believed to be induced by photolysis, possibly as a result of enhanced ozone within the enclosure. Daytime SQT recovery loss has not been reported in the literature (when care is taken to eliminate ozone and other reactive gases from the enclosure purge flow) and warrants further investigation. For future studies, we recommend monitoring additional parameters such as ozone and NO_X at the enclosure inlet and outlet to help interpret any sort of active photochemistry. Additionally, it would be beneficial to select additional heavy SQT such as α-farnesene and cedrol for further investigation into diurnal recovery cycling that has been observed in other studies for NB. Care should be taken to make certain the compounds generated by the CDS due not co-elude during GC/MS analysis. Repeating this study for a complete range of SQT volatility as well as a comprehensive photochemistry analysis would be beneficial for a complete assessment of expected recovery rates when using the bag enclosure technique.

References:

Helmig, D, Revermann, T., Pollmann, J., Kaltschmidt, O., Jimenez-Hernandez, A., Bocquet, F., David, D., 2003. Calibration system and analytical considerations for quantitative Sesquiterpene measurements in air. Journal of ChromatographyA. 1002, 193-211.

Pollmann, J., Ortega, J., Helmig, D., 2005. Sampling of atmospheric sesquiterpenes: sampling losses and mitigation of ozone interference. Environmental Science Technology, 39, 9620.

Ortega, J., Helmig, D., Daly, R.W., Tanner, D.M., Guenther, A.B., Herrick, J.D., 2008. Approaches for quantifying reactive and low-volatility biogenic organic compound emissions by vegetation enclosure techniques – Part B: Applications. Chemosphere 72, 365-380.

Appendix E: Analyte Recovery from Branch Enclosure Studies

Introduction

Biogenic volatile organic compounds (BVOC) are technically difficult to measure due to low ambient concentrations, low-volatility and short atmospheric lifetimes. A measurement technique often used to overcome these measurement challenges has been termed the branch enclosure technique. In this study, an external gas standard composed of compound chosen to encompass the volatility range of monoterpene (MT) and sesquiterpene (SQT) was used to measure the recovery rate of BVOC while utilizing the branch enclosure method. Results of the observed recovery are discussed here.

Experimental Methods

The branch enclosure method used in this study is described in detail by Ortega et al. (2008). A reference standard of ppm-level aromatic compounds was introduced to the enclosure purge-line as a method of monitoring analyte recovery rates (Helmig et al., 2006). The gas standard was composed of low-reactivity and non-biogenically emitted aromatic compounds (deuterated toluene [TOL]; 1,3,5-trimethylbenzene [IPB]; 1,2,3,4-tetrahyrdronaphthalene [THN]; 1,3,5-tri-isopropylbenzene [TIPB]; n-nonylbenzene [NB]) selected to bound the retention times of MT and SQT GC elution. This mixture was added to the enclosure purge line to achieve mixing ratios near a 10 ppb level. By simultaneously sampling from the inlet and outlet of the branch enclosure, recovery rates for these five compounds were monitored throughout the sampling season.

Results

Figure E1 reports the recovery rate, defined as the ratio of outlet to inlet concentration, for samples collected in January 2010. All compounds other than NB display good agreement between inlet and outlet sample lines. This indicates full recovery of MT and at least low-volatility SQT may be expected. However, NB clearly exhibits a strong diurnal pattern with low recovery rates (as low as 50%) in cold and dark conditions and high recovery (in excess of 200%) during warmer daylight periods. This trend may be explained by compounds adsorbing to material surfaces (likely the enclosure bag and vegetation) in cold temperatures resulting in low recovery, followed by excessive concentrations with warming conditions. While this case illustrates poor recovery in the cold winter months, similar patterns were observed in the warmest summer months as well. In August, recovery of NB varied from 60% at a temperature low of 10 ^{o}C at night and peaked at 150% during the hottest sample of 40 ^{o}C.

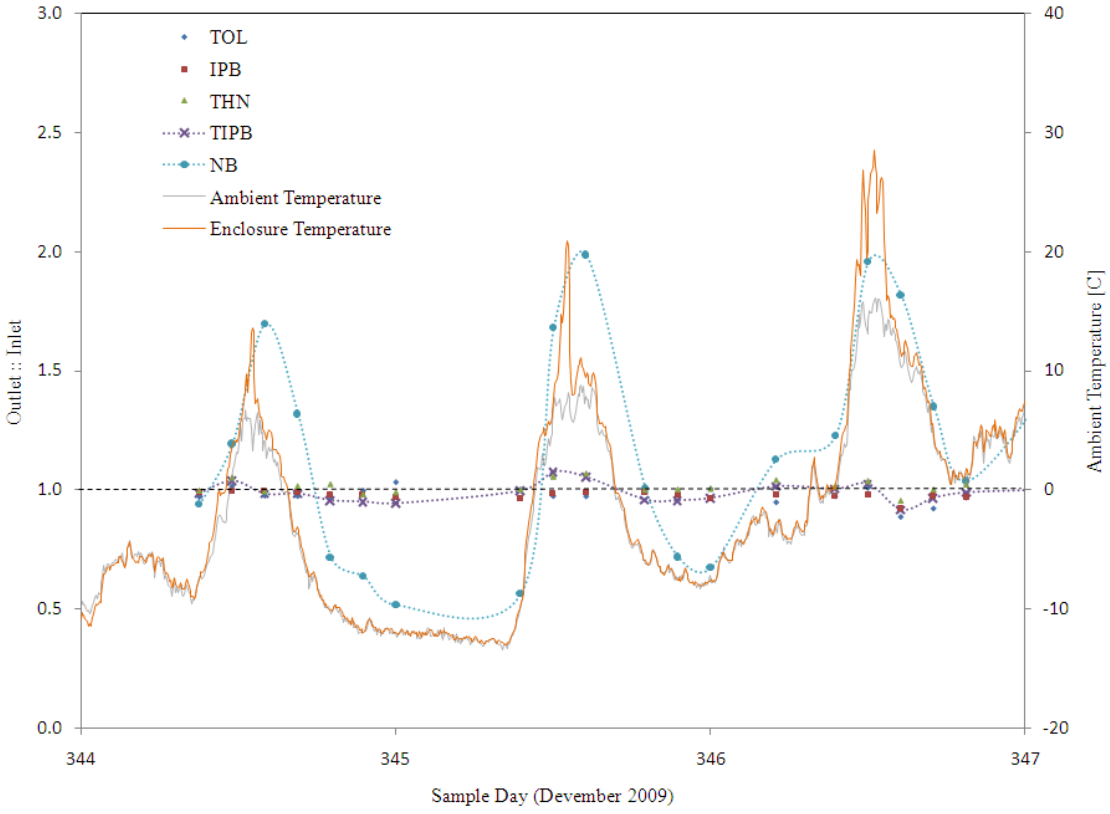

Figure E1: Aromatic recovery rate outlet::inlet for the five reference standard compounds. TIPB and NB are shown with basic curved lines to help illustrate the diurnal recovery rates. Ambient outdoor and enclosure temperatures are shown as solid lines.

These findings draw into question whether or not all SQT are fully recovered with enclosure methods or if heavier SQT may exhibit similar diurnal loss rates analogous to that of NB. In this study, SQT were not found in large enough quantities to further investigate potential recovery loss. The Gamble Oak was the largest SQT emitter, predominantly of germacrene B which falls more or less in the middle of the SQT volatility range. Minimal losses of germacrene B are expected.

References:

Helmig, D., Bocquet, F., Pollmann, J., Revermann, T., 2004. Analytical techniques for Sesquiterpene emission rate studies in vegetation enclosure experiments. Atmospheric Environment 38, 557-572.

Ortega, J., Helmig, D., Daly, R.W., Tanner, D.M., Guenther, A.B., Herrick, J.D., 2008. Approaches for quantifying reactive and low-volatility biogenic organic compound emissions by vegetation enclosure techniques – Part B: Applications. Chemosphere 72, 365-380.

Appendix F – Published Paper: PTR-MS for measuring SQT

'Measurement of atmospheric sesquiterpenes by proton transfer Reaction-mass spectrometry (PTR-MS)'

By S., Kim, T., Karl, D., Helmig, R., Daly, R., Rasmussen, and A., Guenther.

Published in Atmospheric Measurement Techniques, 2, 99-112, 2009.

Project Duration: May – June 2008
Conducted by Saewung Kim with the assistance of Ryan Daly. Saewung was participating in NCAR's Advanced Study Program.

Goal: A laboratory study to explore the feasibility of measuring atmospheric sesquiterpenes (SQT) concentrations using Proton-Transfer-Reaction Mass Spectrometry (PTR-MS)

Introduction

Sesquiterpenes (SQT) ($C_{15}H_{24}$) represent a class of terpinoid compounds commonly emitted from vegetation. SQT have received increasing amounts of attention due to their role in plant biology and atmospheric chemistry. SQT are believed to act as biological signals acting in plant to plant communication as well as defense against herbivory attack. Additionally, SQT are believed to participate in ozone and secondary organic aerosol chemistry with important impacts on human and plant health, radiative forcing and atmospheric composition. Measurements of SQT have proven difficult due their low volatility and reactive nature. SQT are most commonly measured using pre-concentration techniques with subsequent analysis by GC/MS from enclosed vegetation. Very few studies have attempted measurements of SQT in ambient air. Proton-Transfer-Reaction Mass Spectrometry (PTR-MS) has recently emerged as a potentially powerful tool for measuring SQT due to its high sensitivity and fast time resolution. Due to the limited number of studies have attempted measurement of SQT using PTR-MS, several unknowns remain to be answered (Steinbacher et al., 2004; Lee et al., 2006; Boy et al., 2008).

In this study, an intercomparison between PTR-MS and GC/MS provided a method for assessing the capabilities of PTR-MS for the measurement of atmospheric SQT. These results contributed to a larger evaluation of PTR-MS for measuring SQT including instrument mass discrimination, SQT fragmentation patterns and other analytical characteristics which were applied to estimating ambient air measurements of SQT at the PROPHET Field site collected in 2005. The combination of these findings has led to a publication by Saewung Kim in 2009:

Kim, S., Karl, T., Helmig, D., Daly, R., Rasmussen, R., Guenther, A., 2009. Measurement of atmospheric sesquiterpenes by proton transfer reaction-mass spectrometry (PTR-MS). Atmospheric Measurement Techniques 2, 99-112.

Experimental Methods

A Capillary Diffusion System (CDS) described in detail by Helmig et al. (2003) was used to generate a mixture of six sesquiterpenes and one aromatic compound. Briefly, each SQT was generated by diffusion through a specified glass capillary, mixed with scrubbed N2. This gas mixture was then diluted to mixing ratios on the order of 1-10 ppbV using zero-air. Theoretical concentrations of each compound were measured by GC-FID after direct injection from the CDS. Measurement of the diluted gas stream occurred simultaneously by PTR-MS. Through a comparison of the mixing ratios estimated by both systems, the PTR-MS was assessed for its capability to measure SQT. A schematic describing the CDS is shown in Figure F1.

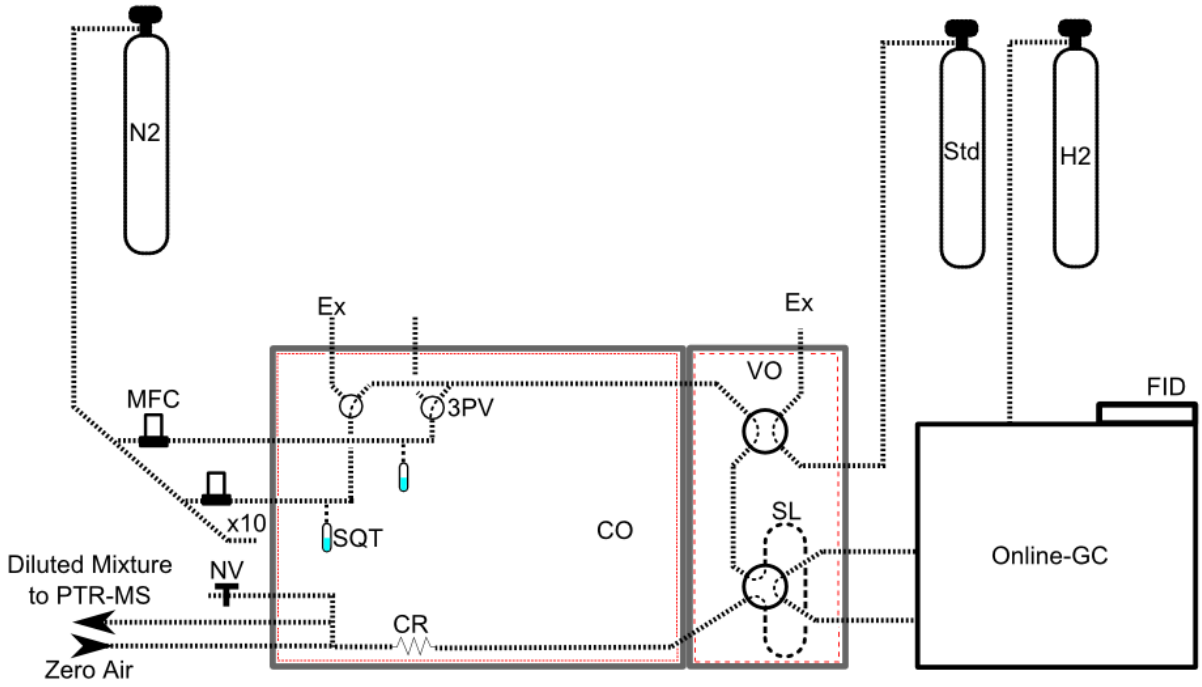

Figure F1: Schematic of CDS for generating SQT mixture. Abbreviations are the following: CO: capillary vial oven, heated to 75°C; CR: capillary resistance; Ex: exhaust; MFC: mass flow controller; NV: needle valve, used for further dilution; SL: sample loop; SQT: vial housing liquid sesquiterpenes standard with capillary; Std: hydrocarbon reference standard (isoprene, isooctane, n-dodecane – n-hexadecane) used from GC calibration; VO: switching valve oven, heated to 170°C; 3PV: manual three port valve.

Results / Discussion

Mass Discrimination

Studies have found that PTR-MS sensitivity begins to decrease for mass-to-charge ratios (m/z) greater than 80 due to fringing field effects of the quadrupole mass filter. An experimental transmission curve using an aromatic gas standard covering mass ranges between m/z 79^{+}-181^{+} in addition to 1,3,5-triisopropylbenzene (TIPB) generated by the CDS for a total mass range of m/z 79^{+}-205^{+}. TIPB is representative of the SQT compounds studied

here. Results of this study are shown in Figure F2, marked as 'experiment 3', clearly show the effects of mass discrimination where heavy compounds displayed lowest transmission. An empirically fit curve was used to estimate the actual abundances for each of the compounds studied here.

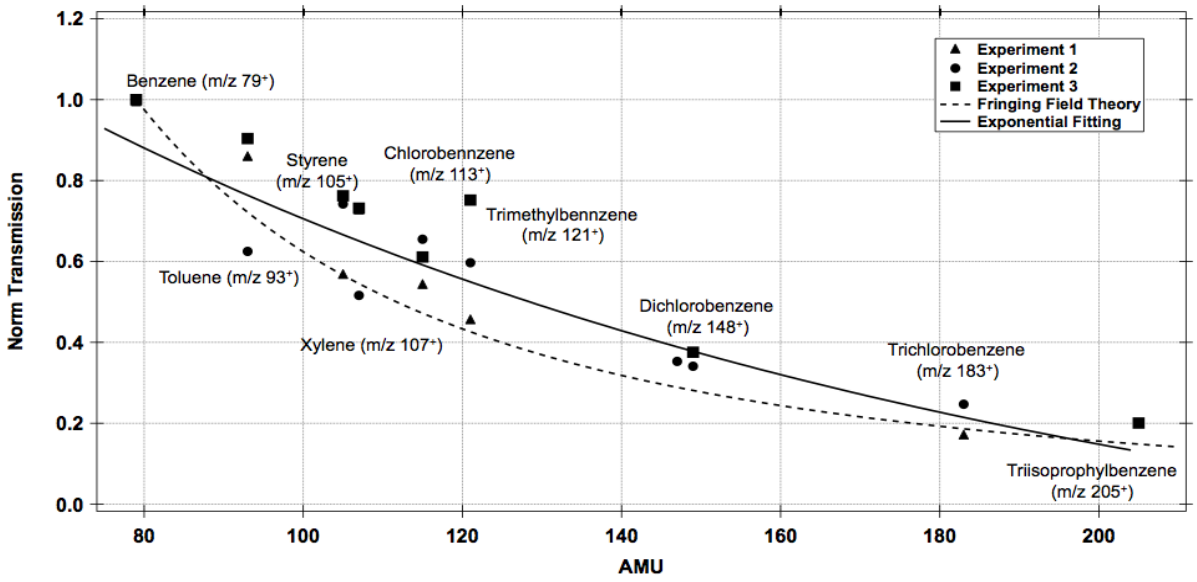

Figure F2: Transmission curve for masses ranging between m/z 79^+ - 205^+. Transmissions from three different experimental data sets are shown. Two transmission curves, based on fringing field theory (dashed) and exponentially fit curve (solid) were used for interpreting observed abundances. Figure copied from Kim et al. (2009).

Ion Fragmentation

Ion fragmentation is used for quantification of selective compound families. Few studies have examined SQT using a PTR-MS, therefore the expected fragmentation for each compound was unknown. Before quantification of SQT compounds, each compound was analyzed for its fragmentation pattern. Figure F3 shows raw (b) and mass discrimination corrected (d) PTR-MS fragmentation for β-caryophyllene. Ion fragmentation was observed for all seven SQT compounds, finding the most abundant ions to be 81^+, 95^+, 109^+, 123^+, 125^+, 137^+, 149^+, 205^+. Table F1 shows an example of the measured abundance of each ion for β-caryophyllene. Of these eight ions, measurements were found to be accurate to within 20% by using only the two most abundant ions, m/z 149^+ and 205^+. Furthermore, measurements were found to be accurate to 30% when using only m/z 205^+. These findings were significant as monitoring fewer fragmentation ions simplifies measurements and increase time resolution.

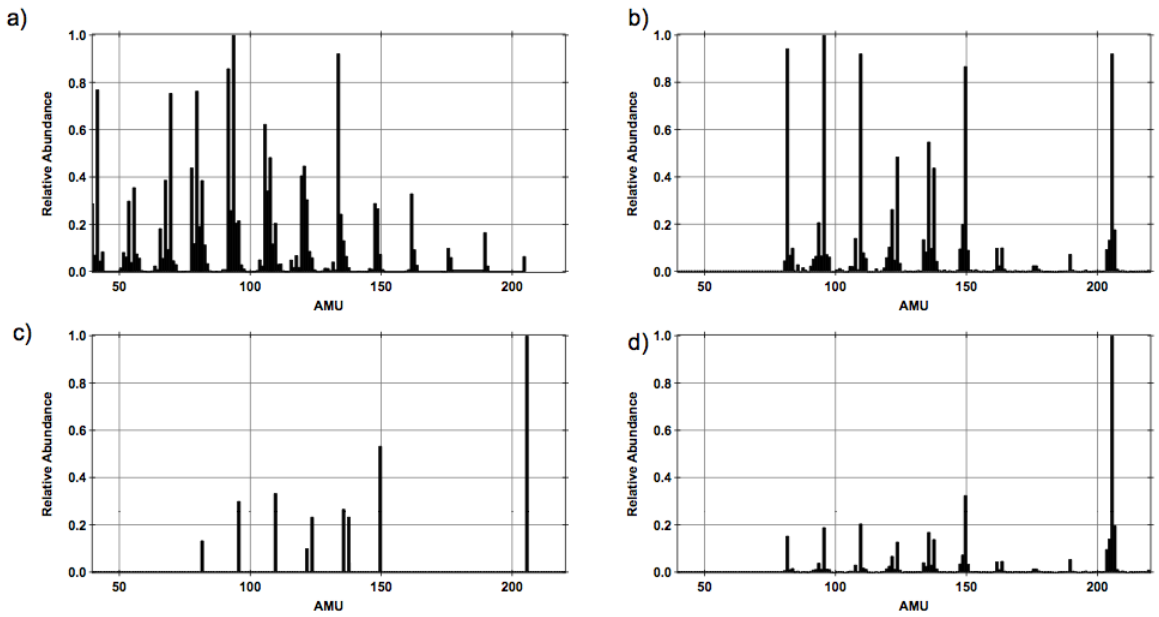

Figure 2. Mass spectra of β-caryophyllene a) electron impact (EI; from NISt Standard Reference Database), b) PTR-MS (this study), c) SIFT-MS (Dhooghe et al., 2008) with the mass discrimination correction. The mass discrimination corrected PTR-MS spectrum from this study is presented in d).

Figure F3: Mass spectra of β-caryophyllene a) electron impact (from NIST Standard Reference Database), b) PTR-MS (this study), c) SIFT-(MS) (Dhooghe et al., 2008) with mass discrimination correction, d) mass discrimination corrected PTR-MS (this study). Figure copied from Kim et al. (2009).

Table F1: List of major fragmentation ions observed for β-caryophyllene. * Mass discrimination corrected. **Mass discrimination corrected findings by Dhooghe et al. (2008) included for comparison. Figure copied from Kim et al. (2009).

Species	Fragment Ions	Abundance (%) at 117 Td		
		PTR-MS	*PTR_MS T.C.	**SIFT-MS
β-Caryophyllene 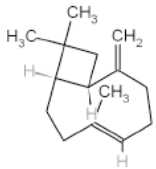	MS 81 ($C_6H_9^+$)	16	6.7	4
	MS 95 ($C_7H_{11}^+$)	18	8.2	9
	MS 109 ($C_8H_{13}^+$)	15	8.6	10
	MS 123 ($C_9H_{15}^+$)	6.9	5.3	7
	MS 135 ($C_{10}H_{15}^+$)	8.1	7.1	8
	MS 137 ($C_{10}H_{17}^+$)	7.3	6.6	7
	MS 149 ($C_{11}H_{17}^+$)	11	14	16
	MS 205 ($C_{15}H_{25}^+$)	10	44	30

Comparison between GC and PTR-MS

Each SQT compound was simultaneously monitored by direct injection to GC and dilution sampling by PTR-MS. Accounting for dilution rates, the mixing ratio of each compound were estimated for both systems and compared. Table F2 reports the ratio of GC to PTR-MS findings, accounting for varying levels of fragmentation. Results show that the PTR-MS agrees with GC within 10% when all product ions are accounted for. When only accounting for m/z 149^+ and 205^+, the systems agree to a systematic error of 50% (20% when averaged over all SQT compounds). Using the dilution capabilities of the CDS, a multipoint calibration curve could be generated for examining fragmentation ion signal with varying mixing ratios. Figure F4 shows curve for β-caryophyllene with mixing ratios varying between 10 – 70 ppbV. High linearity was observed, illustrated by the high R^2. For one minute integration time of m/z 205^+, detection limits were estimated at 91 pptV.

Table F2: Ratio of GC to PTR-MS mixing ratios for each studied SQT compound. Ratios are shown for two PTR-MS settings. Additionally, the table is broken into a case accounting for a product ions and a second case where only m/z 149^+ and 205^+ are considered. Figure copied from Kim et al. (2009).

Species	All Fragments		*m/z* 205^+ and *m/z* 149^+	
	EN105	EN117	EN105	EN117
β-caryophyllene	1.10	1.04	0.63	0.58
α-humulene	0.91	0.79	0.63	0.55
aromadendrene	1.10	0.86	0.92	0.71
α-cubebene	1.28	1.19	1.11	0.74
neoclovene	1.07	0.91	0.93	0.79
isolongifolene	0.66	0.75	0.66	0.75
δ-cadinene	1.19	1.04	1.13	1.04
Average	1.04	0.94	0.86	0.74
STD	0.203	0.157	0.218	0.161

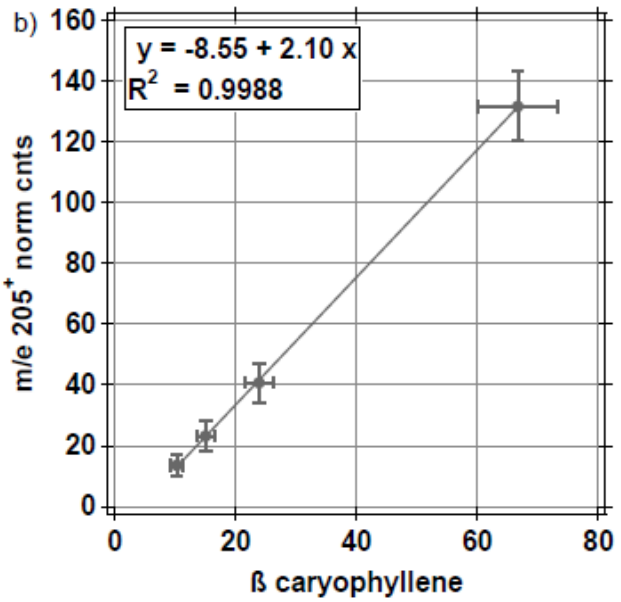

Figure F4: Signal calibration curve for varied sample mixing ratios. Figure copied from Kim et al. (2009).

These findings suggest that PTR-MS may be a viable method for monitoring total SQT emissions from vegetation sources either by vegetation enclosure methods or ambient air sampling. Kim et al. (2009) applied lessons learned to an investigation of ambient levels of SQT generated by a mixed hardwood forest at the PROPHET tower (Michigan, USA) measurements collected by PTR-MS in 2005.

References

Boy, M., Karl, T., Turnipseed, A., Mauldin, R. L., Kosciuch, E., Greenberg, J., Rathbone, J., Smith, J., Held, A., Barsanti, K., Wehner, B., Bauer, S.,Wiedensohler, A., Bonn, B., Kulmala, M., Guenther, A., 2008. New particle formation in the Front Range of the Colorado Rocky Mountains, Atmosopheric Chemistry and Physics 8, 1577–1590.

Dhooghe, F., Amelynck, C., Schoon, N., Debie, E., Bultinck, P., Vanhaecke, F., 2008. A selected ion flow tube study of the reactions of H3O+, NO+ and O2 with a series of sesquiterpenes. International Journal of mass Spectrometry 272, 137–148.

Helmig, D., Revermann, T., Pollmann, J., Kaltschmidt, O., Hernandez, A. J., Bocquet, F., David, D., 2003. Calibration system and analytical considerations for quantitative sesquiterpene measurements in air. Journal of Chromatographic Analysis 1002, 193–211.

Kim, S., Karl, T., Helmig, D., Daly, R., Rasmussen, R., Guenther, A., 2009. Measurement of atmospheric sesquiterpenes by proton transfer reaction-mass spectrometry (PTR-MS). Atmospheric Measurement Techniques 2, 99-112.

Lee, A., Goldstein, A. H., Keywood, M. D., Gao, S., Varutbangkul, V., Bahreini, R., Ng, N. L., Flagan, R. C., and Seinfeld, J. H., 2006. Gas-phase products and secondary aerosol yields from the ozonolysis of ten different terpenes. Journal of Geophysical Research 111, D07302.

Steinbacher, M., Dommen, J., Ammann, C., Spirig, C., Neftel, A., and Pr´evˆot, A. S. H., 2004. Performance characteristics of a protontransfer- reaction mass spectrometer (PTR-MS) derived from laboratory and field measurements. International Journal of Mass Spectrometry 239, 117–128.

Appendix G – 2009 & 2010 CABINEX Field Campaign

This work still in progress and is expected to result in a published paper.

Project Duration: Summer 2009, Spring – Fall 2010

Persons involved: Detlev Helmig, Ryan Daly, Jacques Hueber, Éva Joó, Romain Baghi, Chris Borke

Goal: To report biogenic emission flux data present at the PROPHET and FASET tower sites. Additionally, a novel ozone reactivity study was performed to examine possible differences in ozone reactivity rates observed in the field and lab studies.

Introduction

This research effort was part of the CABINEX (Community Atmosphere Biosphere INteractions and EXchange) field campaign, a collaborative effort of nearly four dozen researchers that took place at the University of Michigan Biological Station, MI. As described in the CABINEX main webpage (http://aoss-research.engin.umich.edu/prophet/CABINEX.html):

> 'Past research has found that biogenic volatile organic compounds (BVOCs), originating in forest canopies, can influence basic processes within the troposphere. Additionally, forest succession and climate change share in the responsibility of the changing face of these forest canopies. Motivated by the concurring Forest Accelerated Succession Experiment (FASET), CABINEX aims to examine the effects on microscale atmospheric chemistry within the canopy layer owing to forest succession.'

A number of recent studies on BVOC released in the forest atmosphere have pointed out that identified emissions cannot account for the entire chemical reactivity seen in the forest atmosphere. To further investigate these findings, BVOC emissions and their reactivity with ozone were studied with a newly developed ozone reactivity instrument. Experiments were conducted on the tree species red oak, white pine, big tooth aspen, and red maple, representing ~ 87% of the canopy leaf area index at this site. Experiments were performed over several days to capture emission changes under varying ambient temperature and light conditions. Additionally, INSTAAR served to examine and report BVOC emission speciation and rate data of these tree species from the both the PROPHET and FASET site forest canopies. This data was shared with other groups for microscale atmospheric chemistry modeling studies. BVOC emission rates and compound speciation were measured during the summers of 2009 and 2010. The ozone reactivity study was completed in the summer of 2010.

Experimental Setup

BVOC emission rates and compound speciation

BVOC emission rates and chemical compound speciation were measured by branch enclosure experiment, adsorbent cartridge sampling, and thermal desorption GC/MS analysis, described in section 2.3.2 of Chapter 2. Sun exposed upper canopy branches were selected

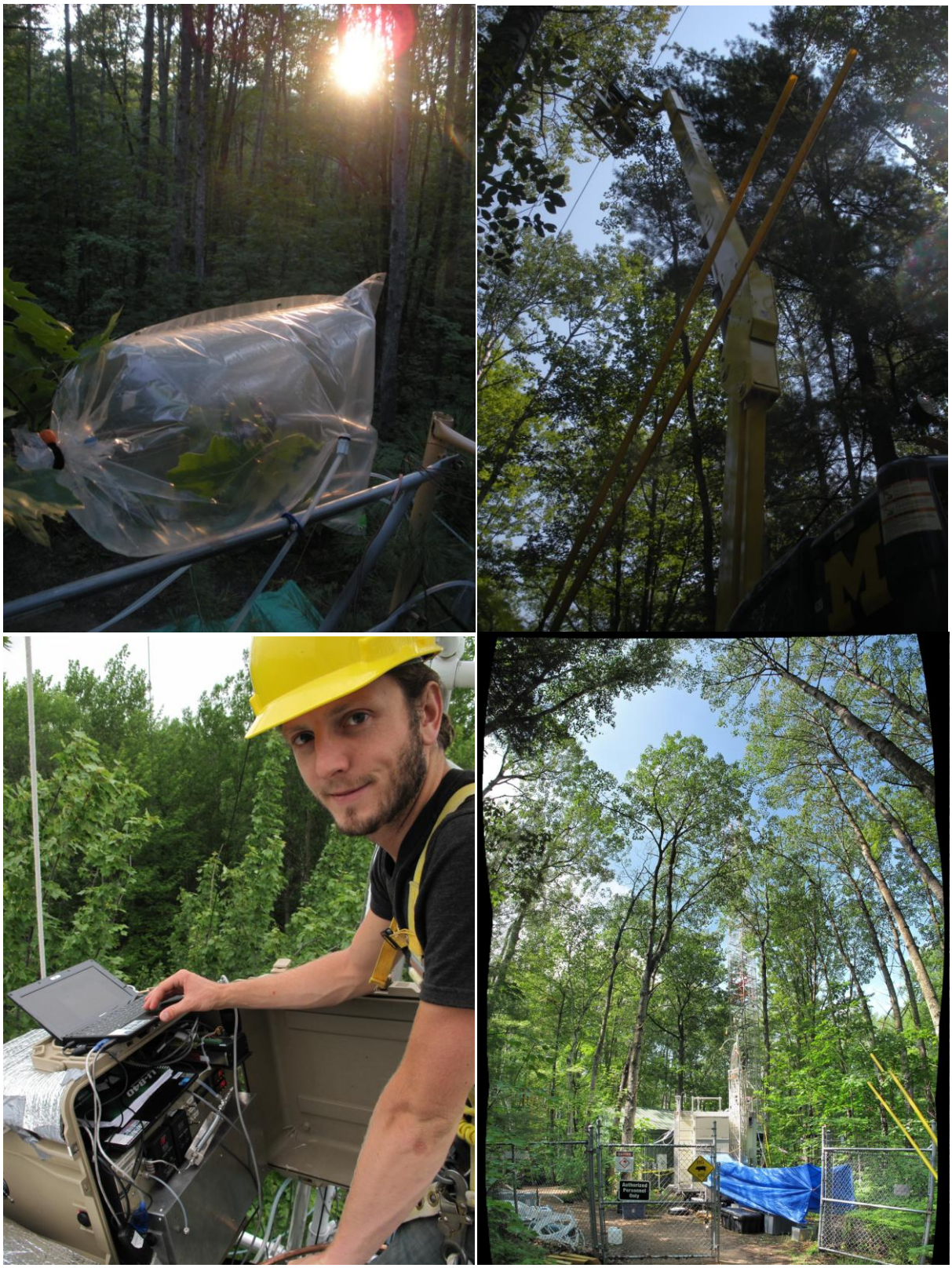

Figure G1: Clockwise from top left: branch enclosure experiment of a red oak tree at the PROPHET site, sampling of a girdled big tooth aspen from the FASET site, PROPHET tower and lab facilities, Ryan Daly attending equipment at the top of the PROPHET tower.

for measurement at both the PROPHET and FASET sites. Branches were accessed from the PROPHET tower, stand alone scaffolding, or by an electrically motorized zero emission cherry picker. Red oak, white pine, big tooth aspen, and red maple, representing ~ 87% of the canopy leaf area index were studied from the PROPHET site. Additionally, girdled big tooth aspen trees were examined from the FASET site.

Ozone reactivity experiment

Tree branches in the lower canopy area were accessed from scaffolding. Dynamic branch enclosures were installed and allowed to equilibrate for at least 12 hours before experiments commenced. Sampling was then conducted over 2-4 diurnal cycles. Instrumentation was operated in a van parked at the base of the tower. Ambient air was scrubbed of ozone and particulates, dried with an ice bath, mixed with a 5-component reference standard, and then delivered to the enclosure at 15 l min^{-1}. A flow of 3 l min^{-1} was pulled from an inlet inside the enclosure. A small addition of ozone-enriched air was mixed with the enclosure air to result in a 100 ppbV ozone mixing ratio. This mixture was then directed through a series of 4 glass flask reaction vessels (10 liters total). The loss of ozone (reaction rate) was measured with an ozone UV absorption monitor. The monitor was operated in a differential mode to directly measure the difference in ozone before and after

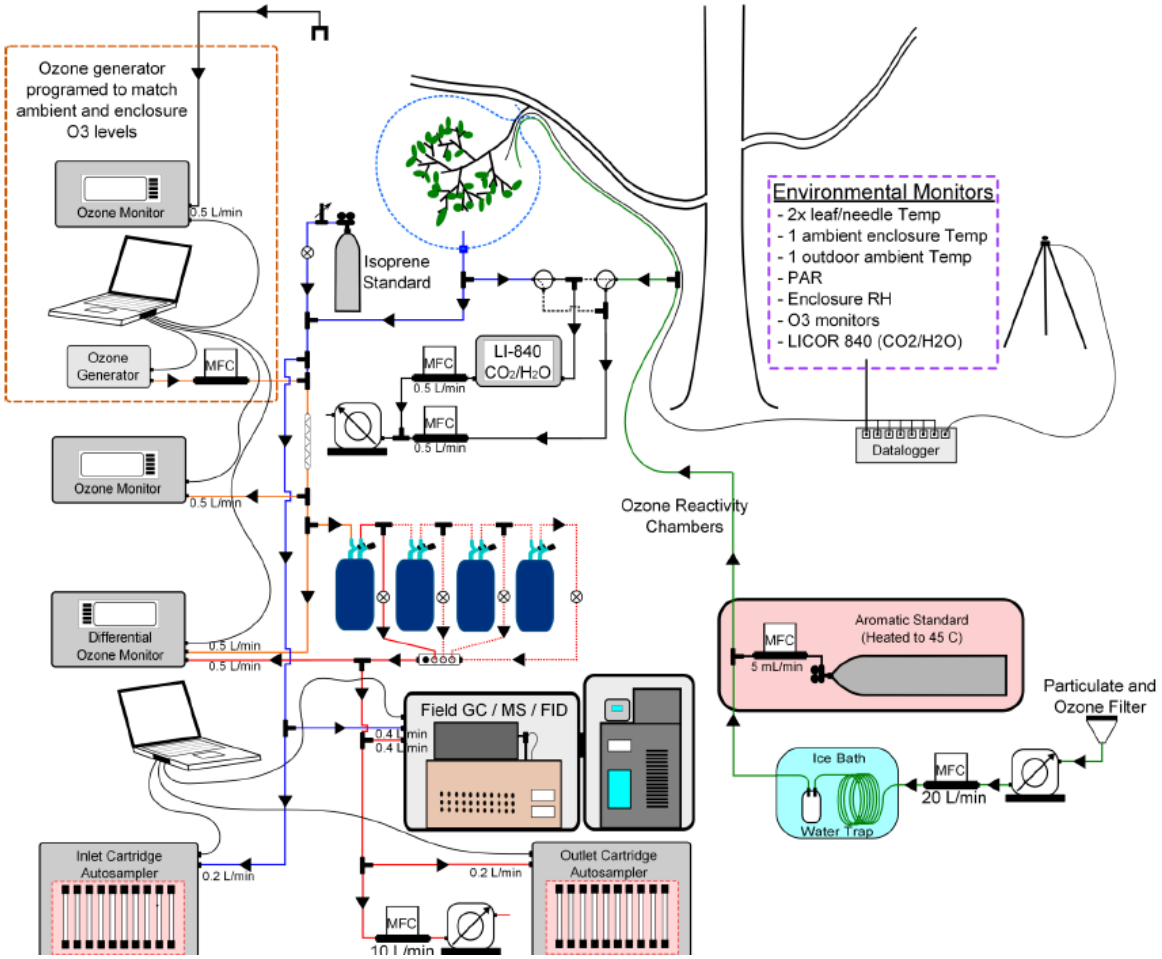

Figure G2: Experimental setup of the ozone reactivity experiment.

the reaction vessel. Both air streams were directed through a Nafion dryer to reduce water content. CO_2 and water vapor were measured in both the air delivered to the enclosure as well as the air drawn from the enclosure every 5 min. Other variables recorded included ambient ozone mixing ratio, temperature inside the enclosure, leaf temperatures, ambient temperature and incoming solar radiation. A detailed schematic is shown in Figure G2.

Results

BVOC emission rates and compound speciation

BVOC emission rates were observed to be predominantly temperature dependant from all tree species. Normalized basal emission rates and pertinent enclosure data are reported for each of the tree species in Table G1. Litter trap data that may be useful in calculating canopy flux rates is included in Table G2 for reference. This data has been compiled from litter trap findings reported by Ortega et al. (2007) from the PROPHET site as well as 2008 litter trap data provided by Chris Vogel, UMBS faculty, from the nearby Ameriflux tower site. The observed BVOC compound speciation is shown in Table G3.

These findings have been made available to other groups within the CABINEX project. Kerri Pratt, under the guidance of Paul Shepson of Purdue University, has used this emission rate data in a microscale atmospheric chemistry model of the PROPHET forest canopy. Her findings have been used in presentations and will likely result in a written manuscript.

Table G1: Basal emission rate data for each tree specie studied between 2009 and 2010.

CABINEX 2009-2010 BVOC Summary

						Isoprene		Monoterpenes					Sesquiterpenes				
Common name	genus/species	Sample Dates	Min Bag Temp (deg. C)	Max Bag Temp (deg. C)	Total samples	# of samples	Normalized ER ($\mu gC\ g^{-1}\ hr^{-1}$)	# of samples	# of Identified compounds	Total ER ($\mu gC\ g^{-1}\ hr^{-1}$)	β	R^2	# of samples	# of Identified compounds	Total ER ($\mu gC\ g^{-1}\ hr^{-1}$)	β	R^2
Red Oak	*Quercus rubra*	7/10/2009 - 7/12/2009	10.1	28.9	32	26	**1.96**[b]	29	3	**0.16 (0.10)**[e]	-	-	9	1	**0.015 (0.006)**[f]	-	-
		7/24/2010 - 7/26/2010	13.9	33.9	15	15	**1.29**[b]	13	11	**0.07**[d]	0.23	0.75	11	2	**0.024**[d]	0.22	0.89
White Pine	*Pinus strobus*	7/16/2009 - 7/18/2009	11.5	21.3	25	0	-	25	5	**0.38 (0.24)**[e]	-	-	0	-	-	-	-
		7/26/2010 - 7/28/2010	16.6	37.0	13	0	-	13	7	**0.16**[d]	0.12	0.70	0	-	-	-	-
Red Maple	*Acer rubrum*	7/28/2010 - 7/30/2010	12.5	31.7	14	0	-	11	3	**0.14**[d]	0.15	0.58	14	1	**0.14**[d]	0.15	0.70
Bigtooth Aspen	*Populus grandider*	7/31/2010 - 8/2/2010	15.8	31.4	16	16	**1.12**[b]	0	-	-	-	-	0	-	-	-	-
Red Pine	*Pinus resinosa*	7/19/2009 - 7/20/2009	9.1	30.3	26	0	-	26	10	**0.56**[d]	0.12	0.63	26	2	**0.028**[d]	0.11	0.77
American Beech	*Fagus grandifolia*	7/20/2009 - 7/22/2009	13.1	24.5	20	0	-	20	12	**7.46**[d]	0.74	0.80	0	-	-	-	-

[a] All samples collected from one branch-enclosure applied to one tree per species

[b] Isoprene emission rates of the form x.xx were corrected for standard *light* (PAR = 1000 μmol $m^{-2}\ s^{-1}$) and *temperature* (20 C) conditions using methods suggested by Guenther et al. (1993)

$ER(K, PAR) = ER_s * C_L * C_T$

$C_L = (0.0029*PAR)/(1+(0.0027*PAR)^2)^{0.5}$ $C_T = \exp(((95{,}000\ J\ mol^{-1})*(T - 293K)) / ((8.314\ J\ K^{-1})*(293K)*T)) / (1+ \exp(((230{,}000\ J\ mol^{-1})*(T - 314K)) / ((8.314\ J\ K^{-1})*(293K)*T)))$

[d] Basal emission rates calculated using an exponential equation, fit to emission rate vs. temperature data and normalized to 20 C. ER(k) = exp(B * 20C)

[e] Basal emission rates of the form x.xx (y.yy) were not fitted to an exponential curve, rather they are reported as the mean (with standard deviation in parenthesis) after normalizing each measurment result to 20 °C using a β of 0.11 $°C^{-1}$

[f] Basal emission rates of the form x.xx (y.yy) were not fitted to an exponential curve, rather they are reported as the mean (with standard deviation in parenthesis) after normalizing each measurment result to 20 °C using a β of 0.17 $°C^{-1}$

Table G2: Litter Trap Data

Species	Leaf Area (cm^2)	Leaf Dry Mass (g)	Specific Leaf Mass (SLM) (g/m^2)	Leaf Area Index (LAI) ($m^2\ m^{-2}$)
Acer Rubrum (red maple)	1019.1	6.6	64.8	0.71[a], 0.61[b]
Populus grandidentata (bigtooth aspen)	621.8	4.2	67.2	1.04[a], 0.92[b]
Quercus rubra (red oak)	1173.7	7.5	63.7	0.81[a], 0.84[b]
Fagus grandifolia (beech)	783.4	2.6	33.4	0.21[a], 0.10[b]
Betula papyrifera (paper birch)	498.1	3.0	59.2	0.25[a], 0.28[b]
Acer saccharum(sugar maple)	1356.0	4.5	33.4	
Pinus strobus (white pine)	144.0	3.9	268.8	0.14[a], 0.35[b]
Populus tremuloides (quaking aspen)	1428.0	10.1	70.9	

Table G3: BVOC compound speciation (percent of the total emission) listed by tree specie and chemical compound emitted. Numbers represent the percent contribution of each compound to the total emission.

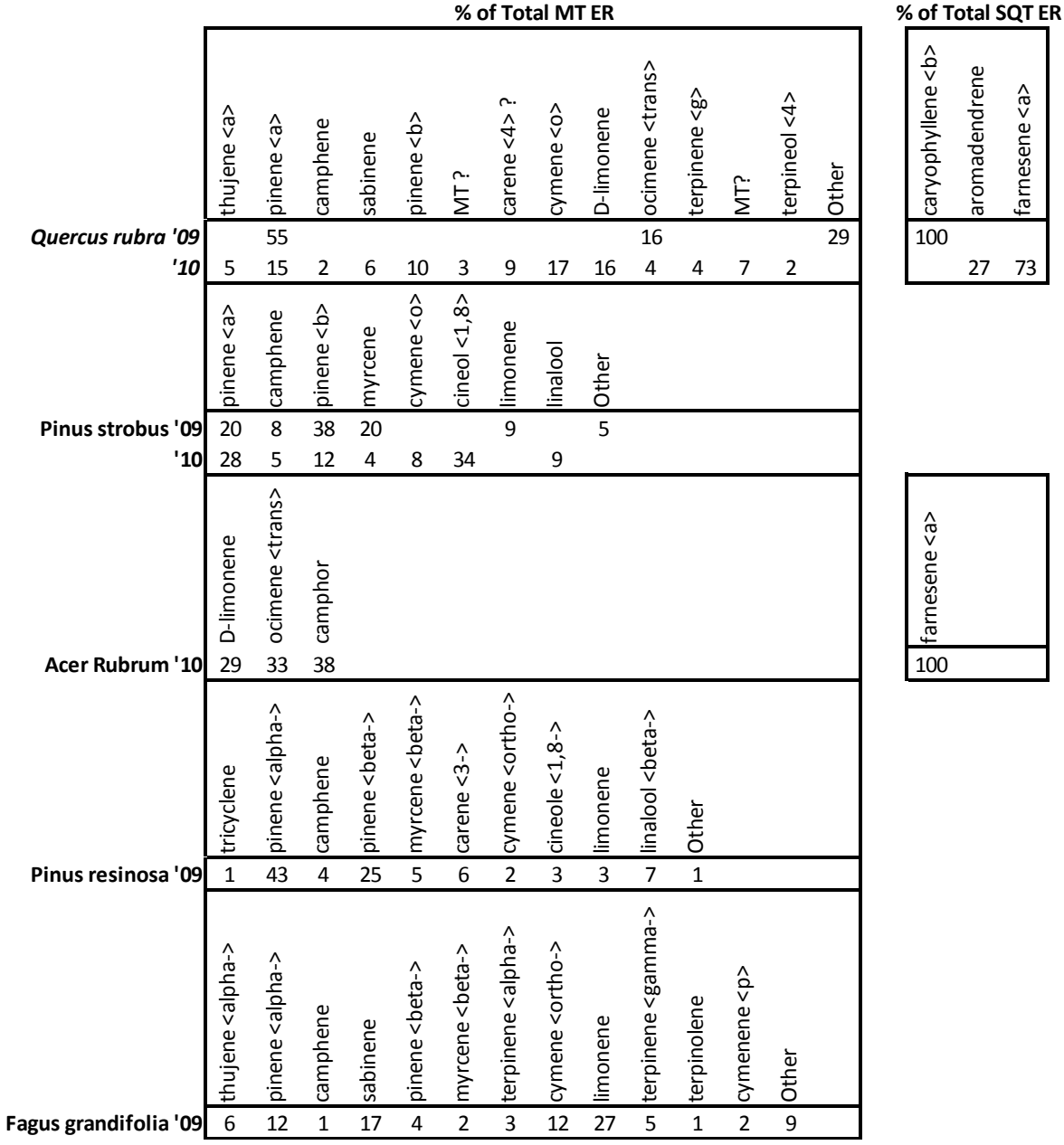

	% of Total MT ER														% of Total SQT ER		
	thujene <a>	pinene <a>	camphene	sabinene	pinene <b>	MT ?	carene <4> ?	cymene <o>	D-limonene	ocimene <trans>	terpinene <g>	MT?	terpineol <4>	Other	caryophyllene <b>	aromadendrene	farnesene <a>
Quercus rubra '09		55								16				29	100		
'10	5	15	2	6	10	3	9	17	16	4	4	7	2			27	73
	pinene <a>	camphene	pinene <b>	myrcene	cymene <o>	cineol <1,8>	limonene	linalool	Other								
Pinus strobus '09	20	8	38	20			9		5								
'10	28	5	12	4	8	34		9									
	D-limonene	ocimene <trans>	camphor												farnesene <a>		
Acer Rubrum '10	29	33	38												100		
	tricyclene	pinene <alpha->	camphene	pinene <beta->	myrcene <beta->	carene <3->	cymene <ortho->	cineole <1,8->	limonene	linalool <beta->	Other						
Pinus resinosa '09	1	43	4	25	5	6	2	3	3	7	1						
	thujene <alpha->	pinene <alpha->	camphene	sabinene	pinene <beta->	myrcene <beta->	terpinene <alpha->	cymene <ortho->	limonene	terpinene <gamma->	terpinolene	cymenene <p>	Other				
Fagus grandifolia '09	6	12	1	17	4	2	3	12	27	5	1	2	9				

Ozone reactivity experiment

Figure G3 shows an excerpt with two days of data from collected from the ozone reactivity experiments conducted on a red oak and red maple tree. Data from top to bottom represent the (raw) differentially measured ozone reactivity signal, the difference in water vapor and CO2 mole fraction in air delivered and drawn from the enclosure, photosynthetically active radiation (PAR) measured outside the bag, adjacent to the enclosure, air temperatures measured outside the bag, inside the bag, and from two thermocouples attached to leaves inside the enclosure. The lower two graphs show results from the chemical analyses of samples collected over 60-min from air withdrawn from the enclosure. The first one depicts the mixing ratio of identified BVOC present within the enclosure system. The bottom set shows emission rates calculated from these chemical analysis data, flow rates, and biomass dry weight determination.

Figure G4 illustrates the comparison of ozone reactivity to temperature for the four tree species investigated at 1000 ppbV ozone reactant concentration. Here, the ozone reactivity was normalized to the enclosure purge flow rate and amount of dry leaf biomass for each of the four tree species investigated.

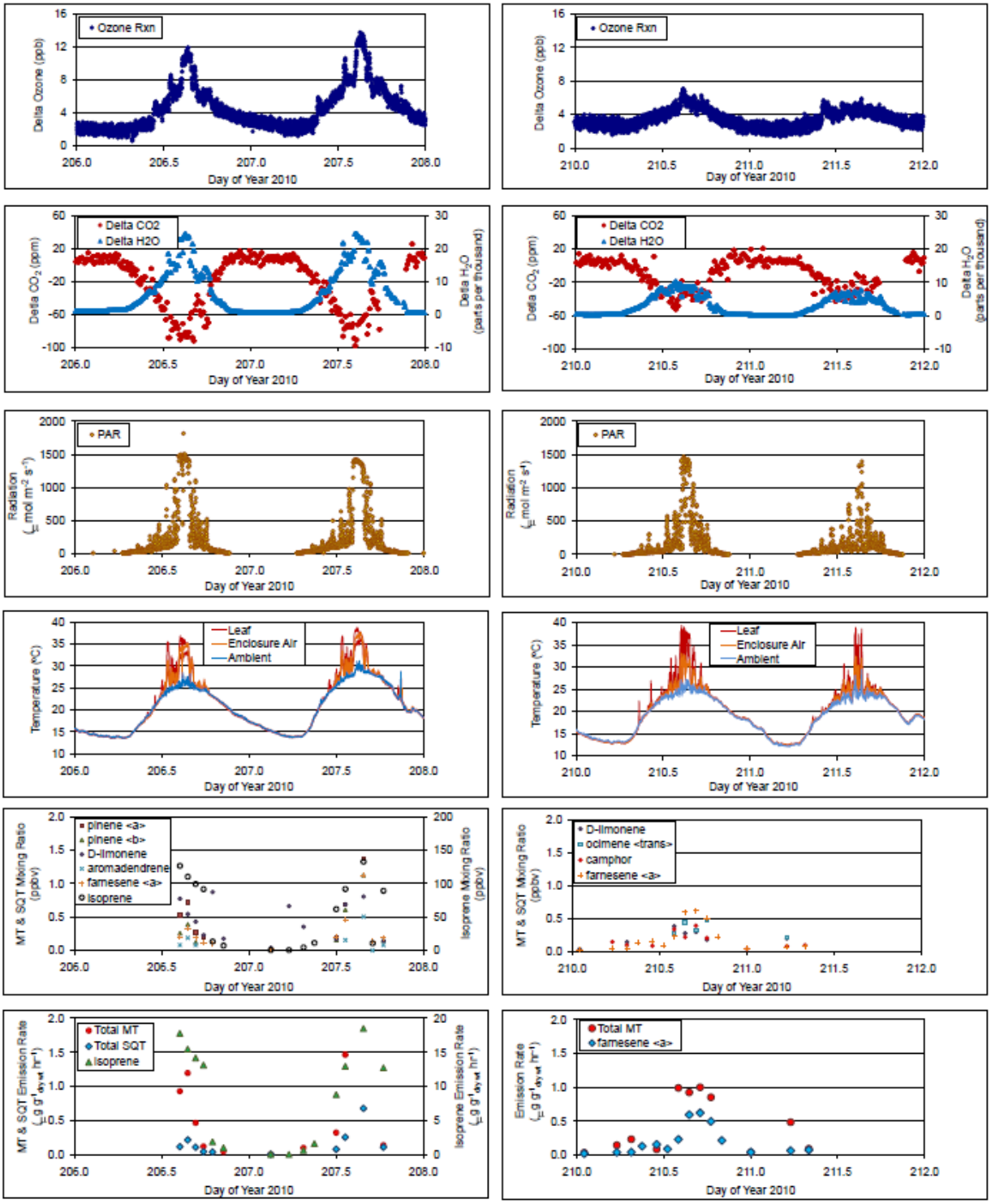

Figure G3: Ozone reactivity data, ΔCO_2, ΔH_2O, environmental conditions, and MT & SQT emission data are shown over a complete two day time period for the red oak (left) and red maple (right).

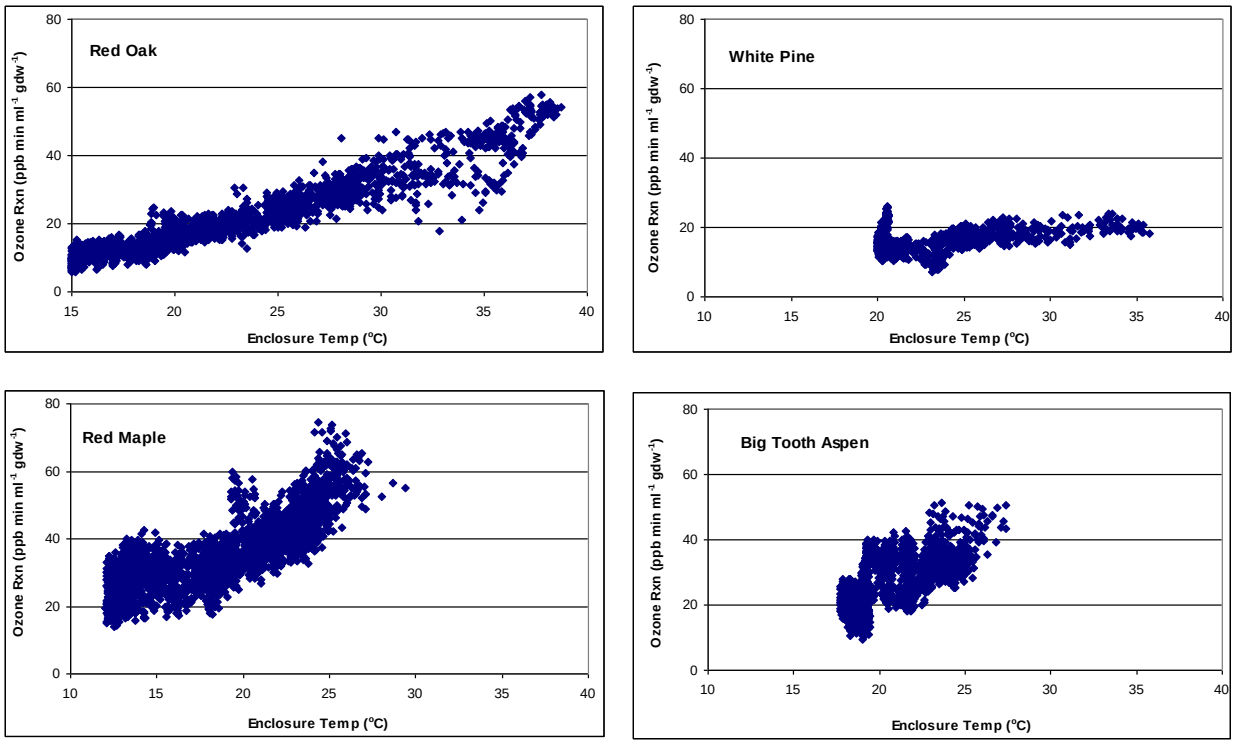

Figure G4: Comparison of ozone reactivity-temperature dependency for the four tree species investigated at 100 ppbV ozone reactant concentration.

The work-up of this data is still in progress. Unexpected convolution between the observed ozone reactivity with fluctuations in BVOC emissions and/or changes in water vapor has proven to be confusing, resulting in further qualification of the ozone reactivity equipment and setup. Lab work is currently being conducted by a visiting PhD student, Éva Joó, who is examining how changes in water vapor content may alter ozone reactivity rates. A written manuscript is expected to result and will be submitted to Atmospheric Environment or to Chemosphere.

References

Ortega, J., Helmig, D., Guenther, A., Harley, P., Pressley, S., Vogel, C., 2007. Flux estimates and OH reaction potential of reactive biogenic volatile organic compounds (BVOCs) from a mixed northern hardwood forest. Atmospheric Environment, 41, 5479-5495.

Appendix H – Contribution of flowering trees to urban atmospheric biogenic volatile organic compound emissions

The following manuscript is in progress and is expected to be published by the end of 2011.

Project Duration: Summer 2009

Authors: Romain Baghi, Detlev Helmig, Alex Guenther, Tiffany Duhl, Ryan Daly

Abstract

Emissions of biogenic volatile organic compounds (BVOC) from urban trees during and after blooming stage were estimated during spring and early summer 2009 in Boulder, Colorado. Air samples were collected by the branch enclosure method from crabapple, horse chestnut, honey locust and hawthorn tree species, which constitute 80% of the flowering tree biomass of the City of Boulder street trees. Samples were analyzed using a Gas Chromatograph coupled to a Flame Ionization Detector and a Mass Spectrometer (GC/FID/MS). Monoterpenes emissions were identified and quantified for Honey Locust, Horse Chestnut and Hawthorn. Sesquiterpenes were observed in Horse Chestnut and Hawthorn samples. Changes in speciation during and after the flowering period were observed on every tree studied. Crabapple flowers were found to emit benzyl alcohol and benzaldehyde. Honey locust total monoterpenes emissions were 3.7 fold higher during flowering. However no significant changes in emissions rates (ER) were observed on Horse Chestnut and hawthorn. Using these experimental results along with existing VOC emission rates database, simulations were performed to estimate the contribution of flower VOC emissions to the total urban BVOC. The cumulated flower BVOC flux during full bloom was 271ug.m2 which represents 4.4% of the total light independent monoterpenes urban flux.
Keywords: biogenic volatile organic compounds, emission factors, tree blossoms, GC/FID/MS.

Introduction

Volatile organic compounds play an important role in atmospheric chemistry, in particular in secondary pollutants formation (e.g. tropospheric ozone and secondary organic aerosols). Emissions from vegetation are highly dependent on vegetation activity and biomass which are governed by seasonal changes. BVOC flux estimates used in chemistry models and air quality models rely on emission rates, vegetation characteristics and weather conditions. Seasonal changes are difficult to account for and especially blooming time for which BVOC emissions resulting from the flowers are generally not described. Ornamental vegetation with colorful flowers or fragrances is planted to brighten up urban area. This artificial vegetation class contributes to VOC concentrations to certain extend that could impact indirectly air quality. To our knowledge only one study in the literature address the possibility of increased VOC production during the blooming period (Müller et al, 2002). Flower volatiles are of interest for botanical research, plant-pollinators interactions or insect pests of trees. Therefore, an abundant body of literature on BVOC emissions from flowers is available. However most studies on flower BVOC emissions report only on qualitative results e.g. *(Buchbauer, Jirovetz et al. 1993), (Deng, Song et al. 2004), (Dudareva, Raguso et al. 1998), (Effmert, Grosse et al. 2005), (Goodwin, Kolosova et al. 2003), (Granero, Gonzalez et al. 2005), (Johne, Weissbecker et al. 2006), (Li, Lee et al. 2006), (Loughrin, Hamiltonkemp et al. 1990), (MacTavish, Davies et al. 2000), (Martin, Toub et al. 2009), (Robertson, Griffiths et al. 1993), (Schuurink, Haring et al.*

2006), (Vallat, Gu et al. 2005), (van Schie, Haring et al. 2006), (Yamaguchi and Shibamoto 1980), (Zhuang, Klingeman et al. 2008). A few of those with quantitative results are not always presented a way that can be used for atmospheric model (e.g. *Baraldi, Rapparini et al. 1999, reports emission rates in ug/100flowers/h*).
Fewer studies of flower voc emission reports qualitative and quantitative results: (Ibrahim, Egigu et al. 2010), (Jakobsen, Friis et al. 1994), (Muller, Pelzing et al. 2002), (Rapparini, Baraldi et al. 2001), (Vallat and Dorn 2005).
Significant amount of BVOC are emitted by flowers but there is a high variability. Some studies shows significantly higher voc emission rates from flowering branches than vegetative branches (Ibrahim et al, 2010).

Experimental

Site description

The field site was located in a tree nursery in Boulder: Creekside tree nursery. An enclosed trailer sitting within the tree nursery was used as a field laboratory. The trees dedicated for this experiment were surrounding the south side of the trailer/lab. Available flowering trees were borrowed from the nursery during the measurements period corresponding to the blooming season. Four trees were studied: Crabapple(Malus), Hawthorne (Crataegus Laevigata 'Pauls Scarlet'), Horse chestnut (Aesculus Carnea 'Ft. McNair'), and a Honey locust (Gleditsia Triacanthos 'Sunburst'). Honey locust, Crabapple and hawthorn represent 80% of flowering trees in Boulder city according to the municipal tree resource analysis report from the city of boulder. All trees were between 2 and 3 meters tall and were kept in their planting pots

Sampling

Sampling methods and specific materials suitable for VOC measurements were required therefore experimental protocol was following procedure described in Ortega et al. (2008). The studied vegetation was enclosed in a Tedlar bag such that the bag does not touch the vegetation. Particulate and ozone filtered purge air was sent at 25 liters per minute toward the enclosure providing a pressure excess. The bag was attached at the branch base with Velcro tape, thus preventing outside air from entering by the pressure excess. A water trap was used to reduce moisture and cool the air inside the enclosure. Flow rates through the sample lines were dependant on the use of the ozone monitor but ranged between 200 ml.min-1 and 700ml.min-1. Two automated sampling devices (AS) developed by Helmig et al. (2004) were used for this experiment allowing for 10 to 20 samples to be collected in a row with a minimum of 30 min between two samples. An additional ozone scrubber composed of 25 MnO2-coated copper screens (Hansen and Seufert, 2003; Helmig et al., 2006) was placed at the auto-sampler inlet. Samples were collected with glass tubes filled with a multi-adsorbent bed composed of half Tenax GR and half Carboxen 1016. An extra adsorbent cartridge called “break through” cartridge was placed in series with the sample cartridge corresponding to the predicted hottest temperature sample. The breakthrough cartridges ensure that sampled compounds do not make their way through the entire adsorbent package.

For each tree a branch was chosen to be sampled repeatedly over the course of the study. Sampling on a branch enclosure started at least half a day after the enclosure bag was put in place and all the equipment had been set up. This delay allowed the plant and the enclosure to reach an equilibrium state. Sampling times varied from one hour during daytime to 2 hours during nighttime. Two sets of enclosure equipment were used simultaneously when several trees

were blooming at the same time. Approximately 400 samples were collected over the course of this study, from April 16th to June 19th: 99 samples on the hawthorn, 40 on the crabapple, 145 on the chestnut and 70 samples on the honey locust. In addition, 20 inlet samples were also collected to achieve an inlet/outlet comparison and to determine aromatic recovery rates due to the experimental setup.

Samples collected at the field site were brought back to the laboratory for analysis. Thermal desorption using a Perkin-Elmer ATD 400 allowed the sample to be transferred from the cartridge to a GC (Hewlett-Packard 5890). The detector was a Mass spectrometer coupled to a flame ionization detector. Similar instrumentation and calibration procedures are described in Helmig et al. (2004). Compound identification was conducted using the retention times, along with comparing to literature (Adams R.) and mass spectrometry chromatograms.

Aromatic Standard

An aromatics standard was introduced to the purge flow to aid in analyte recovery analysis as well as compound identification. The standard was composed of 5 aromatic compounds ranging in molecular weight and therefore retention time when analyzed by gas chromatography. These compounds include toluene, isopropyl-benzene, tetrahydronaphthalene, triisopropyl-benzene and nonyl-benzene. Concentrations were calculated using an online gas chromatography instrument calibrated with a known n-alkane gas standard (Helmig et al., 2003). The aromatic mixture was introduced in the main purge flow at a controlled (Mass flow controller) flow rate of 6.5 ml.min-1.

Environmental monitoring

Several environmental variables were monitored including: ambient air temperature, enclosure temperature, leaf temperature, relative humidity, photo-synthetically active radiation (PAR), and ozone concentrations. BVOCs and particularly sesquiterpenes are very reactive. It was therefore important that oxidant level inside the enclosure were kept low. Ozone concentrations for this experiment were usually below 2 ppb. Data were recorded every 5 minutes by a Campbell Scientific CR10X datalogger.

Normalized Emission rate calculations

Temperature dependence for emissions of monoterpenes, benzenoids, oxygenated monoterpenes and sesquiterpenes were observed in this study. Light dependency was poor for all compounds. Normalized emission rates also mentioned basal emission rates (BER) were calculated using algorithm from Guenther et al (1993).

Results / Discussion

Blooming occurred at different times for each tree and lasted between 7 and 18 days. Figure 1 shows flowering period along with sampling schedule.

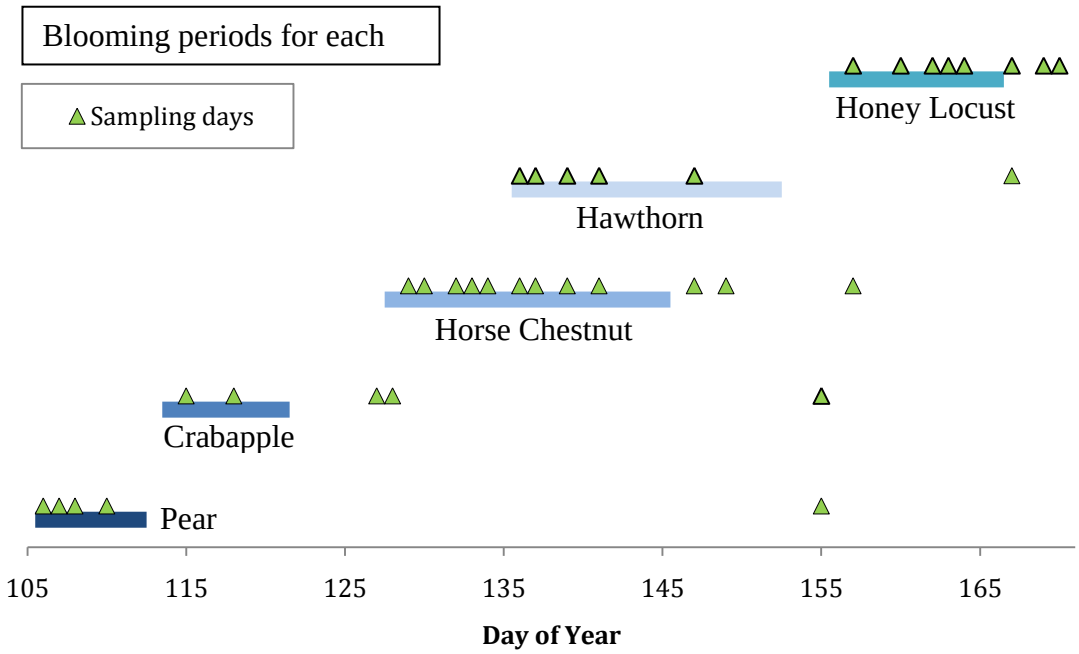

Figure 1: Blooming period for pear, crabapple, horse chestnut, hawthorn and honey locust with concurrent sampling days, in 2009.

Crabapple flowers appeared first, in late April, at a time when leaves at bud stage. Benzylalcohol and benzaldehyde were the only volatiles identified from branch enclosure samples. Figure 2 shows a typical day with emission rates for each compound.

Average temperature inside the enclosure during sampling ranged from 4ºC to 23ºC for the blooming period and from 8ºC to 29ºC after flowering. These emissions present good temperature dependence as shown in Figure 3.

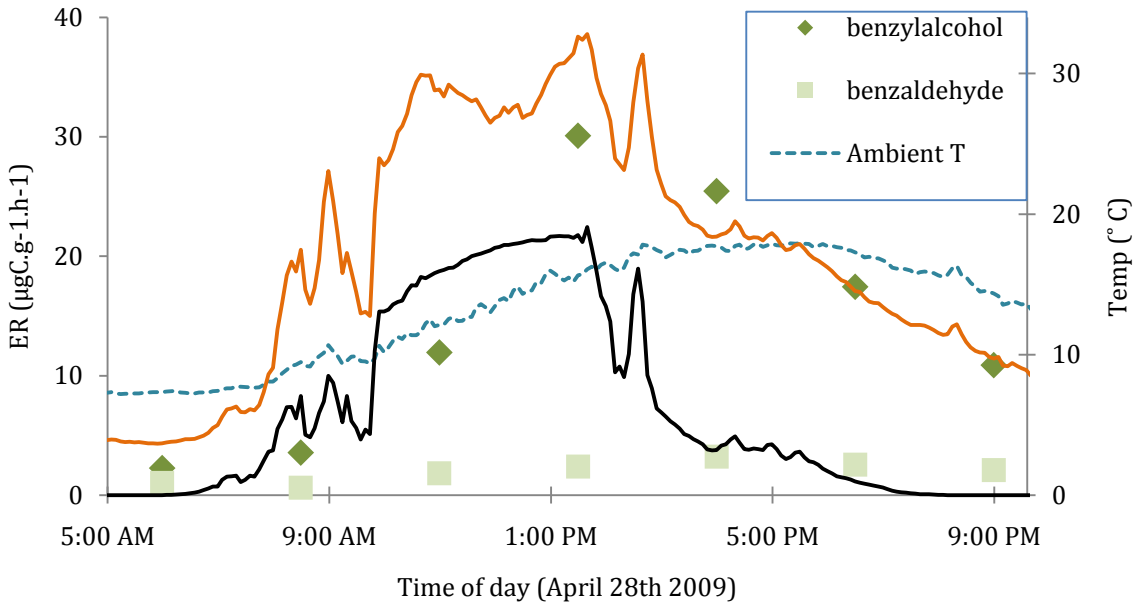

Figure 2: Profile for benzylalcohol and benzaldehyde emission rates from crabapple for a day of measurements at full bloom with concurrent ambient temperature, enclosure temperature and PAR.

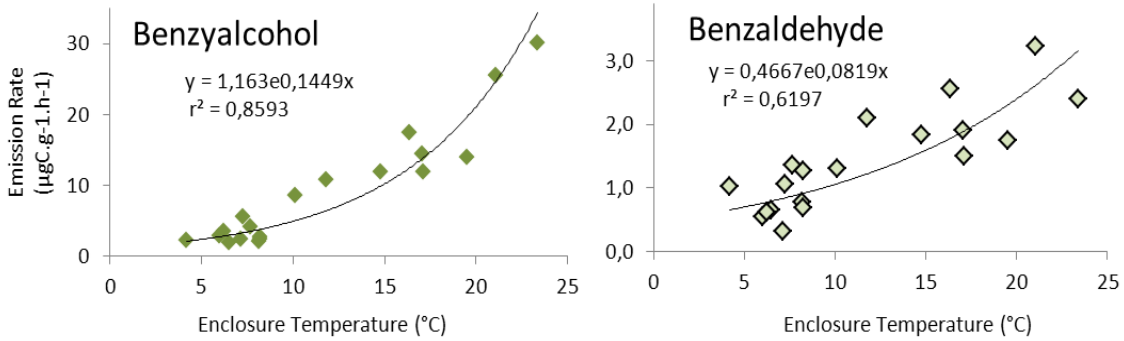

Fig 3: Benzyl alcohol and benzaldehyde emission rates as a function of temperature. Data from crabapple enclosure experiment.

Benzenoids have been reported as being the most abundant floral scent molecules in floral volatiles studies (Van Schie et al, 2006; Dudareva N. and Pichersky E., 2000). The results shown here agree with Loughrin J. et al, (1990) where benzyl alcohol as well as benzaldehyde was identified from apple flowers. Contribution of benzyl alcohol and benzaldehyde to the overall emissions was respectively 79% and 21%. The averaged total normalized emission rate during the flowering period was 2.21µgC$g^{-1}h^{-1}$. Emissions of both compounds dropped to detection limits when the flowers had withered (Figure 4). This shows that VOC emissions from crabapple are mostly relevant at the blooming stage.

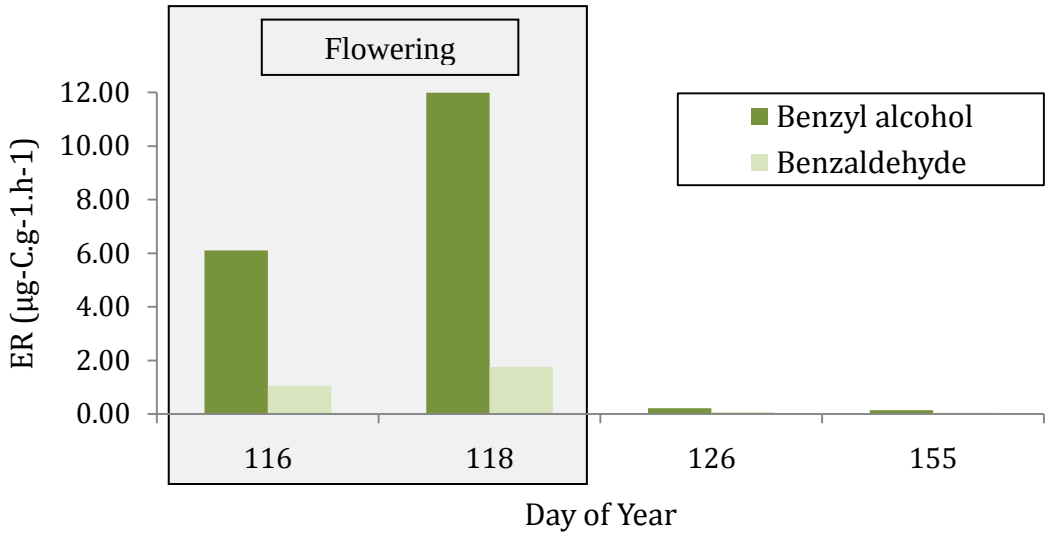

Figure 4: Emission rates observed for crabapple. The two first days fall during the flowering period and the two last days after the flowering.

Compounds identified in horse chestnut branch enclosure samples include thujene, α-pinene, β-pinene, camphene, 2-carene, α-terpinene, o-cimene, β-phellandrene, γ-terpinene, terpinolene, 4-terpineol, methyl salicylate, α-terpineol and D-limonene. Normalized emission rates were calculated for horse chestnut using a β factor of 0.192 for the flowering period and 2.12 after flowering. Average VOC emission rate during flowering was 9.2µgCg^{-1}h^{-1} whereas after the flowering period this value reached 16.5µgCg^{-1}h^{-1}.

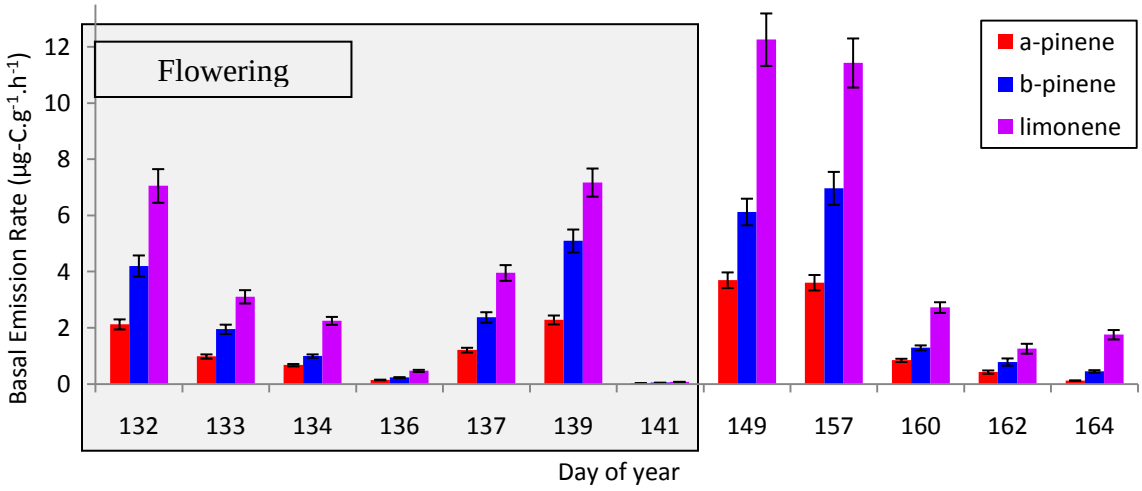

Figure #: Daily averaged normalized emission rates for α-pinene, β-pinene and D-limonene from Horse Chestnut. Error bars show observed maxima and minima values.

α-pinene, β-pinene and D-limonene were the most abundant compounds emitted. In figure # there is no visible trend for emission rates during and after the blooming stage for horse chestnut.

Forty samples were collected during flowering period on the honey locust tree and twenty more samples after flowering. Monoterpenes and oxygenated monoterpenes including α-thujene, α-pinene, β-pinene, 2-carene, o-cimene, β-phellandrene, D-limonene, γ-terpinene and

α-terpineol were identified from honey locust emissions. Average normalized emission rate during the flowering period was 0.76μgCg^{-1}h^{-1} with α-pinene, β-pinene and D-limonene as dominant VOCs. After flowering, averaged emission rates dropped to 0.20μgCg^{-1}h^{-1}, γ-terpinene, β-phellandrene and D-limonene are the major VOCs emitted.

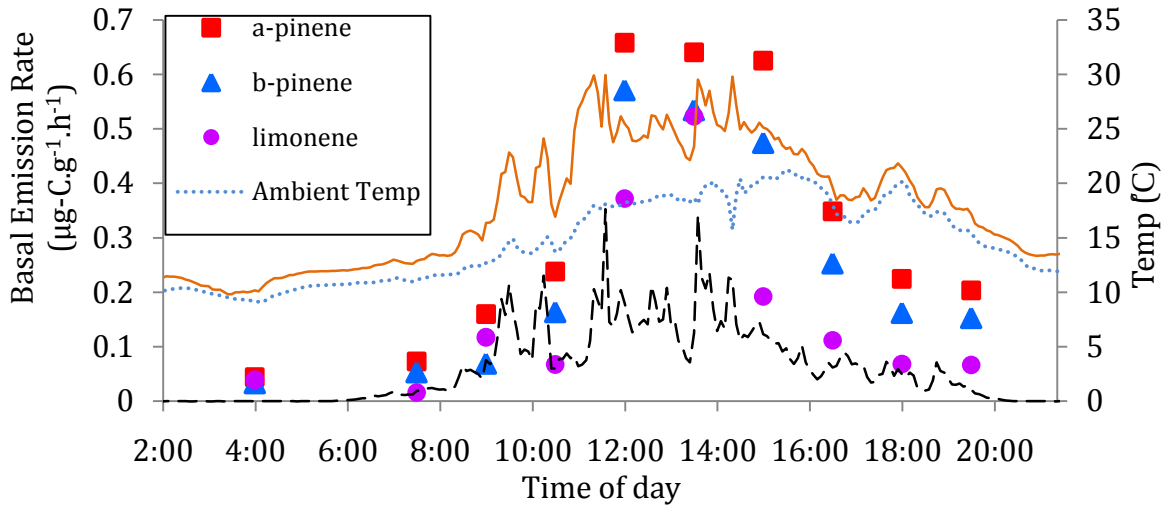

Figure #: Normalized emission rates for α-pinene, β-pinene and D-limonene from Honey Locust branch enclosure on June 9th with concurrent environmental parameters.

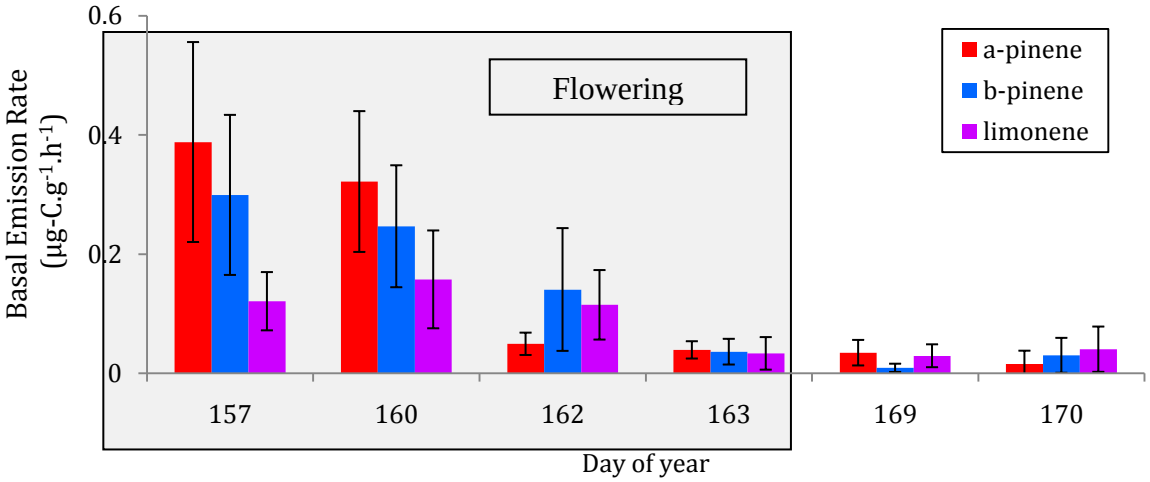

Figure #: Daily averaged normalized emission rates for α-pinene, β-pinene and D-limonene from Honey Locust. Error bars show standard deviation.

Two sesquiterpenes were identified in the hawthorn emission during flowering. The averaged emission rate for β-carophyllene was 15.1ng-C.g^{-1}.h^{-1} and 4.4ng-C.g^{-1}.h^{-1} for α-humulene during flowering, respectively 4.0ng-C.g^{-1}.h^{-1} and 0.5ng-C.g^{-1}.h^{-1} after flowering. A third sesquiterpenes α-farnesene and a monoterpene D-limonene appeared in the hawthorn emissions after flowering.

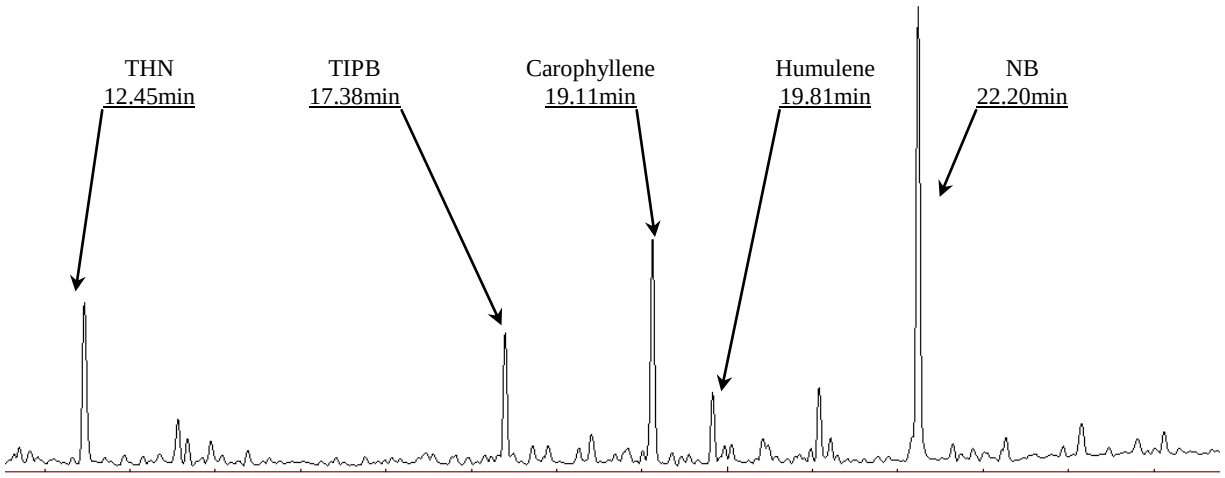

Figure #: Example of chromatogram obtained from GC-FID analysis of Hawthorn sample showing sesquiterpenes compounds.

Modeling

The case study focuses on Boulder city area where a model for VOC emission from natural sources was used to estimate the contribution of flowers to the total emissions. Model inputs comprised the city's tree inventory and an urban vegetation cover fraction estimate. Vegetation cover was estimated by analyzing visually Google earth images. Boulder city area was divided in nine hundred cells. Three hundred fifty cells were randomly evaluated and the average vegetation cover fraction was found to be 15%. A more detailed study aimed to estimate vegetation cover fraction for residential and industrial areas, respectively 25% and 3%. Moreover Boulder city is composed of 58% of residential areas versus 26% for industrial zones. Vegetation type information for Boulder city relied on the municipal tree resource analysis report by Boulder city's foresters (Table#). The city was assumed as a point source of VOC using the Model of Emissions of Gases and Aerosols from Nature (MEGAN). Isoprene and monoterpenes emissions were calculated for april 2009 to june 2009. Meteorological data from University of Colorado weather station were utilized to run the model. Emissions from flowers were included in the model for honey locust and crabapple using experimental results. Both species represent 80% of flowering street trees in boulder and 11% of total street tree according to table #. Tree from private property were assumed to be of the same composition as city street tree and are estimated to be ten times more than city street trees. Emission estimates were compared for the flowering period of each of the two trees. Crabapple flower emissions represent 3% of light independent monoterpenes emission, for honey locust flower emissions it is 6%. These figures need to be interpreted carefully since vegetation type is only representative of city managed trees. As a comparison, in a southern city, Riverside in California, flowering trees represent 40% of total street trees with more than 10 different blooming species.

Table #: municipal tree resource analysis of Boulder city.

Species	No. of trees	% of total trees	Leaf area (m^2)	% of total leaf area	Canopy cover (m^2)	% of total canopy cover
green ash	4901	13.8	1067839	11.8	251497	13.1
siberian elm	3004	8.5	1553048	17.2	229550	12
cottonwood	2626	7.4	932782	10.3	207159	10.8
honeylocust	2318	6.5	572389	6.3	148966	7.8
Silver maple	2145	6	1751984	19.4	335041	17.5
Crabapple	1693	4.8	126021	1.4	58395	3
Blue spruce	1421	4	173733	1.9	34917	1.8
Austrian pine	1317	3.7	127727	1.4	31273	1.6
Juniper	1113	3.1	39360	0.4	11166	0.6
Russian olive	1091	3.1	77160	0.9	37505	2
Norway maple	1052	3	160481	1.8	36594	1.9
Willow	830	2.3	554438	6.1	108834	5.7
Littleleaf linden	731	2.1	90490	1	20013	1
White ash	705	2	123449	1.4	23063	1.2
Pinyon pine	647	1.8	17145	0.2	5796	0.3
Boxelder	620	1.7	162371	1.8	38443	2
Cockspur hawthorn	509	1.4	9346	0.1	3767	0.2
Sugar maple	483	1.4	137299	1.5	33698	1.8
Quaking aspen	478	1.3	43720	0.5	8542	0.4
Red oak	447	1.3	150503	1.7	31130	1.6
Hackberry	434	1.2	64261	0.7	13225	0.7
American linden	428	1.2	124595	1.4	17443	0.9
Red maple	414	1.2	18461	0.2	5543	0.3
Amur maple	409	1.2	9278	0.1	4240	0.2
TOTAL	29816	84	8087883	89.4	1695803	88.5

Flowering VOCs related literature

Baraldi, R., F. Rapparini, et al. (1999). "Volatile organic compound emissions from flowers of the most occurring and economically important species of fruit trees." Physics and Chemistry of the Earth Part B-Hydrology Oceans and Atmosphere 24(6): 729-732.

Buchbauer, G., L. Jirovetz, et al. (1993). "Headspace and essential oil analysis of apple flowers." Journal of Agricultural and Food Chemistry 41(1): 116-118.

Deng, C. H., G. X. Song, et al. (2004). "Rapid determination of volatile compounds emitted from Chimonanthus praecox flowers by HS-SPME-GC-MS." Zeitschrift Fur Naturforschung C-a Journal of Biosciences 59(9-10): 636-640.

Dudareva, N., R. A. Raguso, et al. (1998). "Floral scent production in Clarkia breweri - III. Enzymatic synthesis and emission of benzenoid esters." Plant Physiology 116(2): 599-604.

Effmert, U., J. Grosse, et al. (2005). "Volatile composition, emission pattern, and localization of floral scent emission in Mirabilis jalapa (Nyctaginaceae)." American Journal of Botany 92(1): 2-12.

Flament, I., C. Debonneville, et al. (1993). "Volatile constituents of roses – characterization of cultivars based on the headspace analysis of living flower emissions." Acs Symposium Series 525: 269-281.

Goodwin, S., N. Kolosova, et al. (2003). "Cuticle characteristics and volatile emissions of petals in Antirrhinum majus. (vol 117, pg 435, 2003)." Physiologia Plantarum 119(4): 605-605.

Granero, A. M., F. J. E. Gonzalez, et al. (2005). "Analysis of biogenic volatile organic compounds in zucchini flowers: Identification of scent sources." Journal of Chemical Ecology 31(10): 2309-2322.

Ibrahim, M. A., M. C. Egigu, et al. (2010). "Diversity of volatile organic compound emissions from flowering and vegetative branches of Yeheb, Cordeauxia edulis (Caesalpiniaceae), a threatened evergreen desert shrub." Flavour and Fragrance Journal 25(2): 83-92.

Jakobsen, H. B., P. Friis, et al. (1994). "Emission of volatiles from flowers and leaves of Brassica-napus in-situ." Phytochemistry 37(3): 695-699.

Johne, A. B., B. Weissbecker, et al. (2006). "Volatile emissions from Aesculus hippocastanum induced by mining of larval stages of Cameraria ohridella influence oviposition by conspecific females." Journal of Chemical Ecology 32(10): 2303-2319.

Li, Z. G., M. R. Lee, et al. (2006). "Analysis of volatile compounds emitted from fresh Syringa oblata flowers in different florescence by headspace solid-phase microextraction-gas chromatography-mass spectrometry." Analytica Chimica Acta 576(1): 43-49.

Loughrin, J. H., T. R. Hamiltonkemp, et al. (1990). “Volatiles from flowers of Nicotiana-sylverstris, Nicotiana-otophora and Malus X domestica- headspace components and day night changes in their relative concentrations.” Phytochemistry 29(8): 2473-2477.

MacTavish, H. S., N. W. Davies, et al. (2000). "Emission of volatiles from brown boronia flowers: Some comparative observations." Annals of Botany 86(2): 347-354.

Martin, D. M., O. Toub, et al. (2009). "The bouquet of grapevine (Vitis vinifera L. cv. Cabernet Sauvignon) flowers arises from the biosynthesis of sesquiterpene volatiles in pollen grains." Proceedings of the National Academy of Sciences of the United States of America 106(17): 7245-7250.

Muller, K., M. Pelzing, et al. (2002). "Monoterpene emissions and carbonyl compound air concentrations during the blooming period of rape (Brassica napus)." Chemosphere 49(10): 1247-1256.

Rapparini, F., R. Baraldi, et al. (2001). "Seasonal variation of monoterpene emission from Malus domestica and Prunus avium." Phytochemistry 57(5): 681-687.

Robertson, G. W., D. W. Griffiths, et al. (1993). "A comparison of the flower volatiles from Haethorn and 4 Raspberry cultivars.” Phytochemistry 33(5): 1047-1053.

Schuurink, R. C., M. A. Haring, et al. (2006). "Regulation of volatile benzenoid biosynthesis in petunia flowers." Trends in Plant Science 11(1): 20-25.

Vallat, A. and S. Dorn (2005). "Changes in volatile emissions from apple trees and associated response of adult female codling moths over the fruit-growing season." Journal of Agricultural and Food Chemistry 53(10): 4083-4090.

Vallat, A., H. N. Gu, et al. (2005). "How rainfall, relative humidity and temperature influence volatile emissions from apple trees in situ." Phytochemistry 66(13): 1540-1550.

Van Schie, C. C. N., M. A. Haring, et al. (2006). "Regulation of terpenoid and benzenoid production in flowers." Current Opinion in Plant Biology 9(2): 203-208.

Yamaguchi, K. and T. Shibamoto (1980). "Volatile constituents of the Chestnut flower." Journal of Agricultural and Food Chemistry 28(1): 82-84.

Zhuang, X. F., W. E. Klingeman, et al. (2008). "Emission of Volatile Chemicals from Flowering Dogwood (Cornus florida L.) Flowers." Journal of Agricultural and Food Chemistry 56(20): 9570-9574.

Appendix

Dry biomass weight is needed to calculate emission rates, however, cutting the branch for a weight estimate is very disruptive for the plant and induces an abnormal emission response. Considering the relatively small size of the trees in this experiment, it was possible to cut the sampled branches only at the very end of the project. Blossoms stayed on the branch a limited amount of time, thus flowers were counted on the sampled branches and similar flowers were collected elsewhere in the nursery for weight measurements. Biomass dry weight determination was completed for leaves and flowers of every tree. Flower were counted in each enclosure, an equivalent number was collected on a different tree. Leaves were collected on sampled branches after the experiment. Collected biomass was then dried for 24h at 50°C in an oven.